

**The mitochondrial aspartate/glutamate carrier (AGC or Aralar1) isoforms in *D. melanogaster*: biochemical characterization, gene structure, and evolutionary analysis**

Paola Lunetti<sup>1#</sup>, René Massimiliano Marsano<sup>2#</sup>, Rosita Curcio<sup>3#</sup>, Vincenza Dolce<sup>3\*</sup>, Giuseppe Fiermonte<sup>4</sup>, Anna Rita Cappello<sup>3</sup>, Federica Marra<sup>3</sup>, Roberta Moschetti<sup>2</sup>, Yuan Li<sup>3,5</sup>, Donatella Aiello<sup>6</sup>, Araceli del Arco Martínez<sup>7</sup>, Graziantonio Lauria<sup>3</sup>, Francesco De Leonardis<sup>4</sup>, Alessandra Ferramosca<sup>1</sup>, Vincenzo Zara<sup>1\*</sup>, and Loredana Capobianco<sup>1\*</sup>

<sup>1</sup>Department of Biological and Environmental Sciences and Technologies, University of Salento, 73100 Lecce, Italy

<sup>2</sup>Department of Biology, University of Bari, 70125 Bari, Italy

<sup>3</sup>Department of Pharmacy, Health, and Nutritional Sciences, University of Calabria, 87036 Arcavacata di Rende (Cosenza), Italy.

<sup>4</sup>Department of Biosciences, Biotechnologies and Biopharmaceutics, University of Bari, 70125 Bari, Italy

<sup>5</sup>Faculty of Biological Engineering, Sichuan University of Science and Engineering, Yibin, China

<sup>6</sup>Department of Chemistry, University of Calabria, 87036 Arcavacata di Rende (Cosenza), Italy.

<sup>7</sup>Facultad de Ciencias del Medio Ambiente, Universidad de Castilla La Mancha, Toledo, Spain.

\*Corresponding authors. V. Dolce is to be contacted at Department of Pharmacy, Health, and Nutritional Sciences, University of Calabria, 87036 Arcavacata di Rende (Cosenza), Italy. Tel.: +39 0 984493119; fax: +39 0 984493270. L. Capobianco is to be contacted at Department of Biological and Environmental Sciences and Technologies, University of Salento, 73100 Lecce, Italy. Tel.: +39 0 832298864; fax: +39 0 832298626. V. Zara is to be contacted at Department of Biological and Environmental Sciences and Technologies, University of Salento, 73100 Lecce, Italy. Tel.: +39 0 832298678; fax: +39 0 832298626.

E-mail addresses: [vincenza.dolce@unical.it](mailto:vincenza.dolce@unical.it) (V. Dolce), [loredana.capobianco@unisalento.it](mailto:loredana.capobianco@unisalento.it) (L. Capobianco), [vincenzo.zara@unisalento.it](mailto:vincenzo.zara@unisalento.it) (V. Zara)

# These authors contributed equally to this work.

## Abstract

### Background

In man two mitochondrial aspartate/glutamate carrier (AGC) isoforms, known as aralar and citrin, are required to accomplish several metabolic pathways. In order to fill the existing gap of knowledge in *Drosophila melanogaster*, we have studied *aralar1* gene, orthologue of human AGC-encoding genes in this organism.

### Methods

The blastp algorithm and the “reciprocal best hit” approach have been used to identify the human orthologue of AGCs in Drosophilidae and non-Drosophilidae. Aralar1 proteins have been overexpressed in *Escherichia coli* and functionally reconstituted in liposomes for transport assays.

### Results

The transcriptional organization of *aralar1* comprises six isoforms, three constitutively expressed (*aralar1-RA*, *RD* and *RF*), and the remaining three distributed during the development or in different tissues (*aralar1-RB*, *RC* and *RE*). Aralar1-PA and Aralar1-PE, representative of all isoforms, have been biochemically characterized. Recombinant Aralar1-PA and Aralar1-PE proteins share similar efficiency to exchange glutamate against aspartate, and same substrate affinities than the human isoforms. Interestingly, although Aralar1-PA and Aralar1-PE diverge only in their EF-hand 8, they greatly differ in their specific activities and substrate specificity.

### Conclusions

The tight regulation of *aralar1* transcripts expression and the high request of aspartate and glutamate during early embryogenesis suggest a crucial role of Aralar1 in this *Drosophila* developmental stage. Furthermore, biochemical characterization and calcium sensitivity have identified Aralar1-PA and Aralar1-PE as the human aralar and citrin counterparts, respectively.

### General Significance

The functional characterization of the fruit fly mitochondrial AGC transporter represents a crucial step toward a complete understanding of the metabolic events acting during early embryogenesis.

**Keywords:** *Drosophila melanogaster*; *CG2139*; aspartate/glutamate carrier (AGC); aralar; citrin; phylogenetic footprint;

**Abbreviations:** AGC, aspartate/glutamate carrier; MAS, malate-aspartate shuttle; MCF, mitochondrial carrier family; NRG, nuclear respiratory gene; SDS-PAGE, polyacrylamide gel electrophoresis in the presence of sodium dodecyl sulfate; TSS, transcriptional start site.

## 1.Introduction

The mitochondrial carrier family (MCF) represents one of the largest families of transporters widespread across all species. MCF members share a common structural organization, consisting of three tandemly repeated sequences of approximately 100 amino acids in length, and mediate the transport of metabolites across the inner mitochondrial membrane [1-3]. The aspartate/glutamate carrier (AGC) catalyzes an electrogenic exchange of cytosolic glutamate plus a proton for mitochondrial aspartate [4], and it is one of the most important family member, since it is a key component of the malate-aspartate shuttle (MAS), which transfers the reducing equivalents of NADH from cytosol to mitochondria in order to regenerate NAD<sup>+</sup> necessary for glycolysis. Furthermore, AGC plays an essential role in many other metabolic processes including the synthesis of urea and nitrogen-containing metabolites [5], gluconeogenesis from lactate [5], calcium-mediated regulation of mitochondrial respiration [4, 6-9], insulin secretion from islet cells [10], zygote development [11, 12], N-acetylaspartate (a myelin precursor) synthesis [13-16] and glial synthesis of glutamate and glutamine [17]. Increasing evidences support the hypothesis that MAS activity is crucial for breast cancer cell proliferation [18]. In this regard, it might divert energetic cell metabolism towards glycolysis, promoting cancer cell growth [19]. Furthermore, AGC is involved in taurine metabolism, since it can efficiently transport also cysteinesulfinate [4, 20], an intermediate of cysteine degradation that serves as a precursor of taurine [21].

In *Homo sapiens*, two isoforms named AGC1 and AGC2 (also known as aralar and citrin) and encoded by the *SLC25A12* and *SLC25A13* genes, respectively, have been identified and characterized [4, 22]. They belong to a subfamily of calcium-binding mitochondrial carrier sharing a characteristic bipartite structure, which consists of a C-terminal domain responsible for transport activity, and an N-terminal domain containing 8 EF-hands that regulates transport activity [4, 23].

Aralar is mainly expressed in the heart, retina, skeletal muscle and brain [24, 25], whereas citrin is widely expressed in the liver, epithelial cells and breast [4]. Aralar is involved in retinal visual function [26, 27], in myelination process [13] and in glutamate-induced excitotoxicity [28, 29]. Mutations in the *SLC25A12* gene have been found in autism spectrum disorders [25, 30-32], as well as in a rare human disease (OMIM number 612949) implying developmental delay, epilepsy and hypotonia [15, 33]. *SLC25A13* mutations are responsible for citrin deficiency that causes adult-onset type II citrullinemia (CTLN2, OMIM number 603471), neonatal intrahepatic cholestasis (NICCD, OMIM number 605814) [29, 34-39], as well as failure to thrive and dyslipidemia caused by citrin deficiency (FTTDCD) [40].

1  
2  
3  
4  
5  
6  
7  
8  
9  
10  
11  
12  
13  
14  
15  
16  
17  
18  
19  
20  
21  
22  
23  
24  
25  
26  
27  
28  
29  
30  
31  
32  
33  
34  
35  
36  
37  
38  
39  
40  
41  
42  
43  
44  
45  
46  
47  
48  
49  
50  
51  
52  
53  
54  
55  
56  
57  
58  
59  
60  
61  
62  
63  
64  
65

In *D. melanogaster*, a single gene annotated in FlyBase as *CG2139* or *aralar1* encodes a ortholog of the human AGC isoforms [41]. *Aralar1* gene is involved in high energy demanding processes, together with many other genes, such as those responsible for embryonic epithelial repair [42]. Previous studies indicated that *aralar1* locus is involved in the determination of bristle number in *D. melanogaster*, which are structures that may also have a neurosensory function [43], as well as this locus may influence wing size phenotype [44].

Differently from other fruit fly mitochondrial transporters, such as adenine nucleotide translocase [45], uncoupling protein [46, 47] dicarboxylate [48], thiamine pyrophosphate [49, 50], and glutamate carriers [51], a genomic analysis of this insect has highlighted the presence of a single gene (*CG2139*) encoding various *aralar1* spliced isoforms. The presence of so many alternatively spliced isoforms in mitochondrial carriers [47, 52, 53] and more in general in this organism is not surprising, since alternative splicing is a peculiar mechanism very often used by *D. melanogaster* to tightly control tissue- and stage-specific protein isoforms with different functions in development, as highlighted by Venables et co-workers “*Drosophila uses every alternative splicing strategy imaginable with an elegance and complexity that often eclipses mammals*” [54].

Despite the high metabolic relevance of this transporter, very few data are available on its biological role in fruit fly cellular processes, and no data at all are available on its transport properties in *Drosophila*.

In the present study, we have described (i) the expression profile of *D. melanogaster aralar1* gene in different developmental stages and tissues; (ii) the evolutionary changes that have shaped *aralar1* gene structure in arthropods; (iii) the functional characterization of recombinant Aralar1-PA and Aralar1-PE and their identification as the fruit fly mitochondrial aspartate/glutamate carriers.

## 2. Material and methods

### 2.1. Blast search of AGC orthologs in *D. melanogaster* and other species

The *D. melanogaster* ortholog of human AGCs was identified using the blastp algorithm (<http://flybase.org/blast/>). A BLAST search strategy, using *D. melanogaster* CDS and/or peptides as queries against genomic and ESTs databases, was also adopted to identify putative genes encoding AGC in the genome of other Drosophilidae and several non-Drosophilidae species [55]. A complete list of the species investigated in this study and the accession number in which *aralar1* genes have been identified is shown in Supplementary Table 1. These searches were performed using organism-specific ([www.flybase.org](http://www.flybase.org), [www.vectorbase.org](http://www.vectorbase.org) and <http://hymenoptera.genome.org>) and generalist genomic repositories (NCBI <http://blast.ncbi.nlm.nih.gov/Blast.cgi>). The “reciprocal best

hit” approach was used to identify *aralar1* genes in different species. In this approach, a common evolutionary origin is supposed when in the compared genomes two gene sequences represent each other the best BLAST hit[56].For each genomic sequence identified by using the above-mentioned criteria, exon/intron boundaries were carefully annotated after prediction *in silico* carried out with the aid of ESTs and cDNA sequences, if available, or predicted by the Genscan tool [57], or inferred by sequence similarity with transcript sequences of closely related species. Multiple alignments of amino acids, as well as coding and non-coding DNA sequences, were obtained using the MultAlin 5.4.1 software available at the MultAlin server (<http://multalin.toulouse.inra.fr/multalin/>) [58, 59]. The matrix-scan pattern matching tool of the Regulatory Sequence Analysis Tools from the RSAT server (<http://rsat.ulb.ac.be/>) was used, in combination with multiple alignments to identify Nuclear Respiratory Gene (NRG) elements [60] in the non-coding sequences of Drosophilidae and non-Drosophilidae *aralar1* genes.

## 2.2. Reverse-transcription analyses of *aralar1* transcriptional isoforms

Oregon-R flies were raised on standard culture medium at 24 °C. Total RNA for gene expression analysis was achieved from 0.5- to 1-g samples of Oregon-R individuals at different developmental stages (embryo, larvae, pupae and adult flies). Except for ovaries and testes, male and female tissues equally contributed to each dissection. Total RNA from all the developmental stages and tissues was extracted by employing Trizol. Purified RNA was quantified using a Nanodrop spectrophotometer (Thermo Scientific) and diluted to 1 mg/ml for reverse transcription. RNA (1 µg) was reverse transcribed by employing the Quantitect reverse transcription kit (QIAGEN) [61, 62] following the manufacturer’s protocol. Amplification was carried out using the Platinum Taq DNA Polymerase (Thermo Fisher).

Primers used for amplification were:

aralar\_RA\_F ATTAGACGCGGGAATTGCTC  
aralar\_RA\_R CTCCTCGTGAAAGTCGTGCAG  
aralar\_RB\_F ATAGTGCGAACGTGCCTGA  
aralar\_RB\_R ATGGCGAGATGAACCCAGTG  
aralar\_RC\_F CCGATGCCAAGAATCTCCGT  
aralar\_RC\_R TCCTCGTGAAAGTCGTGCAG  
aralar\_RE\_F CAAATCACGCCGCTGGAGAT  
aralar\_RE\_F GGCCCCTTTATCAAGCGCTA

### 2.3. Construction of the expression plasmids encoding *D. melanogaster* Aralar1 isoforms and mutants in *E. coli* and *S. cerevisiae*

The two protein isoforms Aralar1-PA and Aralar1-PE were considered for the functional characterization of *D. melanogaster* *CG2139* gene. Aralar1-RA and Aralar1-RE were amplified by polymerase chain reaction (PCR) from the cDNA of the fruit fly clones LD35441 and GH21613, respectively. Both clones were provided by Drosophila Genomics Resource Center (Indiana University 1001 East Third St., Bloomington IN, 47405-7107). The oligonucleotide primers (sense and antisense) used in PCR reactions carried suitable restriction sites at their 5' ends for the further cloning of the amplified inserts in the pET-21b/V5-His *E. coli* expression vector [51]. The absence of a stop codon in the reverse primer sequence led to the expression of Aralar1 proteins containing V5/His-tag at their C-termini [63].

The WT Aralar1-RE cDNA was employed as a template to generate mutants named  $\Delta 5$  (deletion from residue 301 to 305),  $\Delta 8$  (deletion from residue 301 to 308 ),  $\Delta 12$  (deletion from residue 299 to 310 ), and 5Ala (replacement of residues K<sub>301</sub>RRRK<sub>305</sub> by consecutive alanines). All of the mutations were introduced by the overlap extension PCR method [64, 65], using oligonucleotides with suitable mutations in their sequences. Primers used for amplification were:

aralar\_PE\_FTAGGAATTCACCAATGCACATCCCGTTTCC and

aralar\_PE\_R CGAAAGCTTGGATCCCGTGGCCGTCG for all mutants.

The following specific primers were used to generate the above-mentioned mutants:

aralar\_PE\_Δ5\_F CCATCAAGCAGGCTGGTGGATACCTCCGAGTAGCCGCA

aralar\_PE\_Δ5\_R TGCGGCTACTCGGAGGTATCCACCAGCCTGCTTGATGG

aralar\_PE\_Δ8\_F CCATCAAGCAGGCTGGTGGAGTAGCCGCATCGACTATAGTGAC

aralar\_PE\_Δ8\_R GTCACTATAGTCGATGCGGCTACTCCACCAGCCTGCTTGATGG

aralar\_PE\_Δ12\_F GCGCCGTCCATCAAGCAGGCCGCATCGACTATAGTGACCTGAGCAA

aralar\_PE\_Δ12\_R TTGCTCAGGTCACTATAGTCGATGCGGCCTGCTTGATGGACGGCGC

aralar\_PE\_5Ala\_F

CCATCAAGCAGGCTGGTGGGCGGCTGCCGCAGCGATACCTCCGAGTAGCCGCA

aralar\_RE\_5Ala\_R

TGCGGCTACTCGGAGGTATCGCTGCGGCAGCCGCCACCAGCCTGCTTGATGG

The aralar1-RA and aralar1-RE ORFs were recovered from pET-21b/V5-His clones by a EcoRI/AgeI digestion and cloned in the modified yeast expression vector pYES2/ V5-His [49], in which the inducible GAL1 promoter had been replaced with the constitutive TDH3 promoter. The

frameshift of transcripts was avoided cloning a KpnI/EcoRI fragment carrying the ATG start codon at '5-end. Fragments used were: GGTACCAGGATCCGATCTTGAAGTACTGACTGAGATGGCGAATTC and GGTACCAGGATCCGATCTTGAAGTACTGACTGAGATGGCGAATTC for aralar1-RA and for aralar1-RE, respectively.

#### 2.4. Bacterial expression and purification of the recombinant proteins

Aralar1 proteins were overexpressed at high levels in *E. coli* BL21(DE3) [49]. Their identities were assessed by MALDI-TOFMS of trypsin digests of the corresponding bands excised from a Coomassie blue-stained polyacrylamide gel [66, 67]. Inclusion bodies were purified using sucrose density gradient centrifugation, next they were washed at 4°C, firstly with TE buffer (10 mM Tris/HCl, 1 mM EDTA, pH 8), then twice with a buffer containing Triton X-114 (2%, w/v) and 10 mM HEPES (pH 8), and finally with 10 mM PIPES pH 6.5. Aralar1-PA and Aralar1-PE were solubilized in 2% sarkosyl (w/v), and a small residue was removed by centrifugation (258000 g, 30 min). Solubilized proteins were diluted 10-fold with 10 mM PIPES pH 6.5 and reconstituted into liposomes [68].

#### 2.5. Reconstitution into liposomes and transport assays

Reconstitution mixture (700 µl) contained 0.5-1 µg of solubilized proteins, Triton X-114 (1,3 % w/v), L- $\alpha$ -phosphatidylcholine from egg yolk (1,3 % w/v), as sonicated liposomes, 10 mM glutamate (except where otherwise indicated), and 20 mM PIPES at pH 6.5 [69]. These components were carefully blended, and the blend was recycled 13 times through the same Amberlite column (Bio-Rad) [69]. External substrate was eliminated from proteoliposomes on Sephadex G-75 columns, pre-equilibrated with 50 mM NaCl and 10 mM PIPES at pH 6.5. Transport at 25°C was started by adding L-[<sup>14</sup>C]glutamate (Scopus Research BV, Wageningen, Netherlands) at the indicated concentrations to substrate-loaded proteoliposomes (exchange reaction), or to empty proteoliposomes (uniport reaction). In both cases, transport was terminated by adding 30 mM pyridoxal phosphate (PLP). In control samples, inhibitor was added together with the external radioactive substrate based on the inhibitor stop method [70, 71]. Finally, external substrate was removed and radioactivity into proteoliposomes was measured. The experimental values were adjusted by subtracting control values. The initial transport rate was measured from the radioactivity taken up by proteoliposomes after 1 min (in the initial linear range of substrate uptake). The free Ca<sup>2+</sup> concentrations were determined fluorimetrically with fura-2-acetoxymethyl ester (Fura-2 AM) (Thermo Fischer Scientific). Fura-2 AM is a membrane-permeable, non-invasive

1 derivative of the ratiometric calcium indicator fura-2. The excitation wavelengths used are 340 nm  
2 and 380 nm for Ca<sup>2+</sup>-bound and Ca<sup>2+</sup>-free fura-2 AM, respectively. In both states, the emission  
3 maximum is about 510 nm. The ratios 510 nm/340 nm and 510 nm/380 nm are directly related to  
4 the amount of Ca<sup>2+</sup> [72]. Calcium dependence on transport activity was determined using de-ionized  
5 ultrapure water. In experiments for evaluating the influence of the membrane potential on the  
6 activity of the recombinant proteins, valinomycin was added to proteoliposomes in order to provide  
7 de-energized conditions. K<sup>+</sup> diffusion potentials were generated using valinomycin and K<sup>+</sup>  
8 gradients. In these experiments, substrate and buffer were neutralized with NaOH [4].  
9  
10  
11  
12  
13  
14  
15

## 16 **2.6. Yeast strains, growth conditions and functional complementation of yeast AGC1Δ by** 17 **ARALAR1-PA and ARALAR1-PE**

18 W303 (wild-type) (*MATa {leu2-3,112 trp1-1 can1-100 ura3-1 ade2-1 his3-11,15}*) yeast strain was  
19 provided by the EUROFAN resource center EUROSCARF (Frankfurt, Germany). The yeast  
20 AGC1 gene deletion (*agc1Δ*) and the cloning of endogenous yeast deleted gene AGC1 were  
21 achieved as described before [73].  
22  
23  
24  
25  
26

27 The recombinant aralar1-RA-pYES2 and aralar1-RE-pYES2 plasmids were introduced into the  
28 *agc1Δ* yeast strain using the lithium acetate method [74], and transformants were selected on  
29 minimal medium lacking uracil, supplemented with 2% glucose.  
30  
31

32 Functional complementation was achieved growing cells on liquid complete medium (1% Bacto  
33 yeast extract, 2% Bacto Peptone, pH 5.0) supplemented with 2% glucose (YPD) or 0.5 mM oleic  
34 acid dissolved in 10% Tween40 (YPO) as carbon sources. Growths were started from medium log  
35 precultures grown on complete medium YPD and diluted with YPO to an optical density of 0.01 at  
36 600 nm.  
37  
38  
39  
40  
41

42 Simultaneously, washed cells were diluted and spotted on complete solid medium YPO, then plates  
43 were incubated for 72 h at 30 °C. Four-fold serial dilutions of both the transformed strains, wild-  
44 type and AGC1Δ cells were analyzed.  
45  
46  
47  
48  
49

## 50 **2.7. Other methods**

51 Proteins were resolved by SDS-PAGE and stained with Coomassie blue dye [75]. The amounts of  
52 recombinant pure Aralar1-PA and Aralar1-PE incorporated into liposomes were measured as  
53 previously described [76] and proved to be approximately 20% of the protein amount added to the  
54 reconstitution mixture. Moreover, recombinant proteins were resolved by SDS-PAGE analysis [77,  
55 78], then transferred to a nitrocellulose membrane and analyzed by Western blotting employing a  
56 mouse anti-V5 monoclonal antibody (Sigma-Aldrich) [79, 80]. A multiple sequence alignment  
57  
58  
59  
60  
61  
62  
63  
64  
65



(MSA) of the fruit fly Aralar1 proteins, human aralar and citrin isoforms was obtained by using ClustalW to insert gaps in the MSA [81]. All data were analyzed using the statistical software GraphPad Prism Software (7.0 version). Pairwise comparisons between means of different groups were performed using a Student's t-test (two tailed, unpaired). Multiple comparisons were performed using a univariate ANOVA. Values at  $P \leq 0.05$  were considered statistically significant, while values at  $P \leq 0.01$  and  $P < 0.001$  were considered very significant [82, 83]. Orientation of functional Aralar-1 in the membrane of reconstituted proteoliposomes was investigated by ELISA assay performed as previously described [84]. ELISA tests were carried out on intact and permeabilized proteoliposomes by using either the rabbit polyclonal antiserum generated against 35-177 amino acids of Drosophila Aralar-1 proteins as described in [85] or the anti-V5 antibody directed against the V5 epitope placed at their C-termini (Sigma-Aldrich).

### 3. Results

#### 3.1. Identification of genes encoding the aspartate/glutamate carrier in Drosophilaspecies

A single gene, annotated in FlyBase as *CG2139* or *alarar1*, encodes a *D. melanogaster* ortholog of the human AGC isoforms (also known as aralar and citrin) [4], with no additional hits obtained throughout database mining. *Aralar1* locus spans roughly 10 Kbp on the third chromosome (3R:30,445,635..30,455,867 [-]) in the 99F4-99F5 cytogenetic band of polytene chromosomes of *D. melanogaster*. The transcriptional organization of *alarar1* reported in FlyBase (Figure 1A) comprises six transcriptional isoforms. The utilization of alternative transcriptional start sites, alternative splicing and alternative UTRs, produces five different transcriptional isoforms (namely RA, RB, RC, RD, RE), which in turn can be translated into four different proteins (PA/PD, PB, PC, PE). An additional translational isoform is reported in FlyBase, Aralar1-PF, which is translated from the *alarar1-RF* transcript that is structurally identical to *alarar1-RA* isoform by mean of a read-through translational mechanism [86]. In this regard, *alarar1-RA* transcript is translated into a 682 amino acids long protein (Aralar1-PA), whereas *alarar1-RF* transcriptional isoform is translated into a polypeptide having 12 additional aminoacids at its C-terminus due to translation progression beyond the canonical stop codon. Three different promoters contribute to the transcription of *alarar1* locus. *Aralar1-RA* (identical to *alarar1-RF*) and *alarar1-RD* are transcribed from the same downstream promoter, with *alarar1-RD* transcript possessing a shorter 3'UTR if compared to that of *alarar1-RA/RF* isoforms. *Aralar1-RB* arises from the central promoter, whereas *alarar1-RC* and *alarar1-RE* are originated from the upstream promoter. The two latter isoforms differ by a short, 36 bp long exon, which is specifically incorporated into the *alarar1-RE* transcript. Given the availability of a wide range of sequenced Arthropoda genomes, we have surveyed *alarar1* gene structure in Arthropoda.

1 Orthologous genes in Drosophilidae have been retrieved using a BLAST strategy, and locus  
2 structure has been inferred with the aid of ESTs and cDNA sequences annotated in FlyBase and  
3 NCBI databases. Sequences with significant similarity to *D. melanogaster aralar1* gene have been  
4 detected in the genome of 22 additional Drosophila species (Supplementary Table 1), and their  
5 organization has been compared. Similarly to *D. melanogaster* annotation, in all the investigated  
6 Drosophila species three transcriptional start sites can be inferred from ESTs and cDNAs comparison  
7 and from inter-species similarity. In order to give a better snapshot of *aralar1* locus, its organization  
8 has been divided into three schemes highlighting the exon/intron organization relative to the three  
9 TSSs (Transcriptional Start Site) (Supplementary Tables 2-5). The comparison clearly suggests that  
10 the exon-intron structure of the locus is highly conserved in the 23 analyzed species. As can be  
11 observed, exon length is poorly variable. The first exon of all transcriptional isoforms is the most  
12 variable in length. Indeed, they encode the 5' UTRs and the leader peptides that are expected to be  
13 divergent in sequence, even if closely related species are compared. The length of the coding region  
14 of the last exon, encoding the protein C-terminus, also presents variable length and sequence in the  
15 analyzed Drosophila species. Internal coding exons are instead extremely conserved in length. As  
16 expected, introns are the most plastic regions of eukaryotic genes, and they are longer in species  
17 distantly related to *D. melanogaster*. It is worth to note that although the presence of the *aralar1-RE*  
18 specific exon is not supported by ESTs or cDNAs in the vast majority of the Drosophilidae species  
19 (not shown), it can be inferred by sequence similarity, suggesting that it could be also a functional  
20 exon in other species. In support of this hypothesis, the *aralar1-RE* specific exon, which can be 33-  
21 39 bp long depending upon the species, is flanked by a non-canonical donor splice site  
22 (GC) conserved in all the Drosophila species, suggesting the usage of an atypical splice site in the  
23 common ancestor of Drosophila and Sophophora genera (Supplementary Figure 1).  
24  
25  
26  
27  
28  
29  
30  
31  
32  
33  
34  
35  
36  
37  
38  
39  
40  
41  
42  
43

### 44 **3.2. Conservation of regulatory elements**

45 Inter-species DNA sequence comparison is an excellent tool for the identification of cis-regulatory  
46 DNA sequences interested in eukaryotic gene expression regulation, especially in non-coding DNA  
47 sequence. In the noncoding sequences of Drosophilidae *aralar1* genes we have searched for  
48 conserved motifs by using phylogenetic footprinting and DNA pattern discovery softwares. The  
49 nuclear respiratory gene (NRG) element has been previously reported as a palindromic 8-bp motif  
50 (TTAYRTAA) that is shared by all nuclear OXPHOS genes [87], as well as by many other nuclear  
51 genes involved in biogenesis and function of mitochondria in insects [60]. In *D. melanogaster*,  
52 NRG elements are usually located within an intron, in close proximity to the transcription start site  
53 (TSS), but it can be found in different gene locations, such as upstream the TSS. A NRG element  
54  
55  
56  
57  
58  
59  
60  
61  
62  
63  
64  
65

1 (TTATATAA) associated with high weight and low P value in the RSAT output (8,2 and  $6.0e^{-05}$   
2 respectively) is located in the first intron, 518 bp downstream of the transcription start site related to  
3 *D. melanogaster aralar1-RB* transcriptional isoform. This 8-bp motif is extremely conserved and  
4 located in the first intron in all the Drosophilidae *alarar1* orthologs with high frequency (Figure  
5 1B). An additional NRG element, associated with a slightly lower score and a moderately higher P-  
6 value in the RSAT output (6,7 and  $1,5e^{-04}$  respectively), is located downstream within the same  
7 intron, 686 bp upstream the TSS related to the RA/RD/RF transcriptional isoforms (Figure 1C).

8  
9 The functional importance of the NRG element in *alarar1* genes is suggested by its presence in the  
10 non-coding regions of *alarar1* genes belonging to the 32 non-Drosophilidae Arthropoda species  
11 investigated in this work (Supplementary Table 1). Notwithstanding, the very long divergence times  
12 (divergence between Drosophila and Parasteatoda/Limulus genera is estimated approximately 600  
13 MYA, from Treebase <http://www.timetree.org>) [88], single or multiple NRG elements have been  
14 detected in *alarar1* genes of the majority of Arthropoda species, and their intragenic localization is  
15 often strictly conserved (not shown). However, standing to the availability of transcriptional data in  
16 the vast majority of the studied cases, we have reconstructed the complete exon/intron structure of  
17 *alarar1* related to the shortest transcriptional isoform, which we have arbitrarily assumed to be  
18 homologous to *D. melanogaster* RA-RD-RF transcripts. In many of these species, the NRG  
19 elements have been found in the first intron related to the shortest transcriptional isoform,  
20 suggesting that their positions could have been remodeled during insects' evolution. Also the length  
21 of the first intron, with respect to the most proximal TSS, is on average longer in non-Drosophilidae  
22 insects (mean length=15149 bp, 29 species) than in *D. melanogaster* homologs (mean length=245  
23 bp, 23 species), supporting the hypothesis of a functional role of the NRG elements, although in a  
24 different position.  
25  
26  
27  
28  
29  
30  
31  
32  
33  
34  
35  
36  
37  
38  
39  
40  
41  
42  
43

### 44 **3.3. All eukaryotic *alarar1* genes have a common evolutionary origin.**

45 Sequences homologous to *D. melanogaster aralar1* gene have been found in the genomes of 23  
46 Drosophilidae species. They share not only significant sequence similarity with *D. melanogaster*  
47 genes, but also a strikingly conserved exon/intron organization (Figure 2 and Supplementary Tables  
48 2-5). As a first step towards understanding the evolutionary history of *alarar1* genes, we have  
49 compared the Drosophilidae gene organization with their counterparts in an informative range of 32  
50 Arthropod species consisting of 30 insects species (namely 7 Diptera, two Lepidoptera 1  
51 Coleoptera, 18 Hymenoptera and 2 Hemiptera), an Arachnida (*Parasteatoda tepidariorum*) and a  
52 Xiphosurida (*Limulus polyphemus*).  
53  
54  
55  
56  
57  
58  
59  
60  
61  
62  
63  
64  
65

1 Similarly to what found in Drosophilidae, a single *aralar1* gene has been detected in the genome of  
2 all these species. The complete list of the identified *aralar1* genes and the accession numbers in  
3 which they have been found in the respective genomes is shown in Supplementary Table 1.  
4 Variations in the exon/intron organization of the investigated genes are reported in Supplementary  
5 Table 6. Comparison of all the investigated genes, in particular those in insects and Arachnida  
6 (*Parasteatoda tepidariorum*), as well as in Xiphosura (*Limulus polyphemus*), suggests the presence  
7 of a common ancestor before Arthropods' divergence. Intron loss seemingly occurred in Diptera-  
8 Lepidoptera-Coleoptera, while intron gain suggests a lineage-specific process.

9 The existence of an internal exon, specific for a transcriptional isoform homologous to *D.*  
10 *melanogasteraralar1-RE*, can be inferred in a subset of the analyzed species including Hymenoptera  
11 (14 out of 18 species) and Diptera (6 out of 7 non-Drosophilid species), whereas we have not  
12 detected it in Coleoptera (one species) and Lepidoptera (two species), as well as in the evolutionary  
13 distant Hemiptera species.

14 In humans, the nearly identical exon/intron organization of *ARALAR* (*SLC25A12*) and *CITRIN*  
15 (*SLC25A13*) genes (19 and 21 coding exons, respectively) is consistent with a duplication of an  
16 ancestral gene, which was probably present in the genome of the Vertebrate's ancestor, due to the  
17 existence of two paralogue genes in the genome of extant vertebrate species so far sequenced (not  
18 shown). Alternatively spliced transcript variants have been reported for the human *ARALAR* gene  
19 (as provided by ac.nos NM\_003705, NR\_047549, XM\_011512070). While the NM\_003705 is  
20 translated into the Aralar1 protein (NP\_003696), the functional roles of the predicted  
21 (XM\_011512070) and the putatively non-coding (NR\_047549) transcriptional isoforms are currently  
22 unknown. Comparisons of exon phase, exon length, and intron positions, suggest that Arthropod  
23 and human genes have a unique intron-rich ancestor predating the divergence of such lineages.  
24 Since position conservation in humans and in numerous Arthropod lineages can be supposed in order  
25 to identify retained ancestral introns, we have deduced that such common ancestor gene contained at  
26 least 15 introns.

### 27 **3.4. Expression pattern of *Drosophila melanogasteraralar1* gene**

28 The developmental expression pattern of *aralar1* in *D. melanogaster* is widely described in  
29 FlyBase, which reports the modENCODE mRNA-Seq temporal expression data (mRNA-Seq\_U,  
30 [89]). Relative data are summarized in Figure 3. In order to integrate these data with the expression  
31 pattern of *aralar1* transcriptional isoforms, we have carried out a Reverse Transcriptase-PCR  
32 analysis (RT-PCR) on total RNA samples isolated from distinct *Drosophila* developmental stages  
33 (Figure 4A) or from dissected adult tissues (Figure 4B).

1 With this aim, we have devised a set of primers specific to easily discriminate the five reported  
2 isoforms. Unfortunately, we were not able to find oligos suitable for performing quantitative  
3 analysis, so we could only conduct semiquantitative analyses based on RT-PCR. However, RA/RF  
4 and RD, cannot be distinguished, due to their nearly identical sequence, as described above. We  
5 will refer to *aralar1-RA* to indicate the RA/RD/RF isoforms through this paragraph.  
6

7  
8 The obtained results have revealed a constitutive expression of *aralar1-RA* transcript throughout  
9 development (Figure 4A). By contrast, the expression of the other isoforms is patchy distributed  
10 during the development or in different tissues. *Aralar1-RB* isoforms detected in early embryo  
11 development, during all the pupal stages and in adults, being only limited to females. Finally,  
12 *aralar1-RC* is detected in embryos (at least until 12-15 hours after egg laying), in all the pupal  
13 stages and in both sexes during the adult stage, while *aralar1-RE* is expressed in the early-embryo  
14 development and in both sexes during the adult stage. Consistent with the expression pattern  
15 detected in whole adult males and females, we have found that *aralar1-RA*, *aralar1-RC* and  
16 *aralar1-RE* are ubiquitously expressed in all the main fruit fly body regions (namely head, thorax  
17 and abdomen), whereas *aralar1-RB* expression is limited to the abdomens of females, due to its  
18 ovary-specific expression (Figure 4B).  
19  
20  
21  
22  
23  
24  
25  
26  
27  
28  
29  
30

### 3.5. Bacterial expression and functional characterisation of recombinant Aralar1 proteins

31  
32 A ClustalW alignment of Drosophila Aralar1 with the human AGC isoforms has revealed that all  
33 the proteins conserve the same domain structure organization consisting of an N-terminal domain  
34 with 8 EF-hands, a carrier domain and a C-terminal domain with unknown function (Figure 5) [23].  
35 Five out of the six Drosophila Aralar1 protein isoforms do not present any difference in their N-  
36 terminal EF-hands and carrier domains (Figure 5). Aralar1-PE diverges from the other isoforms  
37 because of an insertion of 12 additional amino acid residues in the loop of its eighth EF-hand (EF-  
38 hand 8) [23]. In order to check if this peculiarity may affect its transport activity, we have chosen  
39 Aralar1-PE to be biochemically characterized together with Aralar1-PA that also shows a shorter N-  
40 terminus similar to that found in Aralar1-PD and Aralar1-PF (Figure 5).  
41  
42  
43  
44  
45  
46  
47  
48

49 Aralar1-PA and Aralar1-PE have been overexpressed at high levels in *E. coli* BL21(DE3) (Figure  
50 6A, lane 3 for Aralar1-PA, lane 4 for Aralar1-PE). They accumulate as inclusion bodies and have  
51 been purified by centrifugation on sucrose gradient and washing (Figure 6A, lane 5 for Aralar1-PA,  
52 lane 6 for Aralar1-PE), with a yield of 50 – 60 mg/ml bacterial culture. These proteins have been  
53 not revealed in bacterial cells harvested just before the induction of expression (Figure 6A, lane 1  
54 for Aralar1-PA, lane 2 for Aralar1-PE), or in cells harvested after induction but do not carrying the  
55 coding sequence for Aralar1-PA and Aralar1-PE in the expression vector (data not shown). Their  
56  
57  
58  
59  
60  
61  
62  
63  
64  
65

1 identities have been assessed by western blot analysis employing a mouse anti-V5 monoclonal  
2 antibody (Figure 6A, lanes 1-6).

3 Aralar1-PA and Aralar1-PE have been functionally reconstituted into liposomes and the orientation  
4 of their N- and C-terminal regions in the proteoliposomes was performed by ELISA assay,  
5 indicating that both termini of Aralar1 proteins reconstituted into the proteoliposomal membrane  
6 protrude toward the outside, which in intact proteoliposomes is the only side of the membrane  
7 accessible to antibodies (Supplementary Figure 2). Aralar1-PA and Aralar1-PE transport activity  
8 have been tested in homo-exchange experiments (same substrate inside and outside). Using external  
9 and internal substrate concentrations of 1 and 10 mM, respectively, both proteins efficiently  
10 catalyze [<sup>14</sup>C]glutamate/glutamate and [<sup>14</sup>C]aspartate/aspartate exchange reactions. A very active  
11 uptake of [<sup>14</sup>C]glutamate and [<sup>14</sup>C]aspartate has also been observed when proteoliposomes had been  
12 preloaded with 10 mM aspartate or glutamate, respectively (hetero-exchange reactions). Both  
13 proteins do not catalyze any homo-exchange of phosphate, ADP, ATP, malonate, malate,  
14 oxoglutarate, ketoisocaproate, citrate, carnitine, ornithine, lysine, arginine, glutathione, choline,  
15 proline, and threonine (data not shown). No [<sup>14</sup>C]glutamate/aspartate exchange has been observed  
16 using boiled Aralar1-PA and Aralar1-PE for incorporation into liposomes or reconstituting  
17 sarcosyl-solubilized bacterial material deriving either from cells not carrying any expression vector  
18 for Aralar1-PA and Aralar1-PE or from cells collected just before the induction of expression.

19 We have displayed kinetics of Aralar1-PA and Aralar1-PE uptake in Figure 6B. Each protein  
20 reconstituted into proteoliposomes contains 10 mM internal glutamate, and uptake has been  
21 measured in the presence of external 0.5 mM [<sup>14</sup>C]glutamate (exchange). Exchange reactions follow  
22 first-order kinetics, and isotopic equilibrium is approached exponentially, maximum uptake is  
23 reached after 90 min (rate constants 0.066 and 0.080 min<sup>-1</sup> and initial rates of 20.78 and 59.51  
24 nmol/min x mg protein for Aralar1-PA and Aralar1-PE, respectively). Conversely, no  
25 [<sup>14</sup>C]glutamate uptake is observed in the absence of an internal substrate (uniport), highlighting that  
26 both proteins are unable to catalyze a unidirectional transport of glutamate (Figure 6B). After 50  
27 min incubation, when radioactive uptake by proteoliposomes has approached equilibrium, the  
28 addition of 20 mM unlabeled aspartate leads to an extensive efflux of radiolabeled glutamate from  
29 glutamate-loaded proteoliposomes (Figure 6B). A similar efflux of labeled substrate is observed by  
30 adding 20 mM unlabeled glutamate (not shown). This efflux further confirms the strict exchange  
31 mechanism catalyzed by Aralar1-PA and Aralar1-PE. The unidirectional transport has been further  
32 investigated in backward experiment, as it provides a more convenient assay [53], i.e., by  
33 measuring the efflux of [<sup>14</sup>C]glutamate from prelabeled active proteoliposomes; in the absence of an  
34 external substrate no efflux of [<sup>14</sup>C]glutamate has been observed, even after 60 minutes of

1 incubation, but an extensive efflux has occurred upon the addition of 10 mM external glutamate or  
2 aspartate (data not shown).

3 Substrate specificity of recombinant Aralar1-PA and Aralar1-PE has been examined in detail by  
4 measuring the uptake of [<sup>14</sup>C]glutamate into proteoliposomes preloaded with different possible  
5 substrates. Table I reports the results of our explorative statistical analysis. Both proteins efficiently  
6 exchange external [<sup>14</sup>C]glutamate for internal L-glutamate or L-aspartate. Aralar1-PA also catalyzes  
7 a lower but significant uptake of [<sup>14</sup>C]glutamate in the presence of internal L-cysteinesulfinate,  
8 whereas no transport activity has been found with L- $\alpha$ -amino adipate, L-glutamine and L-asparagine  
9 (Table I). Differently from Aralar1-PA and yeast AGC [90], but similarly to the human AGC  
10 isoforms [4], Aralar1-PE exchanges external [<sup>14</sup>C]glutamate for internal cysteinesulfinate at the  
11 same rate as aspartate, and it shows a significantly high [<sup>14</sup>C]glutamate uptake in the presence of  
12 internal L- $\alpha$ -amino adipate and L-glutamine. Both isoforms are virtually unable to exchange  
13 [<sup>14</sup>C]glutamate for internal D-aspartate and D-glutamate, indicating a high degree of stereo  
14 specificity.  
15

16 The [<sup>14</sup>C]glutamate/glutamate exchange reactions catalyzed by Aralar1-PA and Aralar1-PE are  
17 hampered by many well-known inhibitors of several MCF members, being completely inhibited by  
18 50  $\mu$ M *p*-chloromercuribenzoate [4] and 1 mM pyrocarbonate [90] (100 and 96% inhibition,  
19 respectively for both proteins) and, to a slightly lesser extent by 50  $\mu$ M mersalyl [76] and 0.1%  
20 tannic acid [53] (80 and 85% inhibition, respectively for both proteins), and also by 1 mM *N*-  
21 ethylmaleimide [53] (40 and 50% inhibition for Aralar1-PA and Aralar1-PE, respectively).  
22 Moreover, 10 mM bathophenanthroline or 0.1 mM bromocresol purple [53] are unable to exert a  
23 significant inhibition. Additionally, no inhibition has been observed with 10  $\mu$ M bongkreikic acid  
24 [68] and 2.5 mM 1,2,3-benzenetricarboxylate [81], which are specific inhibitors of the mitochondrial  
25 ADP/ATP and citrate carrier, respectively.  
26

27 Considering that the AGC-catalyzed aspartate/glutamate antiport reaction is electrogenic [4], the  
28 effect of membrane potential has been examined on the aspartate/glutamate exchange reaction  
29 mediated by our Aralar1 carriers. A K<sup>+</sup> diffusion potential has been created across the membrane of  
30 proteoliposomes using valinomycin/KCl (calculated value  $\sim$ 100 mV, positive inside). In such  
31 conditions, the rates of the [<sup>14</sup>C]aspartate<sub>out</sub>/glutamate<sub>in</sub> exchanges of Aralar1-PA and Aralar1-PE are  
32 stimulated (Table II). In the absence of a membrane potential or when homo-exchanges have been  
33 measured, no effect has been observed. As a consequence, Aralar1-PA and Aralar1-PE are able to  
34 catalyze an electrogenic exchange of aspartate for glutamate.  
35

36 We have determined the kinetic constants of the recombinant purified Aralar1-PA and Aralar1-  
37 PE by measuring the initial transport rate at various external [<sup>14</sup>C]glutamate or [<sup>14</sup>C]aspartate  
38  
39  
40  
41  
42  
43  
44  
45  
46  
47  
48  
49  
50  
51  
52  
53  
54  
55  
56  
57  
58  
59  
60  
61  
62  
63  
64  
65

1 concentrations, in the presence of a constant internal saturating concentration (10 mM) of unlabeled  
2 substrates. In five independent experiments carried out at the same internal and external pH (6.5),  
3 the half-saturation constants ( $K_m$ ) of reconstituted Aralar1-PA and Aralar1-PE for glutamate are  
4  $0.26 \pm 0.03$  and  $0.29 \pm 0.07$  mM, respectively, and for aspartate are  $47 \pm 2.3$  and  $51 \pm 2.6$   $\mu$ M,  
5 respectively. Interestingly, the two isoforms significantly differ in their  $V_{max}$  values, which are  $32.25$   
6  $\pm 1.69$  and  $94.29 \pm 5.40$  nmol/min/mg protein, for Aralar1-PA and Aralar1-PE, respectively for  
7 both substrates. The activity has been normalized by determining the amount of recombinant  
8 proteins recovered into proteoliposomes after reconstitution. We have further analyzed whether the  
9 differences in transport rates (Table I) and  $V_{max}$  values found between the two isoforms could arise  
10 from the 12 additional amino acid residues present in the loop of the helix-loop-helix structure of  
11 the eighth EF-hand (EF-hand 8) of Aralar1-PE. First of all, we have checked, in de-ionized  
12 ultrapure water, the effect of  $Ca^{2+}$  or EGTA (a divalent ion chelator) on Aralar1-PA and Aralar1-PE  
13 transport activity (Figure 6C). The activities of both isoforms are increased of about 35% by the  
14 addition of 1 mM  $CaCl_2$  and diminished by the addition of 0.5 mM EGTA. The inhibitory effect of  
15 EGTA is abolished in the presence of 1 mM  $CaCl_2$  (Figure 6C). These results indicate that both  
16 isoforms are highly sensitive to calcium, since low calcium contamination in the reconstitution  
17 mixture is able to activate transport activity of both isoforms, whereas its removal by a  $Ca^{2+}$   
18 chelator exerts an inhibitory effect. The  $Ca^{2+}$ -dependence of the transport activities of Aralar1-PA  
19 and Aralar1-PE has been further studied by measuring their transport rates as a function of the free  
20  $Ca^{2+}$  concentration (Figure 6D). Both isoforms are highly  $Ca^{2+}$ -sensitive, since Aralar1-PA and  
21 Aralar1-PE have a half-maximal activation of about 0.34 and 0.15  $\mu$ M, respectively.  
22  
23  
24  
25  
26  
27  
28  
29  
30  
31  
32  
33  
34  
35  
36  
37  
38  
39

### 40 **3.6. Influence of the eighth EF-hand on the activity of ARALAR1 PE isoform**

41 Once established that in our reconstituted system calcium is able to regulate transport activity of both  
42 isoforms, we have checked if the shortening of the insertion consisting of 12 additional residues in  
43 Aralar1-PE or the replacement of some residues might affect its transport activity. In particular, the  
44 five positive charged residues (KRRRK from 301 to 305) have been replaced by consecutive  
45 alanine residues (5Ala mutant) or deleted ( $\Delta 5$  mutant). Two further deletions have also been  
46 investigated, the first encompassing residues 301-308 ( $\Delta 8$  mutant), and the second including  
47 residues 299-310 ( $\Delta 12$  mutant); in this latter mutant the insertion characterizing Aralar1-PE has  
48 been completely removed. Substrate specificity of recombinant Aralar1-PE mutants has been  
49 examined in detail by measuring the uptake of [ $^{14}C$ ]glutamate into proteoliposomes preloaded with  
50 different possible substrates. As reported in figure 7, the substitution of the five charged residues  
51 with Ala deeply increases transport activity of all the tested substrates, whereas its deletion  
52  
53  
54  
55  
56  
57  
58  
59  
60  
61  
62  
63  
64  
65



1  
2  
3  
4  
5  
6  
7  
8  
9  
10  
11  
12  
13  
14  
15  
16  
17  
18  
19  
20  
21  
22  
23  
24  
25  
26  
27  
28  
29  
30  
31  
32  
33  
34  
35  
36  
37  
38  
39  
40  
41  
42  
43  
44  
45  
46  
47  
48  
49  
50  
51  
52  
53  
54  
55  
56  
57  
58  
59  
60  
61  
62  
63  
64  
65

decreases transport activity proportionally with the size of the deletion gradually leading Aralar1-PE to have the same substrate specificity of Aralar1-PA. The kinetic constants of the recombinant Aralar1-PE mutants are reported in Table III. The half-saturation constants ( $K_m$ ) of reconstituted mutants do not vary with respect to the wild type, whereas as regards transport activity a significant change has been observed. In particular, 5Ala mutant shows a transport activity three-fold higher than that of the wild-type protein, whereas deletions negatively affect transport activity, which decreases proportionally with the size of the deletion. Interestingly,  $\Delta 12$  mutant exhibits the same transport activity as Aralar1-PA.

### 3.7. Aralar1-PA and Aralar1-PE function as an AGC transporter in *S. cerevisiae*

The yeast *AGC1* null mutant does not grow on oleate even in rich medium [90]. This phenotype is explained since MAS is required for reduction of the cytosolic NADH derived from peroxisomal oleate oxidation [90]. Thus, the expression of a mitochondrial carrier protein able to exchange aspartate with glutamate should abolish the growth defect of the *agc1* $\Delta$  knockout. Aralar1-PA and Aralar1-PE expressed in *AGC1* null cells have fully restored growth of the *agc1* $\Delta$  strain on oleate, similarly to the yeast Agc1p (Figure 8), indicating that both *Drosophila* proteins function as AGC transporters. By contrast, in *agc1* $\Delta$  cells transformed with the empty vector no growth rescue has been observed.

## Discussion

By allowing the mitochondrial re-oxidation of the cytosolic NADH, the MAS plays a central role in the redox homeostasis and in different metabolisms such as glucose homeostasis and nitrogen metabolism. The MAS requires the concerted functioning of six proteins, two located in the cytosol, the malate dehydrogenase 1 (MDH1) and the aspartate aminotransferase 1 (GOT1), two located in the mitochondrial matrix, the malate dehydrogenase 2 (MDH2) and the aspartate aminotransferase 2 (GOT2), and the last two located in the inner mitochondrial membrane, the aspartate/glutamate and the oxoglutarate/malate (OGC) carriers, which connect MAS cytosolic reactions to the mitochondrial ones. Despite the central role in energetic metabolism, very little is known about MAS components in the fruit fly, and up to date no functional data are available on AGC and OGC. In mammals, there are two genes encoding AGC, *ARALAR*, also known as AGC1, more widely expressed but absent in the liver, and *CITRIN* also known as AGC2, expressed in fewer tissues but present in the liver [24]. By searching the FlyBase database (<http://flybase.org/>) for human AGC homologs, we have found 6 alternatively spliced-isoforms annotated as *aralar1* and none as citrin.

1 The expression profile of *aralar1* transcriptional variants studied in this work suggests that three  
2 isoforms (namely *aralar1-RA/RF* and *aralar1-RD*) are constitutively transcribed throughout the  
3 development and in adult tissues. Due to their overlapping sequences, it is not possible to  
4 discriminate the expression profile of these transcriptional isoforms, which are transcribed from the  
5 innermost promoter. The slight differences observed in their organization suggest that they might  
6 have a different stability (i.e. half-life of their mRNA molecules) due to the length of the 3' UTR  
7 (*aralar1-RD* and *aralar1-RA* isoforms). Similarly, the stability of Aralar1-PF protein, encoded by  
8 *aralar1-RF* transcript (identical to *aralar1-RA* transcript), could be affected by the presence of the  
9 additional 12 amino acids introduced upon the translational read-through process [86].

10 Conversely, *aralar1-RB*, *aralar1-RC* and *aralar1-RE* transcriptional isoforms have a more complex  
11 expression pattern, as described in the Results section. While *aralar1-RB* is undetectable by RT-  
12 PCR in adult males, it can be specifically detected in adult ovary, suggesting its role in oogenesis.  
13 We do not know whether *aralar1-RB* detected during the early embryo development is the result of  
14 a maternal contribution or of the active transcription in embryos, as instead appears evident for  
15 *aralar1-RC* and *aralar1-RE*, which are undetectable in female germline and are present in early  
16 embryo developmental stages. Furthermore, while *aralar1-RC* expression persists in the whole  
17 adult tissues with the exclusion of the germline tissues, *aralar1-RE* expression is confined in the  
18 early stages of embryo development and in somatic adult tissues. The expression of the more active  
19 *aralar1-RE* in the early embryogenesis might be related to the very active aspartate and glutamate  
20 metabolism occurring in this stage [91]. *Aralar1-RB* and *aralar1-RC*, together with the  
21 constitutively expressed isoforms, seem to be also important during metamorphosis. It is  
22 noteworthy that all the *aralar1* transcriptional isoforms contribute to the strong *aralar1* expression  
23 observed in adult fat bodies (mainly located in the abdomen), as can be inferred by the combination  
24 of our results (see Figure 4) and the modENCODE Tissue Expression Data. Fat bodies are  
25 important energy storages and utilization organs in *Drosophila*, as well as in other insects [92], and  
26 they play a fundamental role in the post-metamorphic energy metabolism and egg development.  
27 Taken together, these results suggest that an isoform-specific expression pattern becomes defined  
28 after the initial embryo development, when all the isoforms are transcribed, and its establishment  
29 appears to be important for certain developmental stages or in specific adult tissues.

30 It can be speculated that the observed transcriptional pattern could be related to the presence of two  
31 evolutionary conserved DNA motifs, located between the TSSs of *aralar1-RB* and *aralar1-  
32 RA/RF/RD* transcripts. Although we have not performed functional studies aimed to demonstrate  
33 their involvement in transcriptional regulation, it could be hypothesized that NRG elements might  
34 influence *aralar1* gene expression for two reasons. Firstly, its evolutionary conservation in 23

1 Drosophila species belonging to two distinct sub-genera indicates a constrained role. Indeed, intron  
2 sequences are less conserved, even in related species, and only functionally constrained motifs are  
3 maintained. The divergence between *D. melanogaster* and *D. grimshawi* is thought to have occurred  
4 50Mya (Russo et al. 2003), and the conservation of such putative *cis*-acting sequence suggests a  
5 functional role. The NRG element can also be detected in non-Drosophilidae insects  
6 (Supplementary Table 6), thus enforcing its putative functional role, although its position related to  
7 the expressed transcriptional isoforms in these organisms is not easy to be determined.

8  
9 Secondly, previous studies reported that NRG elements are conserved in a subset of Drosophila  
10 genes encoding mitochondrial proteins, while they have been lost in duplicated genes, which in turn  
11 have acquired testis-specific transcription patterns. Since *alarar1* gene lacks paralogues in *D.*  
12 *melanogaster* (and in all the analyzed Drosophila species), the presence of two NRG elements  
13 within it might have acquired a different role, such as the establishment of a regulated expression  
14 pattern of all, or at least some, of the transcriptional *alarar1* isoforms. In this view, the two NRG  
15 elements detected could act either cooperatively or independently, as positive or negative  
16 regulators. Whether or not the two NRG elements are functional to *alarar1* expression cannot be  
17 determined without the aid of mutant or transgenic strains carrying *alarar1* genes containing  
18 disrupted NRG elements, which necessarily calls for future analyses.

19  
20 In order to verify if this complex tissue- and developmental stage-specific transcriptional regulation  
21 is associated to the expression of functionally different isoforms, the transport properties of Aralar1-  
22 PA and Aralar1-PE, representing the two main encoded products of all *alarar1* transcripts, have  
23 been determined. The two recombinant proteins, once reconstituted into liposomes, catalyze a very  
24 efficient aspartate/glutamate electrogenic exchange reaction and are able to restore the yeast defect  
25 of the *AGC1* null gene (Figure 8), confirming their identity as the *D. melanogaster* mitochondrial  
26 AGC. Similarly to the human isoforms [4], fruit fly Aralar1 isoforms do not show any significant  
27 difference in their substrate affinity, moreover, as the human isoforms, the Km value for aspartate  
28 was significantly lower than that for glutamate. Interestingly, although Aralar1-PA and Aralar1-PE  
29 differ only in their N-terminal halves, i.e., region known to interact with calcium [23], they showed  
30 a significant different specific activity, being Aralar1-PE more active than Aralar1-PA. A similar  
31 situation had been previously found in *H. sapiens*, where citrin resulted more active than aralar [4].  
32 Although fruit fly and human AGC isoforms showed this overlapping behavior, it should be  
33 emphasized that the different specific activities found in the latter are mainly due to their different  
34 carrier domains [4], whereas all *D. melanogaster* AGC isoforms share the same carrier domain and  
35 differ in their N-terminal domains. In fact, the recombinant carrier domain reconstituted into  
36 liposomes, shows the same kinetic properties of Aralar1-PA (data not shown).

1  
2  
3  
4  
5  
6  
7  
8  
9  
10  
11  
12  
13  
14  
15  
16  
17  
18  
19  
20  
21  
22  
23  
24  
25  
26  
27  
28  
29  
30  
31  
32  
33  
34  
35  
36  
37  
38  
39  
40  
41  
42  
43  
44  
45  
46  
47  
48  
49  
50  
51  
52  
53  
54  
55  
56  
57  
58  
59  
60  
61  
62  
63  
64  
65

Interestingly, this N-terminal domain was also able to alter substrate specificity of the fruit fly AGC isoforms; since Aralar1-PE, similarly to human citrin [4], is able to exchange glutamate against cysteinesulfinatate at the same rate as that of aspartate, while Aralar1-PA, similarly to human aralar, shows a glutamate/cysteinesulfinatate exchange rate about one half lower than that of glutamate/aspartate. Furthermore, Aralar1-PE, differently from Aralar1-PA, significantly exchanges glutamate for L- $\alpha$ -aminoadipate and L-glutamine, suggesting a wider range of substrate specificity if compared to the latter.

A ClustalW alignment of *Drosophila* Aralar1 with human AGC isoforms has clarified that all proteins conserved the same structural organization including an N-terminal domain having 8 EF-hands with different functions (i.e. EF-hands 1-3 constitute a calcium-responsive unit, whereas EF-hands 4-8 are part of a static unit), a carrier domain and a C-terminal domain with unknown role (Figure 5) [23]. Furthermore, calcium (EF-hands 1-3) and substrate binding sites are almost completely conserved between man and *Drosophila*, with a single conservative variation present in the calcium-binding site, where a threonine was replaced by a serine in the fruit fly isoforms (Figure 5). The most variable regions in the fruit fly Aralar1 isoforms are located in the N-terminus and into the loop of the helix-loop-helix structure of EF-hand 8 (Figure 5, green shaded) [23], where Aralar1-PE has an extra highly positive charged amino acid sequence. In the light of this observation, it is evident that N-terminus variations could play a fundamental role on the functional differences found between Aralar1-PA and Aralar1-PE. Site-direct mutagenesis experiments conducted on this additional region in EF-hand 8 have showed that the substitution of the charged residues by alanine can significantly affect substrate specificity and increase initial transport rate, whereas the progressive removal of these extra amino acids reduce initial transport rate and change substrate specificity until making Aralar1-PE similar to Aralar1-PA. Furthermore, this data are in agreement with the role proposed for the human AGC isoforms, in which the EF-hands 1–3 form a calcium-responsive mobile unit, EF-hands 4–8 form a static unit while the N-terminus region, external to the first EF-hand motif, seems not to be involved in any crucial regulatory function [23]. Finally, we have demonstrated that both proteins are Ca<sup>2+</sup>-dependent, and similarly to citrin, Aralar1-PE shows a higher sensitivity to calcium being S<sub>0.5</sub> about 2 times lower than that of Aralar1-PA. Hence, biochemical characterization and calcium sensitivity have identified Aralar1-PA and Aralar1-PE as the human aralar and citrin counterparts, respectively (Figure 6 C-D).

The functional characterization of the fruit fly mitochondrial AGC transporter represents a crucial step toward a complete understanding of the metabolic events acting during early embryogenesis, and it might strengthen the use of *D. melanogaster* as a model for genetics and developmental biology. Nevertheless, further studies of gain and loss of function are required to better understand

1  
2  
3  
4  
5  
6  
7  
8  
9  
10  
11  
12  
13  
14  
15  
16  
17  
18  
19  
20  
21  
22  
23  
24  
25  
26  
27  
28  
29  
30  
31  
32  
33  
34  
35  
36  
37  
38  
39  
40  
41  
42  
43  
44  
45  
46  
47  
48  
49  
50  
51  
52  
53  
54  
55  
56  
57  
58  
59  
60  
61  
62  
63  
64  
65

how the complex transcriptional and expression patterns of Aralar1 regulates specific metabolic pathways in the different developmental stages of the fruit fly.

### Acknowledgements

This work was supported by Associazione Italiana per la Ricerca sul Cancro (FG grant n. 15404/2014); by the Italian Ministero dell'Istruzione, dell'Università e della Ricerca, MIUR, 2017PAB8EM\_003; Drosophila clones were provided by Drosophila Genomics Resource Center NIH grant 2P40OD010949. The authors acknowledge “Sistema Integrato di Laboratori per L’Ambiente — SILA for providing lab tools.

### References

- [1] R. Curcio, P. Lunetti, V. Zara, A. Ferramosca, F. Marra, G. Fiermonte, A.R. Cappello, F. De Leonardis, L. Capobianco, V. Dolce, Drosophila melanogaster Mitochondrial Carriers: Similarities and Differences with the Human Carriers, *Int J Mol Sci* 21(17) (2020).
- [2] F. Palmieri, The mitochondrial transporter family SLC25: identification, properties and physiopathology, *Molecular aspects of medicine* 34(2-3) (2013) 465-84.
- [3] F. Palmieri, M. Monne, Discoveries, metabolic roles and diseases of mitochondrial carriers: A review, *Biochimica et biophysica acta* 1863(10) (2016) 2362-78.
- [4] L. Palmieri, B. Pardo, F.M. Lasorsa, A. del Arco, K. Kobayashi, M. Iijima, M.J. Runswick, J.E. Walker, T. Saheki, J. Satrustegui, F. Palmieri, Citrin and aralar1 are Ca(2+)-stimulated aspartate/glutamate transporters in mitochondria, *The EMBO journal* 20(18) (2001) 5060-9.
- [5] F. Palmieri, The mitochondrial transporter family (SLC25): physiological and pathological implications, *Pflugers Arch* 447(5) (2004) 689-709.
- [6] B. Pardo, L. Contreras, A. Serrano, M. Ramos, K. Kobayashi, M. Iijima, T. Saheki, J. Satrustegui, Essential role of aralar in the transduction of small Ca<sup>2+</sup> signals to neuronal mitochondria, *The Journal of biological chemistry* 281(2) (2006) 1039-47.
- [7] F.M. Lasorsa, P. Pinton, L. Palmieri, G. Fiermonte, R. Rizzuto, F. Palmieri, Recombinant expression of the Ca(2+)-sensitive aspartate/glutamate carrier increases mitochondrial ATP production in agonist-stimulated Chinese hamster ovary cells, *The Journal of biological chemistry* 278(40) (2003) 38686-92.
- [8] F.N. Gellerich, Z. Gizatullina, O. Arandarcikaite, D. Jerzembek, S. Vielhaber, E. Seppet, F. Striggow, Extramitochondrial Ca<sup>2+</sup> in the nanomolar range regulates glutamate-dependent oxidative phosphorylation on demand, *PloS one* 4(12) (2009) e8181.
- [9] I. Llorente-Folch, C.B. Rueda, I. Amigo, A. del Arco, T. Saheki, B. Pardo, J. Satrustegui, Calcium-regulation of mitochondrial respiration maintains ATP homeostasis and requires ARALAR/AGC1-malate aspartate shuttle in intact cortical neurons, *The Journal of neuroscience : the official journal of the Society for Neuroscience* 33(35) (2013) 13957-71, 13971a.
- [10] B. Rubi, A. del Arco, C. Bartley, J. Satrustegui, P. Maechler, The malate-aspartate NADH shuttle member Aralar1 determines glucose metabolic fate, mitochondrial activity, and insulin secretion in beta cells, *The Journal of biological chemistry* 279(53) (2004) 55659-66.
- [11] M. Lane, D.K. Gardner, Mitochondrial malate-aspartate shuttle regulates mouse embryo nutrient consumption, *The Journal of biological chemistry* 280(18) (2005) 18361-7.
- [12] N. Moscatelli, P. Lunetti, C. Braccia, A. Armirotti, F. Pisanello, M. De Vittorio, V. Zara, A. Ferramosca, Comparative Proteomic Analysis of Proteins Involved in Bioenergetics Pathways Associated with Human Sperm Motility, *Int J Mol Sci* 20(12) (2019).
- [13] M. Ramos, B. Pardo, I. Llorente-Folch, T. Saheki, A. Del Arco, J. Satrustegui, Deficiency of the mitochondrial transporter of aspartate/glutamate aralar/AGC1 causes hypomyelination and neuronal defects unrelated to myelin deficits in mouse brain, *Journal of neuroscience research* 89(12) (2011) 2008-17.

- 1 [14] E. Profilo, L.E. Pena-Altamira, M. Corricelli, A. Castegna, A. Danese, G. Agrimi, S. Petralla,  
2 G. Giannuzzi, V. Porcelli, L. Sbano, C. Viscomi, F. Massenzio, E.M. Palmieri, C. Giorgi, G.  
3 Fiermonte, M. Virgili, L. Palmieri, M. Zeviani, P. Pinton, B. Monti, F. Palmieri, F.M. Lasorsa,  
4 Down-regulation of the mitochondrial aspartate-glutamate carrier isoform 1 AGC1 inhibits  
5 proliferation and N-acetylaspartate synthesis in Neuro2A cells, *Biochimica et biophysica acta*  
6 1863(6) (2017) 1422-1435.
- 7 [15] R. Wibom, F.M. Lasorsa, V. Tohonen, M. Barbaro, F.H. Sterky, T. Kucinski, K. Naess, M.  
8 Jonsson, C.L. Pierri, F. Palmieri, A. Wedell, AGC1 deficiency associated with global cerebral  
9 hypomyelination, *The New England journal of medicine* 361(5) (2009) 489-95.
- 10 [16] M.A. Jalil, L. Begum, L. Contreras, B. Pardo, M. Iijima, M.X. Li, M. Ramos, P. Marmol, M.  
11 Horiuchi, K. Shimotsu, S. Nakagawa, A. Okubo, M. Sameshima, Y. Isashiki, A. Del Arco, K.  
12 Kobayashi, J. Satrustegui, T. Saheki, Reduced N-acetylaspartate levels in mice lacking aralar, a  
13 brain- and muscle-type mitochondrial aspartate-glutamate carrier, *The Journal of biological*  
14 *chemistry* 280(35) (2005) 31333-9.
- 15 [17] B. Pardo, L. Contreras, J. Satrustegui, De novo Synthesis of Glial Glutamate and Glutamine in  
16 Young Mice Requires Aspartate Provided by the Neuronal Mitochondrial Aspartate-Glutamate  
17 Carrier Aralar/AGC1, *Frontiers in endocrinology* 4 (2013) 149.
- 18 [18] J.M. Thornburg, K.K. Nelson, B.F. Clem, A.N. Lane, S. Arumugam, A. Simmons, J.W. Eaton,  
19 S. Telang, J. Chesney, Targeting aspartate aminotransferase in breast cancer, *Breast cancer research*  
20 : BCR 10(5) (2008) R84.
- 21 [19] C. Wang, H. Chen, M. Zhang, J. Zhang, X. Wei, W. Ying, Malate-aspartate shuttle inhibitor  
22 aminooxyacetic acid leads to decreased intracellular ATP levels and altered cell cycle of C6 glioma  
23 cells by inhibiting glycolysis, *Cancer letters* 378(1) (2016) 1-7.
- 24 [20] F. Palmieri, I. Stipani, V. Iacobazzi, The transport of L-cysteinesulfinatate in rat liver  
25 mitochondria, *Biochimica et biophysica acta* 555(3) (1979) 531-46.
- 26 [21] T. Ubuka, A. Okada, H. Nakamura, Production of hypotaurine from L-cysteinesulfinatate by rat  
27 liver mitochondria, *Amino acids* 35(1) (2008) 53-8.
- 28 [22] K. Kobayashi, D.S. Sinasac, M. Iijima, A.P. Boright, L. Begum, J.R. Lee, T. Yasuda, S. Ikeda,  
29 R. Hirano, H. Terazono, M.A. Crackower, I. Kondo, L.C. Tsui, S.W. Scherer, T. Saheki, The gene  
30 mutated in adult-onset type II citrullinaemia encodes a putative mitochondrial carrier protein, *Nat*  
31 *Genet* 22(2) (1999) 159-63.
- 32 [23] C. Thangaratnarajah, J.J. Ruprecht, E.R. Kunji, Calcium-induced conformational changes of  
33 the regulatory domain of human mitochondrial aspartate/glutamate carriers, *Nature communications*  
34 5 (2014) 5491.
- 35 [24] A. del Arco, J. Morcillo, J.R. Martinez-Morales, C. Galian, V. Martos, P. Bovolenta, J.  
36 Satrustegui, Expression of the aspartate/glutamate mitochondrial carriers aralar1 and citrin during  
37 development and in adult rat tissues, *European journal of biochemistry* 269(13) (2002) 3313-20.
- 38 [25] J. Liu, A. Yang, Q. Zhang, G. Yang, W. Yang, H. Lei, J. Quan, F. Qu, M. Wang, Z. Zhang, K.  
39 Yu, Association between genetic variants in SLC25A12 and risk of autism spectrum disorders: An  
40 integrated meta-analysis, *American journal of medical genetics. Part B, Neuropsychiatric genetics* :  
41 the official publication of the International Society of Psychiatric Genetics 168B(4) (2015) 236-46.
- 42 [26] J. Du, A. Rountree, W.M. Cleghorn, L. Contreras, K.J. Lindsay, M. Sadilek, H. Gu, D.  
43 Djukovic, D. Raftery, J. Satrustegui, M. Kanow, L. Chan, S.H. Tsang, I.R. Sweet, J.B. Hurley,  
44 Phototransduction Influences Metabolic Flux and Nucleotide Metabolism in Mouse Retina, *The*  
45 *Journal of biological chemistry* 291(9) (2016) 4698-710.
- 46 [27] L. Contreras, L. Ramirez, J. Du, J.B. Hurley, J. Satrustegui, P. de la Villa, Deficient glucose  
47 and glutamine metabolism in Aralar/AGC1/Slc25a12 knockout mice contributes to altered visual  
48 function, *Mol Vis* 22 (2016) 1198-1212.
- 49 [28] I. Llorente-Folch, C.B. Rueda, I. Perez-Liebana, J. Satrustegui, B. Pardo, L-Lactate-Mediated  
50 Neuroprotection against Glutamate-Induced Excitotoxicity Requires ARALAR/AGC1, *The Journal*  
51 *of neuroscience* : the official journal of the Society for Neuroscience 36(16) (2016) 4443-56.
- 52  
53  
54  
55  
56  
57  
58  
59  
60  
61  
62  
63  
64  
65

- [29] C.B. Rueda, I. Llorente-Folch, J. Traba, I. Amigo, P. Gonzalez-Sanchez, L. Contreras, I. Juaristi, P. Martinez-Valero, B. Pardo, A. Del Arco, J. Satrustegui, Glutamate excitotoxicity and Ca<sup>2+</sup>-regulation of respiration: Role of the Ca<sup>2+</sup> activated mitochondrial transporters (CaMCs), *Biochimica et biophysica acta* 1857(8) (2016) 1158-1166.
- [30] L. Palmieri, V. Papaleo, V. Porcelli, P. Scarcia, L. Gaita, R. Sacco, J. Hager, F. Rousseau, P. Curatolo, B. Manzi, R. Militerni, C. Bravaccio, S. Trillo, C. Schneider, R. Melmed, M. Elia, C. Lenti, M. Saccani, T. Pascucci, S. Puglisi-Allegra, K.L. Reichelt, A.M. Persico, Altered calcium homeostasis in autism-spectrum disorders: evidence from biochemical and genetic studies of the mitochondrial aspartate/glutamate carrier AGC1, *Molecular psychiatry* 15(1) (2010) 38-52.
- [31] N. Ramoz, J.G. Reichert, C.J. Smith, J.M. Silverman, I.N. Bespalova, K.L. Davis, J.D. Buxbaum, Linkage and association of the mitochondrial aspartate/glutamate carrier SLC25A12 gene with autism, *The American journal of psychiatry* 161(4) (2004) 662-9.
- [32] J.A. Turunen, K. Rehnstrom, H. Kilpinen, M. Kuokkanen, E. Kempas, T. Ylisaukko-Oja, Mitochondrial aspartate/glutamate carrier SLC25A12 gene is associated with autism, *Autism research : official journal of the International Society for Autism Research* 1(3) (2008) 189-92.
- [33] M.J. Falk, D. Li, X. Gai, E. McCormick, E. Place, F.M. Lasorsa, F.G. Otieno, C. Hou, C.E. Kim, N. Abdel-Magid, L. Vazquez, F.D. Mentch, R. Chiavacci, J. Liang, X. Liu, H. Jiang, G. Giannuzzi, E.D. Marsh, Y. Guo, L. Tian, F. Palmieri, H. Hakonarson, Erratum to: AGC1 Deficiency Causes Infantile Epilepsy, Abnormal Myelination, and Reduced N-Acetylaspartate, *JIMD reports* 14 (2014) 119.
- [34] T. Saheki, K. Kobayashi, M. Iijima, M. Horiuchi, L. Begum, M.A. Jalil, M.X. Li, Y.B. Lu, M. Ushikai, A. Tabata, M. Moriyama, K.J. Hsiao, Y. Yang, Adult-onset type II citrullinemia and idiopathic neonatal hepatitis caused by citrin deficiency: involvement of the aspartate glutamate carrier for urea synthesis and maintenance of the urea cycle, *Molecular genetics and metabolism* 81 Suppl 1 (2004) S20-6.
- [35] Z.H. Zhang, Z.G. Yang, F.P. Chen, A. Kikuchi, Z.H. Liu, L.Z. Kuang, W.M. Li, Y.Z. Song, S. Kure, T. Saheki, Screening for five prevalent mutations of SLC25A13 gene in Guangdong, China: a molecular epidemiologic survey of citrin deficiency, *The Tohoku journal of experimental medicine* 233(4) (2014) 275-81.
- [36] Y.Z. Song, Z.H. Zhang, W.X. Lin, X.J. Zhao, M. Deng, Y.L. Ma, L. Guo, F.P. Chen, X.L. Long, X.L. He, Y. Sunada, S. Soneda, A. Nakatomi, S. Dateki, L.H. Ngu, K. Kobayashi, T. Saheki, SLC25A13 gene analysis in citrin deficiency: sixteen novel mutations in East Asian patients, and the mutation distribution in a large pediatric cohort in China, *PloS one* 8(9) (2013) e74544.
- [37] Y.Z. Song, M. Deng, F.P. Chen, F. Wen, L. Guo, S.L. Cao, J. Gong, H. Xu, G.Y. Jiang, L. Zhong, K. Kobayashi, T. Saheki, Z.N. Wang, Genotypic and phenotypic features of citrin deficiency: five-year experience in a Chinese pediatric center, *International journal of molecular medicine* 28(1) (2011) 33-40.
- [38] G. Fiermonte, G. Parisi, D. Martinelli, F. De Leonardis, G. Torre, C.L. Pierri, A. Saccari, F.M. Lasorsa, A. Voza, F. Palmieri, C. Dionisi-Vici, A new Caucasian case of neonatal intrahepatic cholestasis caused by citrin deficiency (NICCD): a clinical, molecular, and functional study, *Molecular genetics and metabolism* 104(4) (2011) 501-6.
- [39] G. Fiermonte, D. Soon, A. Chaudhuri, E. Paradies, P.J. Lee, S. Krywawych, F. Palmieri, R.H. Lachmann, An adult with type 2 citrullinemia presenting in Europe, *The New England journal of medicine* 358(13) (2008) 1408-9.
- [40] T. Saheki, Y.Z. Song, Citrin Deficiency, in: M.P. Adam, H.H. Ardinger, R.A. Pagon, S.E. Wallace, L.J.H. Bean, K. Stephens, A. Amemiya (Eds.), *GeneReviews((R))*, Seattle (WA), 1993.
- [41] A. Del Arco, M. Agudo, J. Satrustegui, Characterization of a second member of the subfamily of calcium-binding mitochondrial carriers expressed in human non-excitabile tissues, *The Biochemical journal* 345 Pt 3 (2000) 725-32.

- 1 [42] I. Campos, J.A. Geiger, A.C. Santos, V. Carlos, A. Jacinto, Genetic screen in *Drosophila*  
2 *melanogaster* uncovers a novel set of genes required for embryonic epithelial repair, *Genetics*  
3 184(1) (2010) 129-40.
- 4 [43] C.L. Dilda, T.F. Mackay, The genetic architecture of *Drosophila* sensory bristle number,  
5 *Genetics* 162(4) (2002) 1655-74.
- 6 [44] H. Okada, H.A. Ebhardt, S.C. Vonesch, R. Aebersold, E. Hafen, Proteome-wide association  
7 studies identify biochemical modules associated with a wing-size phenotype in *Drosophila*  
8 *melanogaster*, *Nature communications* 7 (2016) 12649.
- 9 [45] M.D. Brand, J.L. Pakay, A. Ocloo, J. Kokoszka, D.C. Wallace, P.S. Brookes, E.J. Cornwall,  
10 The basal proton conductance of mitochondria depends on adenine nucleotide translocase content,  
11 *The Biochemical journal* 392(Pt 2) (2005) 353-62.
- 12 [46] I.M. Sokolova, E.P. Sokolov, Evolution of mitochondrial uncoupling proteins: novel  
13 invertebrate UCP homologues suggest early evolutionary divergence of the UCP family, *FEBS*  
14 *letters* 579(2) (2005) 313-7.
- 15 [47] M. Ulgherait, A. Chen, S.F. McAllister, H.X. Kim, R. Delventhal, C.R. Wayne, C.J. Garcia, Y.  
16 Recinos, M. Oliva, J.C. Canman, M. Picard, E. Owusu-Ansah, M. Shirasu-Hiza, Circadian  
17 regulation of mitochondrial uncoupling and lifespan, *Nature communications* 11(1) (2020) 1927.
- 18 [48] D. Iacopetta, M. Madeo, G. Tasco, C. Carrisi, R. Curcio, E. Martello, R. Casadio, L.  
19 Capobianco, V. Dolce, A novel subfamily of mitochondrial dicarboxylate carriers from *Drosophila*  
20 *melanogaster*: biochemical and computational studies, *Biochimica et biophysica acta* 1807(3)  
21 (2011) 251-61.
- 22 [49] D. Iacopetta, C. Carrisi, G. De Filippis, V.M. Calcagnile, A.R. Cappello, A. Chimento, R.  
23 Curcio, A. Santoro, A. Voza, V. Dolce, F. Palmieri, L. Capobianco, The biochemical properties of  
24 the mitochondrial thiamine pyrophosphate carrier from *Drosophila melanogaster*, *FEBS J* 277(5)  
25 (2010) 1172-81.
- 26 [50] C. Carrisi, D. Antonucci, P. Lunetti, D. Migoni, C.R. Girelli, V. Dolce, F.P. Fanizzi, M.  
27 Benedetti, L. Capobianco, Transport of platinum bonded nucleotides into proteoliposomes,  
28 mediated by *Drosophila melanogaster* thiamine pyrophosphate carrier protein (DmTpc1), *J Inorg*  
29 *Biochem* 130 (2014) 28-31.
- 30 [51] P. Lunetti, A.R. Cappello, R.M. Marsano, C.L. Pierri, C. Carrisi, E. Martello, C. Caggese, V.  
31 Dolce, L. Capobianco, Mitochondrial glutamate carriers from *Drosophila melanogaster*:  
32 biochemical, evolutionary and modeling studies, *Biochimica et biophysica acta* 1827(10) (2013)  
33 1245-55.
- 34 [52] A. Louvi, S.G. Tsilou, A cDNA clone encoding the ADP/ATP translocase of *Drosophila*  
35 *melanogaster* shows a high degree of similarity with the mammalian ADP/ATP translocases, *J Mol*  
36 *Evol* 35(1) (1992) 44-50.
- 37 [53] A. Voza, F. De Leonadis, E. Paradies, A. De Grassi, C.L. Pierri, G. Parisi, C.M. Marobbio,  
38 F.M. Lasorsa, L. Muto, L. Capobianco, V. Dolce, S. Raho, G. Fiermonte, Biochemical  
39 characterization of a new mitochondrial transporter of dephosphocoenzyme A in *Drosophila*  
40 *melanogaster*, *Biochimica et biophysica acta* 1858(2) (2017) 137-146.
- 41 [54] J.P. Venables, J. Tazi, F. Juge, Regulated functional alternative splicing in *Drosophila*, *Nucleic*  
42 *acids research* 40(1) (2012) 1-10.
- 43 [55] V. Zara, V. Dolce, L. Capobianco, A. Ferramosca, P. Papatheodorou, J. Rassow, F. Palmieri,  
44 Biogenesis of eel liver citrate carrier (CIC): negative charges can substitute for positive charges in  
45 the presequence, *Journal of molecular biology* 365(4) (2007) 958-67.
- 46 [56] G. Moreno-Hagelsieb, K. Latimer, Choosing BLAST options for better detection of orthologs  
47 as reciprocal best hits, *Bioinformatics* 24(3) (2008) 319-24.
- 48 [57] C. Burge, S. Karlin, Prediction of complete gene structures in human genomic DNA, *Journal of*  
49 *molecular biology* 268(1) (1997) 78-94.
- 50 [58] R. Carrozzo, A. Torraco, G. Fiermonte, D. Martinelli, M. Di Nottia, T. Rizza, A. Voza, D.  
51 Verrigni, D. Diodato, G. Parisi, A. Maiorana, C. Rizzo, C.L. Pierri, S. Zucano, F. Piemonte, E.



1 Bertini, C. Dionisi-Vici, Riboflavin responsive mitochondrial myopathy is a new phenotype of  
2 dihydrolipoamide dehydrogenase deficiency. The chaperon-like effect of vitamin B2,  
3 *Mitochondrion* 18 (2014) 49-57.

4 [59] A.R. Cappello, R. Curcio, R. Lappano, M. Maggiolini, V. Dolce, The Physiopathological Role  
5 of the Exchangers Belonging to the SLC37 Family, *Front Chem* 6 (2018) 122.

6 [60] D. Porcelli, P. Barsanti, G. Pesole, C. Caggese, The nuclear OXPHOS genes in insecta: a  
7 common evolutionary origin, a common cis-regulatory motif, a common destiny for gene  
8 duplicates, *BMC Evol Biol* 7 (2007) 215.

9 [61] S. Avino, P. De Marco, F. Cirillo, M.F. Santolla, E.M. De Francesco, M.G. Perri, D.  
10 Rigracciolo, V. Dolce, A. Belfiore, M. Maggiolini, R. Lappano, A. Vivacqua, Stimulatory actions  
11 of IGF-I are mediated by IGF-IR cross-talk with GPER and DDR1 in mesothelioma and lung  
12 cancer cells, *Oncotarget* 7(33) (2016) 52710-52728.

13 [62] V. Bartella, E.M. De Francesco, M.G. Perri, R. Curcio, V. Dolce, M. Maggiolini, A. Vivacqua,  
14 The G protein estrogen receptor (GPER) is regulated by endothelin-1 mediated signaling in cancer  
15 cells, *Cellular signalling* 28(2) (2016) 61-71.

16 [63] A. Santoro, A.R. Cappello, M. Madeo, E. Martello, D. Iacopetta, V. Dolce, Interaction of  
17 fosfomycin with the glycerol 3-phosphate transporter of *Escherichia coli*, *Biochimica et biophysica*  
18 *acta* 1810(12) (2011) 1323-9.

19 [64] S.N. Ho, H.D. Hunt, R.M. Horton, J.K. Pullen, L.R. Pease, Site-directed mutagenesis by  
20 overlap extension using the polymerase chain reaction, *Gene* 77(1) (1989) 51-9.

21 [65] D. Bonofiglio, A. Santoro, E. Martello, D. Vizza, D. Rovito, A.R. Cappello, I. Barone, C.  
22 Giordano, S. Panza, S. Catalano, V. Iacobazzi, V. Dolce, S. Ando, Mechanisms of divergent effects  
23 of activated peroxisome proliferator-activated receptor-gamma on mitochondrial citrate carrier  
24 expression in 3T3-L1 fibroblasts and mature adipocytes, *Biochimica et biophysica acta* 1831(6)  
25 (2013) 1027-36.

26 [66] A. Napoli, D. Aiello, G. Aiello, M.S. Cappello, L. Di Donna, F. Mazzotti, S. Materazzi, M.  
27 Fiorillo, G. Sindona, Mass spectrometry-based proteomic approach in *Oenococcus oeni* enological  
28 starter, *Journal of proteome research* 13(6) (2014) 2856-66.

29 [67] R. Curcio, D. Aiello, A. Voza, L. Muto, E. Martello, A.R. Cappello, L. Capobianco, G.  
30 Fiermonte, C. Siciliano, A. Napoli, V. Dolce, Cloning, Purification, and Characterization of the  
31 Catalytic C-Terminal Domain of the Human 3-Hydroxy-3-methyl glutaryl-CoA Reductase: An  
32 Effective, Fast, and Easy Method for Testing Hypocholesterolemic Compounds, *Mol Biotechnol*  
33 62(2) (2020) 119-131.

34 [68] V. Kurauskas, A. Hessel, P. Ma, P. Lunetti, K. Weinhaupl, L. Imbert, B. Brutscher, M.S. King,  
35 R. Sounier, V. Dolce, E.R.S. Kunji, L. Capobianco, C. Chipot, F. Dehez, B. Bersch, P. Schanda,  
36 How Detergent Impacts Membrane Proteins: Atomic-Level Views of Mitochondrial Carriers in  
37 Dodecylphosphocholine, *The journal of physical chemistry letters* 9(5) (2018) 933-938.

38 [69] R. Curcio, L. Muto, C.L. Pierri, A. Montalto, G. Lauria, A. Onofrio, M. Fiorillo, G. Fiermonte,  
39 P. Lunetti, A. Voza, L. Capobianco, A.R. Cappello, V. Dolce, New insights about the structural  
40 rearrangements required for substrate translocation in the bovine mitochondrial oxoglutarate carrier,  
41 *Biochimica et biophysica acta* 1864(11) (2016) 1473-80.

42 [70] Y. Li, A.R. Cappello, L. Muto, E. Martello, M. Madeo, R. Curcio, P. Lunetti, S. Raho, F.  
43 Zaffino, L. Frattaruolo, R. Lappano, R. Malivindi, M. Maggiolini, D. Aiello, C. Piazzolla, L.  
44 Capobianco, G. Fiermonte, V. Dolce, Functional characterization of the partially purified Sac1p  
45 independent adenine nucleotide transport system (ANTS) from yeast endoplasmic reticulum, *J*  
46 *Biochem* 164(4) (2018) 313-322.

47 [71] F. Palmieri, M. Klingenberg, Direct methods for measuring metabolite transport and  
48 distribution in mitochondria, *Methods Enzymol* 56 (1979) 279-301.

49 [72] L. Contreras, P. Gomez-Puertas, M. Iijima, K. Kobayashi, T. Saheki, J. Satrustegui, Ca<sup>2+</sup>  
50 Activation kinetics of the two aspartate-glutamate mitochondrial carriers, aralar and citrin: role in  
51  
52  
53  
54  
55  
56  
57  
58  
59  
60  
61  
62  
63  
64  
65

the heart malate-aspartate NADH shuttle, *The Journal of biological chemistry* 282(10) (2007) 7098-106.

[73] S. Raho, L. Capobianco, R. Malivindi, A. Voza, C. Piazzolla, F. De Leonadis, R. Gorgoglione, P. Scarcia, F. Pezzuto, G. Agrimi, S.N. Barile, I. Pisano, S.J. Reshkin, M.R. Greco, R.A. Cardone, V. Rago, Y. Li, C.M.T. Marobbio, W. Sommergruber, C.L. Riley, F.M. Lasorsa, E. Mills, M.C. Vegliante, G.E. De Benedetto, D. Fratantonio, L. Palmieri, V. Dolce, G. Fiermonte, KRAS-regulated glutamine metabolism requires UCP2-mediated aspartate transport to support pancreatic cancer growth, *Nat Metab* 2(12) (2020) 1373-1381.

[74] H. Ito, Y. Fukuda, K. Murata, A. Kimura, Transformation of intact yeast cells treated with alkali cations, *J Bacteriol* 153(1) (1983) 163-8.

[75] L. Frattaruolo, M. Fiorillo, M. Brindisi, R. Curcio, V. Dolce, R. Lacret, A.W. Truman, F. Sotgia, M.P. Lisanti, A.R. Cappello, Thioalbamide, A Thioamidated Peptide from *Amycolatopsis alba*, Affects Tumor Growth and Stemness by Inducing Metabolic Dysfunction and Oxidative Stress, *Cells* 8(11) (2019).

[76] M. Madeo, C. Carrisi, D. Iacopetta, L. Capobianco, A.R. Cappello, C. Bucci, F. Palmieri, G. Mazzeo, A. Montalto, V. Dolce, Abundant expression and purification of biologically active mitochondrial citrate carrier in baculovirus-infected insect cells, *Journal of bioenergetics and biomembranes* 41(3) (2009) 289-97.

[77] J. Dandurand, A. Ostuni, M.F. Armentano, M.A. Crudele, V. Dolce, F. Marra, V. Samouillan, F. Bisaccia, Calorimetry and FTIR reveal the ability of URG7 protein to modify the aggregation state of both cell lysate and amylogenic  $\alpha$ -synuclein, *AIMS Biophysics* 7(3) (2020) 189-203.

[78] O.I. Parisi, M. Fiorillo, L. Scrivano, M.S. Sinicropi, V. Dolce, D. Iacopetta, F. Puoci, A.R. Cappello, Sericin/Poly(ethylcyanoacrylate) Nanospheres by Interfacial Polymerization for Enhanced Bioefficacy of Fenofibrate: In Vitro and In Vivo Studies, *Biomacromolecules* 16(10) (2015) 3126-33.

[79] M. Fiorillo, M. Peiris-Pages, R. Sanchez-Alvarez, L. Bartella, L. Di Donna, V. Dolce, G. Sindona, F. Sotgia, A.R. Cappello, M.P. Lisanti, Bergamot natural products eradicate cancer stem cells (CSCs) by targeting mevalonate, Rho-GDI-signalling and mitochondrial metabolism, *Biochimica et biophysica acta* (2018).

[80] C. Carrisi, A. Romano, P. Lunetti, D. Antonucci, T. Verri, G.E. De Benedetto, V. Dolce, F.P. Fanizzi, M. Benedetti, L. Capobianco, Platinated Nucleotides are Substrates for the Human Mitochondrial Deoxynucleotide Carrier (DNC) and DNA Polymerase  $\gamma$ : Relevance for the Development of New Platinum-Based Drugs., *ChemistrySelect* 1(15) (2016) 4633-7

[81] V. Dolce, A.R. Cappello, L. Capobianco, Mitochondrial tricarboxylate and dicarboxylate-Tricarboxylate carriers: from animals to plants, *IUBMB Life* 66(7) (2014) 462-71.

[82] M. Santoro, C. Guido, F. De Amicis, D. Sisci, E. Cione, V. Dolce, A. Dona, M.L. Panno, S. Aquila, Bergapten induces metabolic reprogramming in breast cancer cells, *Oncol Rep* 35(1) (2016) 568-76.

[83] M. Bonesi, M. Brindisi, B. Armentano, R. Curcio, V. Sicari, M.R. Loizzo, M.S. Cappello, G. Bedini, L. Peruzzi, R. Tundis, Exploring the anti-proliferative, pro-apoptotic, and antioxidant properties of *Santolina corsica* Jord. & Fourr. (Asteraceae), *Biomed Pharmacother* 107 (2018) 967-978.

[84] D. Vergara, M. Bianco, R. Pagano, P. Priore, P. Lunetti, F. Guerra, S. Bettini, S. Carallo, A. Zizzari, E. Pitotti, L. Giotta, L. Capobianco, C. Bucci, L. Valli, M. Maffia, V. Arima, A. Gaballo, An SPR based immunoassay for the sensitive detection of the soluble epithelial marker E-cadherin, *Nanomedicine* 14(7) (2018) 1963-1971.

[85] A. del Arco, J. Satrustegui, Molecular cloning of Aralar, a new member of the mitochondrial carrier superfamily that binds calcium and is present in human muscle and brain, *The Journal of biological chemistry* 273(36) (1998) 23327-34.

- 1 [86] I. Jungreis, C.S. Chan, R.M. Waterhouse, G. Fields, M.F. Lin, M. Kellis, Evolutionary  
2 Dynamics of Abundant Stop Codon Readthrough, *Molecular biology and evolution* 33(12) (2016)  
3 3108-3132.
- 4 [87] M. Sardiello, G. Tripoli, A. Romito, C. Minervini, L. Viggiano, C. Caggese, G. Pesole, Energy  
5 biogenesis: one key for coordinating two genomes, *Trends Genet* 21(1) (2005) 12-6.
- 6 [88] P. Rehm, J. Borner, K. Meusemann, B.M. von Reumont, S. Simon, H. Hadrys, B. Misof, T.  
7 Burmester, Dating the arthropod tree based on large-scale transcriptome data, *Molecular*  
8 *phylogenetics and evolution* 61(3) (2011) 880-7.
- 9 [89] J.B. Brown, N. Boley, R. Eisman, G.E. May, M.H. Stoiber, M.O. Duff, B.W. Booth, J. Wen, S.  
10 Park, A.M. Suzuki, K.H. Wan, C. Yu, D. Zhang, J.W. Carlson, L. Cherbas, B.D. Eads, D. Miller, K.  
11 Mockaitis, J. Roberts, C.A. Davis, E. Frise, A.S. Hammonds, S. Olson, S. Shenker, D. Sturgill,  
12 A.A. Samsonova, R. Weiszmann, G. Robinson, J. Hernandez, J. Andrews, P.J. Bickel, P. Carninci,  
13 P. Cherbas, T.R. Gingeras, R.A. Hoskins, T.C. Kaufman, E.C. Lai, B. Oliver, N. Perrimon, B.R.  
14 Graveley, S.E. Celniker, Diversity and dynamics of the *Drosophila* transcriptome, *Nature* 512(7515)  
15 (2014) 393-9.
- 16 [90] S. Cavero, A. Voza, A. del Arco, L. Palmieri, A. Villa, E. Blanco, M.J. Runswick, J.E.  
17 Walker, S. Cerdan, F. Palmieri, J. Satrustegui, Identification and metabolic role of the  
18 mitochondrial aspartate-glutamate transporter in *Saccharomyces cerevisiae*, *Molecular*  
19 *microbiology* 50(4) (2003) 1257-69.
- 20 [91] P.N. An, M. Yamaguchi, T. Bamba, E. Fukusaki, Metabolome analysis of *Drosophila*  
21 *melanogaster* during embryogenesis, *PloS one* 9(8) (2014) e99519.
- 22 [92] D.K. Hoshizaki, Fat-cell development, In *Complete Molecular Insect Science* 2 (2005) 315-  
23 345.
- 24  
25  
26  
27  
28  
29  
30  
31  
32  
33  
34  
35  
36  
37  
38  
39  
40  
41  
42  
43  
44  
45  
46  
47  
48  
49  
50  
51  
52  
53  
54  
55  
56  
57  
58  
59  
60  
61  
62  
63  
64  
65



1  
2  
3  
4  
5  
6  
7  
8  
9  
10  
11  
12  
13  
14  
15  
16  
17  
18  
19  
20  
21  
22  
23  
24  
25  
26  
27  
28  
29  
30  
31  
32  
33  
34  
35  
36  
37  
38  
39  
40  
41  
42  
43  
44  
45  
46  
47  
48  
49  
50  
51  
52  
53  
54  
55  
56  
57  
58  
59  
60  
61  
62  
63  
64  
65

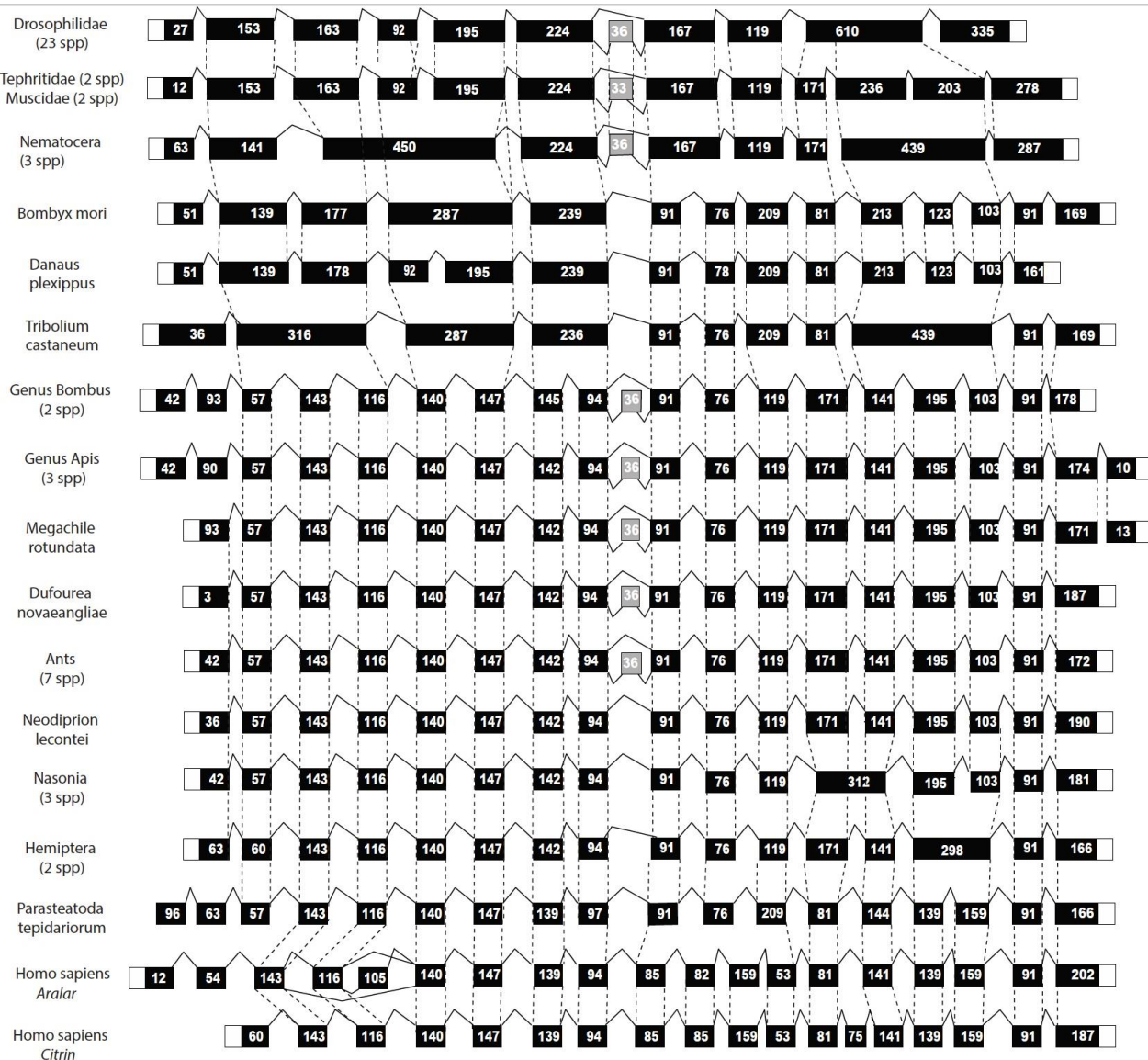


**Figure 2. Eukaryotic AGC-encoding genes share an ancient intron-rich ancestor.** The exon/intron structure of orthologous AGC-encoding genes of representative eukaryotic species is compared considering intron position, exon phase and length. Dashed lines indicate conservation of intron position. Translated AGC1-encoding regions are indicated in black, UTRs as white boxes. Internal *alarar1-RE* specific exons are indicated as gray boxes. Boxes are not in scale.

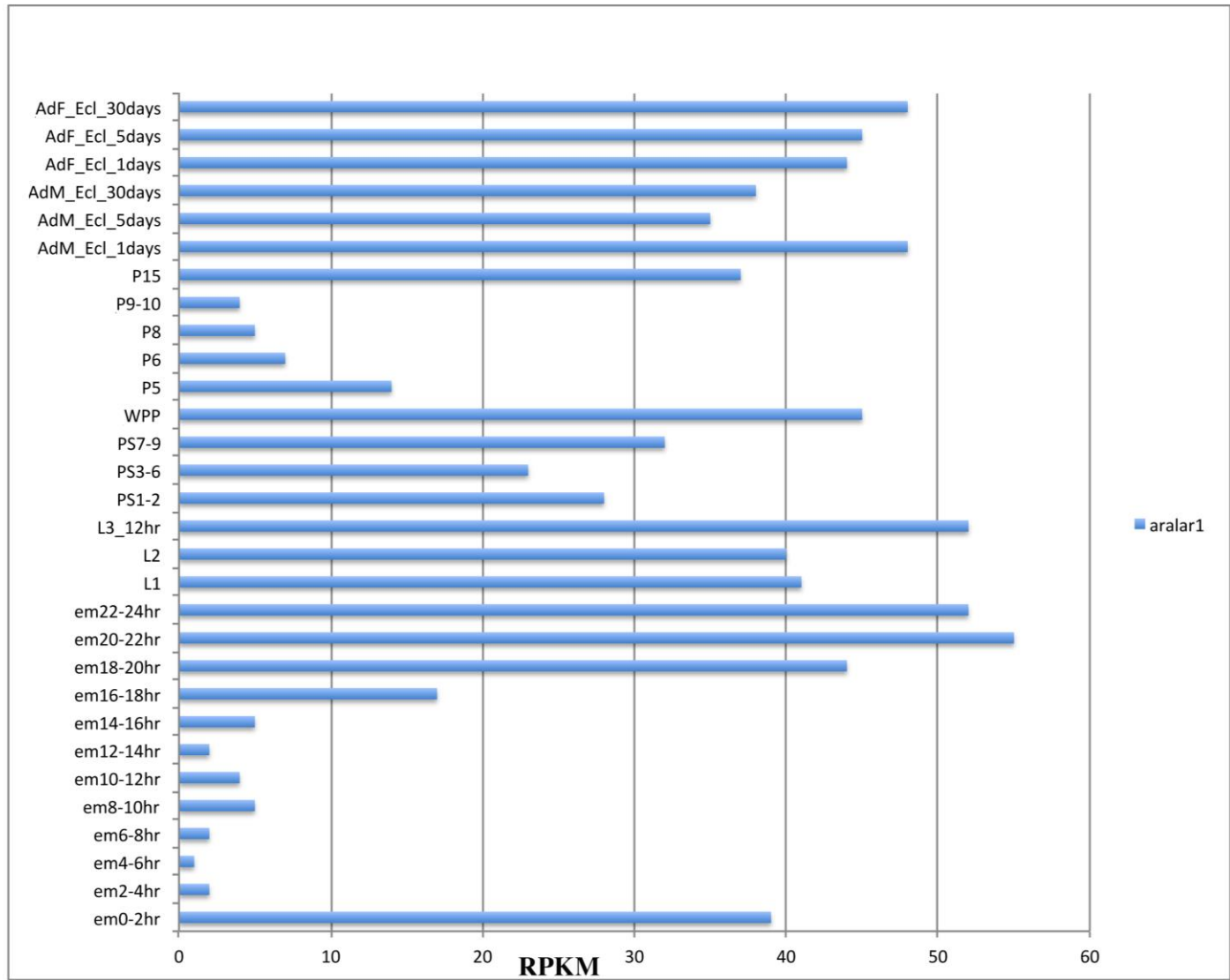


**Figure 3. modEncode expression of *aralar1* through the development.** Cumulative expression of all *aralar1* isoforms through the development is shown. Data were collected from modENCODE. Abbreviations legend. em: embryo stages; L: larval stages; P: pupae stages; AdM: adult males, various ages; AdF: adult females, various ages; RPKM: reads per kilobase million.

1  
2  
3  
4  
5  
6  
7  
8  
9  
10  
11  
12  
13  
14  
15  
16  
17  
18  
19  
20  
21  
22  
23  
24  
25  
26  
27  
28  
29  
30  
31  
32  
33  
34  
35  
36  
37  
38  
39  
40  
41  
42  
43  
44  
45  
46  
47  
48  
49  
50  
51  
52  
53  
54  
55  
56  
57  
58  
59  
60  
61  
62  
63  
64  
65

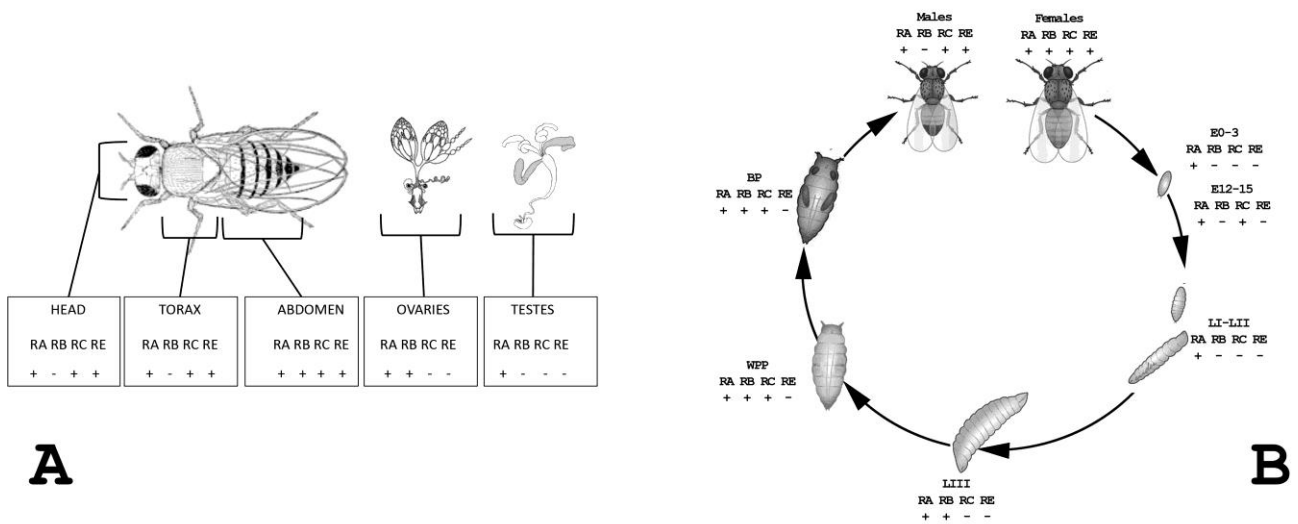


**Figure 4. Transcriptional analysis of *aralar1* in *Drosophila* adult tissues.**

The presence/absence of the indicated *aralar1* isoforms revealed by the detection of RT-PCR fragment in each analyzed RNA sample is indicated with “+” or “-”, respectively.

Panel A. The impact of the four transcriptional isoforms of *aralar1* analyzed in adult heads, thoraces and abdomens, and in the reproductive organs of males and females of *D. melanogaster*.

Panel B. The presence/absence of four transcriptional isoforms of *aralar1* was analyzed by RT-PCR through development in the indicated stages. RNA samples were collected from embryos at two stages of embryonic development (0–3, 12–15 after egg laying), mixed first and second instar larvae (LI-LII), third instar larvae (LIII), white prepupae (WPP), black pupae (BP), and adults (females and males).





the loop of Aralar-1-PE are shaded in green and cyan, respectively. Residues that are involved in the coordination of calcium and the contact points of the substrate-binding site are shaded in yellow and gray, respectively. The alignment was obtained by using ClustalW.

1  
2  
3  
4  
5  
6  
7  
8  
9  
10  
11  
12  
13  
14  
15  
16  
17  
18  
19  
20  
21  
22  
23  
24  
25  
26  
27  
28  
29  
30  
31  
32  
33  
34  
35  
36  
37  
38  
39  
40  
41  
42  
43  
44  
45  
46  
47  
48  
49  
50  
51  
52  
53  
54  
55  
56  
57  
58  
59  
60  
61  
62  
63  
64  
65

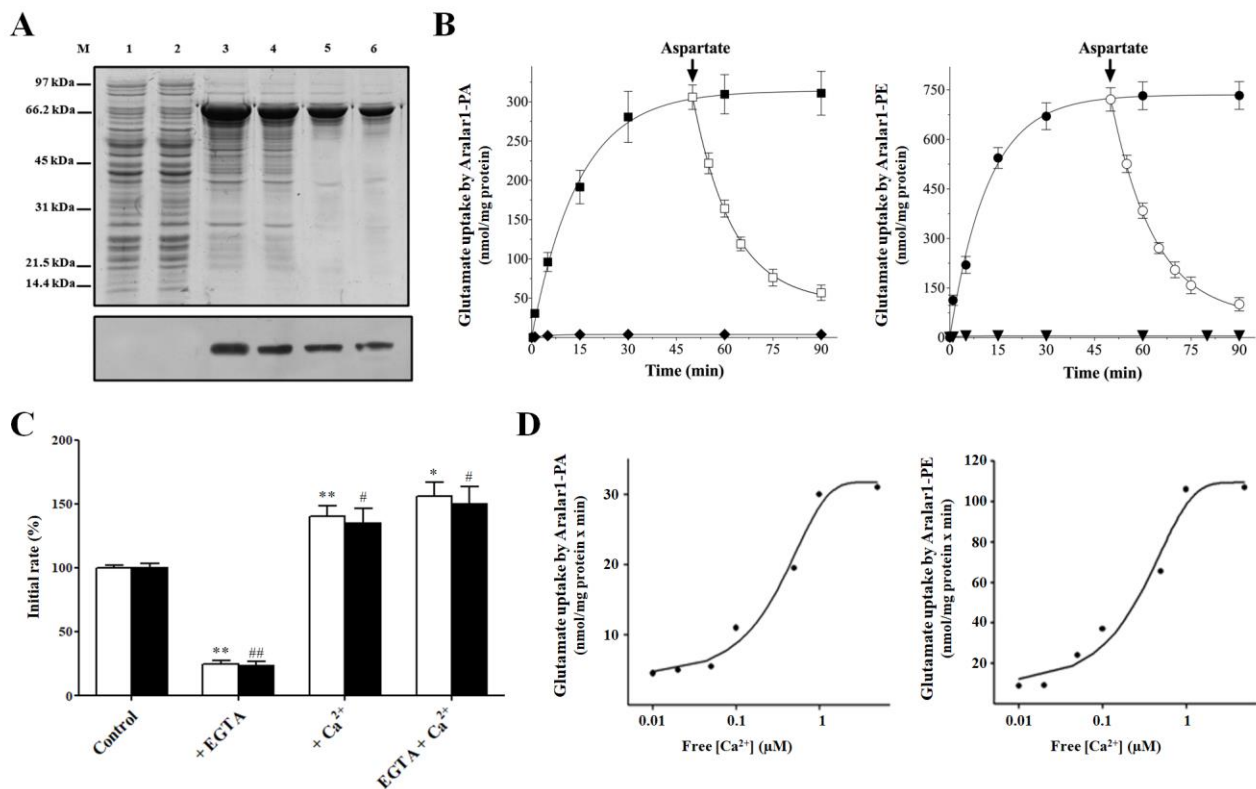


**Figure 6. Bacterial expression and functional characterization of Aralar1-PA and Aralar1-PE.** (A) Expression in *Escherichia coli* of recombinant Aralar1. Proteins were separated by SDS-PAGE and stained with Coomassie blue dye or transferred to nitrocellulose and immunodetected with an anti-V5 monoclonal antibody. Lane M, markers; lanes 1-6, *E. coli* BL21(DE3) containing the expression vector with the coding sequence for Aralar1-PA (lanes 1, 3 and 5) and Aralar1-PE (lanes 2, 4 and 6). Samples were taken at the time of the induction (lanes 1 and 2) and 4 h later (lanes 3 and 4). Lanes 5 and 6, Aralar1-PA and Aralar1-PE originating from bacteria shown in lanes 3 and 4, respectively, purified by centrifugation on sucrose gradient. The same number of bacteria was analyzed in each sample. (B) Kinetics of [<sup>14</sup>C]glutamate/glutamate exchange by Aralar1-PA and Aralar1-PE. Proteoliposomes were reconstituted with Aralar1-PA and Aralar1-PE. 0.5 mM [<sup>14</sup>C]glutamate was added to proteoliposomes containing 10 mM glutamate (■ and ●) or 10 mM NaCl (◆ and ▼). When the uptake approached equilibrium (50 min), 20 mM of aspartate was added outside the proteoliposomes (□ and ○). Similar results were obtained in four independent experiments. (C-D) Effect of Ca<sup>2+</sup> on transport activities of Aralar1-PA and Aralar1-PE. (C) Recombinant Aralar1-PA (open bars) and Aralar1-PE (filled bars), were reconstituted in proteoliposomes, the [<sup>14</sup>C]glutamate/glutamate transport rates were measured in de-ionized ultrapure water without additions (Control) or with the addition of 0.5 mM EGTA, or 1 mM CaCl<sub>2</sub>, or 0.5 mM EGTA in the presence of 1 mM CaCl<sub>2</sub>. Uptake rates of glutamate/glutamate exchange were measured at 60 s. Results are expressed as a percentage of the Aralar1-PA and Aralar1-PE values, which were on average 35.31 ± 1.24 and 110.58 ± 3.76 nmol/min x mg of protein, respectively. The average transport rates were calculated from the average of at least five independent experiments and displayed with the standard error. Different symbols indicate statistical differences, when occurring, between means of values as indicated by ANOVA. \**P* < 0.05, \*\**P* < 0.01 vs Aralar1-PA control, #*P* < 0.05, ##*P* < 0.01 vs Aralar1-PE control. (D) Dependence of Aralar1-PA and Aralar1-PE activities on the free Ca<sup>2+</sup> concentration. The [<sup>14</sup>C]glutamate transport rates were measured in de-ionized ultrapure water in the presence of 0.5 mM EGTA and various concentrations of Ca<sup>2+</sup>. Similar results were obtained in at least three independent experiments.

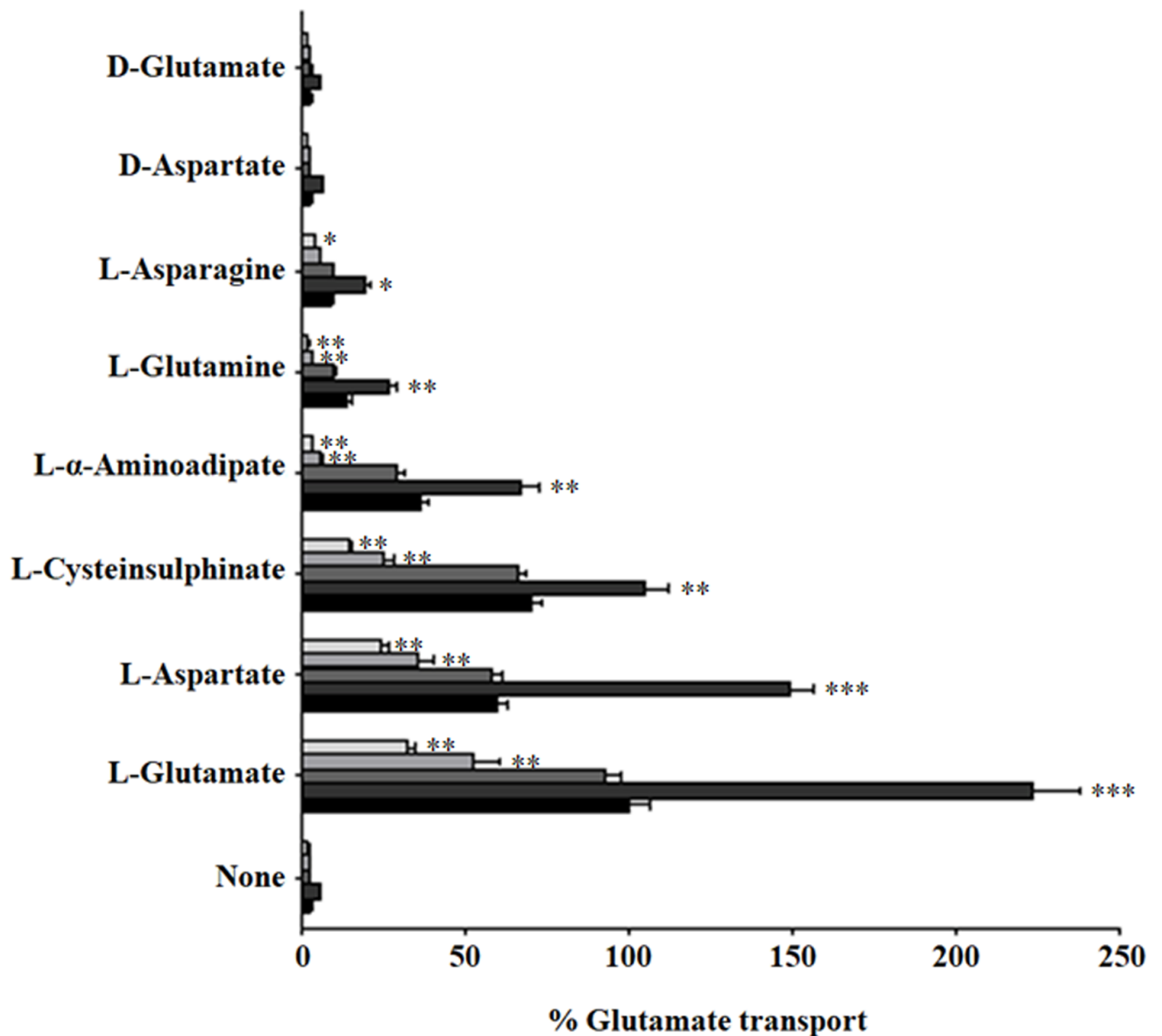


**Figure 7. Dependence on internal substrate of the transport properties of proteoliposomes reconstituted with recombinant Aralar1-PE, 5ALA, Δ5-Aralar1-PE, Δ8-Aralar1-PE and Δ12-Aralar1-PE mutants.** Proteoliposomes reconstituted with Aralar1-PE (black bars), 5ALA (very dark grey bars), Δ5-Aralar1-PE (dark grey bars), Δ8-Aralar1-PE (light grey bars) and Δ12-Aralar1-PE (very light grey bars) were preloaded internally with various substrates (concentration 10 mM). Transport was started by adding 0.5 mM [<sup>14</sup>C]glutamate to proteoliposomes and terminated after 1 min. Data represent the mean of three independent experiments reported as the percent of glutamate transport with respect to the rate of [<sup>14</sup>C]glutamate/glutamate exchange by Aralar1-PE (110 nmol/min/mg protein) setting at 100%. Asterisks indicate the level of statistical significance calculated comparing Aralar1-PE transport activity with that of its mutants in presence of each internal substrate. \**P* < 0.05, \*\**P* < 0.01, \*\*\**P* < 0.001, using ANOVA.

1  
2  
3  
4  
5  
6  
7  
8  
9  
10  
11  
12  
13  
14  
15  
16  
17  
18  
19  
20  
21  
22  
23  
24  
25  
26  
27  
28  
29  
30  
31  
32  
33  
34  
35  
36  
37  
38  
39  
40  
41  
42  
43  
44  
45  
46  
47  
48  
49  
50  
51  
52  
53  
54  
55  
56  
57  
58  
59  
60  
61  
62  
63  
64  
65

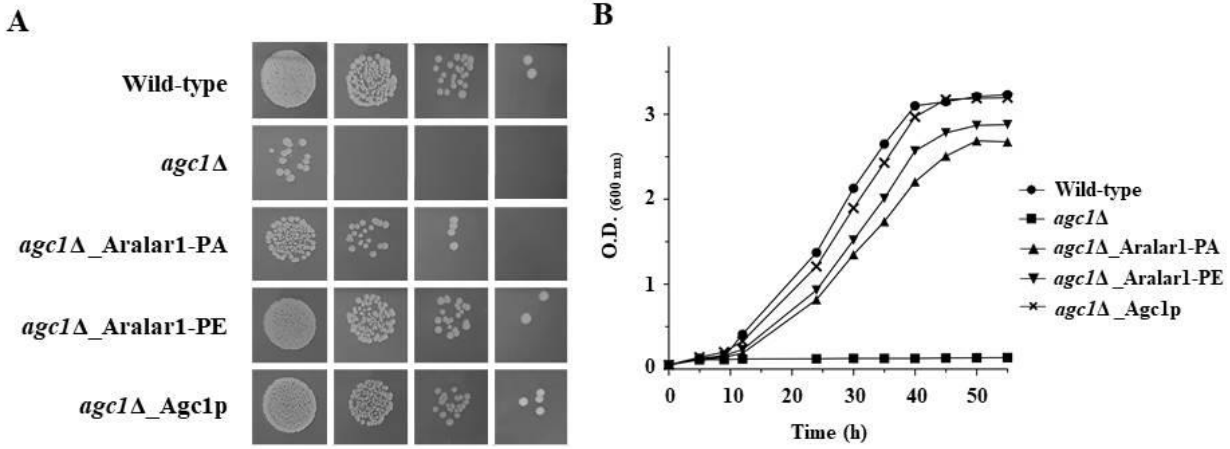


**Figure 8. Complementation of the growth defect of *agc1Δ* yeast strain by Aralar1-PA and Aralar1-PE.** Wild-type, *agc1Δ* cells transformed with the empty vector (*agc1Δ*) and *agc1Δ* cells expressing drosophila Aralar1-PA, Aralar1-PE and yeast Agc1p were plated by using a four-fold serial dilution (A) or inoculated (B) in YP medium supplemented with 0.5 mM oleate. Plates and cell cultures were placed at 30°C. Picture given in A was taken after 3 days to show yeast growth performance, whereas the optical density (O.D.) values at 600 nm given in B refer to cell cultures after the indicated growth times.

TABLE I

Dependence on internal substrate of the transport properties of proteoliposomes reconstituted with recombinant Aralar1-PA and Aralar1-PE.

Proteoliposomes were preloaded internally with various substrates (concentration 10 mM). Transport was started by adding 0.5 mM [<sup>14</sup>C]glutamate to proteoliposomes reconstituted with Aralar1-PA and Aralar1-PE, respectively, and terminated after 1 min. For each internal substrates four independent experiments have been carried out. The means and the standard deviations of Aralar1-PA and Aralar1-PE for each substrate are reported. Different symbols indicate statistical differences between means of values as indicated by ANOVA (\*P ≤ 0.05, \*\*\*P ≤ 0.001 vs uniport reaction by Aralar1-PA, #P ≤ 0.05, ##P ≤ 0.01, ###P ≤ 0.001 vs uniport reaction by Aralar1-PE).

Internal substrate	[ <sup>14</sup> C]Glutamate transport	
	Aralar1-PA	Aralar1-PE
	<i>nmol/min x mg of protein</i>	
None (Cl <sup>-</sup> present)	1.63 ± 0.11	2.85 ± 0.19
L-glutamate	31.27 ± 1.31 <sup>***</sup>	105.5 ± 6.89 <sup>###</sup>
L-aspartate	23.14 ± 1.21 <sup>***</sup>	63.34 ± 2.78 <sup>###</sup>
L-cysteinesulfinat	13.76 ± 0.78 <sup>***</sup>	73.91 ± 3.23 <sup>###</sup>
L-α-aminoadipate	2.34 ± 0.13 <sup>*</sup>	38.05 ± 2.98 <sup>###</sup>
L-glutamine	1.84 ± 0.16	14.68 ± 1.24 <sup>###</sup>
L-asparagine	3.63 ± 0.27 <sup>*</sup>	9.51 ± 1.02 <sup>#</sup>
D-aspartate	1.65 ± 0.10	2.99 ± 0.22
D-glutamate	1.34 ± 0.12	2.77 ± 0.25

**TABLE II**

*Influence of the membrane potential on the activity of recombinant Aralar1-PA and Aralar1-PE.*

The exchange was started by the addition of 50  $\mu\text{M}$  [ $^{14}\text{C}$ ]aspartate to proteoliposomes containing 10 mM of the indicated internal substrate.  $K^+_{\text{in}}$  was included as KCl in the reconstitution mixture, whereas  $K^+_{\text{out}}$  was added as KCl together with the labeled substrate. The differences in osmolarity were compensated for by the addition of appropriate concentrations of sucrose in the opposite compartment. Valinomycin (1.0  $\mu\text{g}/\text{mg}$  phospholipid) was added in 10  $\mu\text{l}$  ethanol/ml of proteoliposomes (+ valinomycin). In the samples without valinomycin (– valinomycin) the only ethanol was added. The exchange reactions were stopped after 1 min. Similar results were obtained in three independent experiments. Asterisks indicate values that are significantly different from those obtained in the same experiment but in absence of valinomycin (\*\* $P \leq 0.01$ , using Student's *t*-test)

Internal substrate	$K^+_{\text{in}}/k^+_{\text{out}}$ (mM/mM)	$[^{14}\text{C}]$ Aspartate uptake (nmol/min x mg protein)			
		Aralar1-PA		Aralar1-PE	
		- valinomycin	+ valinomycin	- valinomycin	+ valinomycin
Aspartate	1/1	28.75 $\pm$ 2.11	30.05 $\pm$ 2.96	100.75 $\pm$ 8.55	102.21 $\pm$ 8.40
	1/50	27.37 $\pm$ 2.41	28.64 $\pm$ 2.05	103.25 $\pm$ 7.20	103.89 $\pm$ 9.10
Glutamate	1/1	21.52 $\pm$ 1.70	22.24 $\pm$ 1.45	76.33 $\pm$ 5.88	77.14 $\pm$ 6.39
	1/50	23.95 $\pm$ 2.35	57.48 $\pm$ 5.74**	75.68 $\pm$ 6.28	154.86 $\pm$ 7.50**

**TABLE III**

*Kinetic constants of recombinant Aralar1-PA, Aralar1-PE, 5ALA, Δ5-Aralar1-PE, Δ8-Aralar1-PE and Δ12-Aralar1-PE mutants.*

The values were calculated from double reciprocal plots of the rate of [<sup>14</sup>C]glutamate uptake versus substrate concentrations. Transport was started by adding 125-750 μM [<sup>14</sup>C]glutamate to proteoliposomes containing 10 mM glutamate, and terminated after 1 min. Similar results were obtained in at least three independent experiments.

<b>Carrier</b>	<b>K<sub>m</sub></b> <i>(mM)</i>	<b>V<sub>max</sub></b> <i>(nmol/min x mg protein)</i>
Aralar1-PA	0.26 ± 0.03	34.60 ± 2.11
Aralar1-PE	0.29 ± 0.07	92.08 ± 4.96
5ALA	0.31 ± 0.062	189.21 ± 10.50
Δ5-Aralar1-PE	0.33 ± 0.075	82.22 ± 7.55
Δ8-Aralar1-PE	0.31 ± 0.072	58.75 ± 5.10
Δ12-Aralar1-PE	0.30 ± 0.055	37.32 ± 3.15

**The mitochondrial aspartate/glutamate carrier (AGC or Aralar1) isoforms in *D. melanogaster*: biochemical characterization, gene structure, and evolutionary analysis**

Paola Lunetti<sup>1#</sup>, René Massimiliano Marsano<sup>2#</sup>, Rosita Curcio<sup>3#</sup>, Vincenza Dolce<sup>3\*</sup>, Giuseppe Fiermonte<sup>4</sup>, Anna Rita Cappello<sup>3</sup>, Federica Marra<sup>3</sup>, Roberta Moschetti<sup>2</sup>, Yuan Li<sup>3,5</sup>, Donatella Aiello<sup>6</sup>, Araceli del Arco Martínez<sup>7</sup>, Graziantonio Lauria<sup>3</sup>, Francesco De Leonardis<sup>4</sup>, Alessandra Ferramosca<sup>1</sup>, Vincenzo Zara<sup>1\*</sup>, and Loredana Capobianco<sup>1\*</sup>

<sup>1</sup>Department of Biological and Environmental Sciences and Technologies, University of Salento, 73100 Lecce, Italy

<sup>2</sup>Department of Biology, University of Bari, 70125 Bari, Italy

<sup>3</sup>Department of Pharmacy, Health, and Nutritional Sciences, University of Calabria, 87036 Arcavacata di Rende (Cosenza), Italy.

<sup>4</sup>Department of Biosciences, Biotechnologies and Biopharmaceutics, University of Bari, 70125 Bari, Italy

<sup>5</sup>Faculty of Biological Engineering, Sichuan University of Science and Engineering, Yibin, China

<sup>6</sup>Department of Chemistry, University of Calabria, 87036 Arcavacata di Rende (Cosenza), Italy.

<sup>7</sup>Facultad de Ciencias del Medio Ambiente, Universidad de Castilla La Mancha, Toledo, Spain.

\*Corresponding authors. V. Dolce is to be contacted at Department of Pharmacy, Health, and Nutritional Sciences, University of Calabria, 87036 Arcavacata di Rende (Cosenza), Italy. Tel.: +39 0 984493119; fax: +39 0 984493270. L. Capobianco is to be contacted at Department of Biological and Environmental Sciences and Technologies, University of Salento, 73100 Lecce, Italy. Tel.: +39 0 832298864; fax: +39 0 832298626. V. Zara is to be contacted at Department of Biological and Environmental Sciences and Technologies, University of Salento, 73100 Lecce, Italy. Tel.: +39 0 832298678; fax: +39 0 832298626.

E-mail addresses: [vincenza.dolce@unical.it](mailto:vincenza.dolce@unical.it) (V. Dolce), [loredana.capobianco@unisalento.it](mailto:loredana.capobianco@unisalento.it) (L. Capobianco), [vincenzo.zara@unisalento.it](mailto:vincenzo.zara@unisalento.it) (V. Zara)

# These authors contributed equally to this work.



## Abstract

### Background

In man two mitochondrial aspartate/glutamate carrier (AGC) isoforms, known as aralar and citrin, are required to accomplish several metabolic pathways. In order to fill the existing gap of knowledge in *Drosophila melanogaster*, we have studied *aralar1* gene, orthologue of human AGC-encoding genes in this organism.

### Methods

The blastp algorithm and the “reciprocal best hit” approach have been used to identify the human orthologue of AGCs in Drosophilidae and non-Drosophilidae. Aralar1 proteins have been overexpressed in *Escherichia coli* and functionally reconstituted in liposomes for transport assays.

### Results

The transcriptional organization of *aralar1* comprises six isoforms, three constitutively expressed (*aralar1-RA*, *RD* and *RF*), and the remaining three distributed during the development or in different tissues (*aralar1-RB*, *RC* and *RE*). Aralar1-PA and Aralar1-PE, representative of all isoforms, have been biochemically characterized. Recombinant Aralar1-PA and Aralar1-PE proteins share similar efficiency to exchange glutamate against aspartate, and same substrate affinities than the human isoforms. Interestingly, although Aralar1-PA and Aralar1-PE diverge only in their EF-hand 8, they greatly differ in their specific activities and substrate specificity.

### Conclusions

The tight regulation of *aralar1* transcripts expression and the high request of aspartate and glutamate during early embryogenesis suggest a crucial role of Aralar1 in this *Drosophila* developmental stage. Furthermore, biochemical characterization and calcium sensitivity have identified Aralar1-PA and Aralar1-PE as the human aralar and citrin counterparts, respectively.

### General Significance

The functional characterization of the fruit fly mitochondrial AGC transporter represents a crucial step toward a complete understanding of the metabolic events acting during early embryogenesis.

**Keywords:** *Drosophila melanogaster*; *CG2139*; aspartate/glutamate carrier (AGC); aralar; citrin; phylogenetic footprint;

**Abbreviations:** AGC, aspartate/glutamate carrier; MAS, malate-aspartate shuttle; MCF, mitochondrial carrier family; NRG, nuclear respiratory gene; SDS-PAGE, polyacrylamide gel electrophoresis in the presence of sodium dodecyl sulfate; TSS, transcriptional start site.

## 1.Introduction

The mitochondrial carrier family (MCF) represents one of the largest families of transporters widespread across all species. MCF members share a common structural organization, consisting of three tandemly repeated sequences of approximately 100 amino acids in length, and mediate the transport of metabolites across the inner mitochondrial membrane [1-3]. The aspartate/glutamate carrier (AGC) catalyzes an electrogenic exchange of cytosolic glutamate plus a proton for mitochondrial aspartate [4], and it is one of the most important family member, since it is a key component of the malate-aspartate shuttle (MAS), which transfers the reducing equivalents of NADH from cytosol to mitochondria in order to regenerate NAD<sup>+</sup> necessary for glycolysis. Furthermore, AGC plays an essential role in many other metabolic processes including the synthesis of urea and nitrogen-containing metabolites [5], gluconeogenesis from lactate [5], calcium-mediated regulation of mitochondrial respiration [4, 6-9], insulin secretion from islet cells [10], zygote development [11, 12], N-acetylaspartate (a myelin precursor) synthesis [13-16] and glial synthesis of glutamate and glutamine [17]. Increasing evidences support the hypothesis that MAS activity is crucial for breast cancer cell proliferation [18]. In this regard, it might divert energetic cell metabolism towards glycolysis, promoting cancer cell growth [19]. Furthermore, AGC is involved in taurine metabolism, since it can efficiently transport also cysteinesulfinate [4, 20], an intermediate of cysteine degradation that serves as a precursor of taurine [21].

In *Homo sapiens*, two isoforms named AGC1 and AGC2 (also known as aralar and citrin) and encoded by the *SLC25A12* and *SLC25A13* genes, respectively, have been identified and characterized [4, 22]. They belong to a subfamily of calcium-binding mitochondrial carrier sharing a characteristic bipartite structure, which consists of a C-terminal domain responsible for transport activity, and an N-terminal domain containing 8 EF-hands that regulates transport activity [4, 23].

Aralar is mainly expressed in the heart, retina, skeletal muscle and brain [24, 25], whereas citrin is widely expressed in the liver, epithelial cells and breast [4]. Aralar is involved in retinal visual function [26, 27], in myelination process [13] and in glutamate-induced excitotoxicity [28, 29]. Mutations in the *SLC25A12* gene have been found in autism spectrum disorders [25, 30-32], as well as in a rare human disease (OMIM number 612949) implying developmental delay, epilepsy and hypotonia [15, 33]. *SLC25A13* mutations are responsible for citrin deficiency that causes adult-onset type II citrullinemia (CTLN2, OMIM number 603471), neonatal intrahepatic cholestasis (NICCD, OMIM number 605814) [29, 34-39], as well as failure to thrive and dyslipidemia caused by citrin deficiency (FTTDCD) [40].

1  
2  
3  
4  
5  
6  
7  
8  
9  
10  
11  
12  
13  
14  
15  
16  
17  
18  
19  
20  
21  
22  
23  
24  
25  
26  
27  
28  
29  
30  
31  
32  
33  
34  
35  
36  
37  
38  
39  
40  
41  
42  
43  
44  
45  
46  
47  
48  
49  
50  
51  
52  
53  
54  
55  
56  
57  
58  
59  
60  
61  
62  
63  
64  
65

In *D. melanogaster*, a single gene annotated in FlyBase as *CG2139* or *aralar1* encodes a ortholog of the human AGC isoforms [41]. *Aralar1* gene is involved in high energy demanding processes, together with many other genes, such as those responsible for embryonic epithelial repair [42]. Previous studies indicated that *aralar1* locus is involved in the determination of bristle number in *D. melanogaster*, which are structures that may also have a neurosensory function [43], as well as this locus may influence wing size phenotype [44].

Differently from other fruit fly mitochondrial transporters, such as adenine nucleotide translocase [45], uncoupling protein [46, 47] dicarboxylate [48], thiamine pyrophosphate [49, 50], and glutamate carriers [51], a genomic analysis of this insect has highlighted the presence of a single gene (*CG2139*) encoding various *aralar1* spliced isoforms. The presence of so many alternatively spliced isoforms in mitochondrial carriers [47, 52, 53] and more in general in this organism is not surprising, since alternative splicing is a peculiar mechanism very often used by *D. melanogaster* to tightly control tissue- and stage-specific protein isoforms with different functions in development, as highlighted by Venables et co-workers “*Drosophila uses every alternative splicing strategy imaginable with an elegance and complexity that often eclipses mammals*” [54].

Despite the high metabolic relevance of this transporter, very few data are available on its biological role in fruit fly cellular processes, and no data at all are available on its transport properties in *Drosophila*.

In the present study, we have described (i) the expression profile of *D. melanogaster aralar1* gene in different developmental stages and tissues; (ii) the evolutionary changes that have shaped *aralar1* gene structure in arthropods; (iii) the functional characterization of recombinant Aralar1-PA and Aralar1-PE and their identification as the fruit fly mitochondrial aspartate/glutamate carriers.

## 2. Material and methods

### 2.1. Blast search of AGC orthologs in *D. melanogaster* and other species

The *D. melanogaster* ortholog of human AGCs was identified using the blastp algorithm (<http://flybase.org/blast/>). A BLAST search strategy, using *D. melanogaster* CDS and/or peptides as queries against genomic and ESTs databases, was also adopted to identify putative genes encoding AGC in the genome of other Drosophilidae and several non-Drosophilidae species [55]. A complete list of the species investigated in this study and the accession number in which *aralar1* genes have been identified is shown in Supplementary Table 1. These searches were performed using organism-specific ([www.flybase.org](http://www.flybase.org), [www.vectorbase.org](http://www.vectorbase.org) and <http://hymenoptera.genome.org>) and generalist genomic repositories (NCBI <http://blast.ncbi.nlm.nih.gov/Blast.cgi>). The “reciprocal best

hit” approach was used to identify *aralar1* genes in different species. In this approach, a common evolutionary origin is supposed when in the compared genomes two gene sequences represent each other the best BLAST hit[56].For each genomic sequence identified by using the above-mentioned criteria, exon/intron boundaries were carefully annotated after prediction *in silico* carried out with the aid of ESTs and cDNA sequences, if available, or predicted by the Genscan tool [57], or inferred by sequence similarity with transcript sequences of closely related species. Multiple alignments of amino acids, as well as coding and non-coding DNA sequences, were obtained using the MultAlin 5.4.1 software available at the MultAlin server (<http://multalin.toulouse.inra.fr/multalin/>) [58, 59]. The matrix-scan pattern matching tool of the Regulatory Sequence Analysis Tools from the RSAT server (<http://rsat.ulb.ac.be/>) was used, in combination with multiple alignments to identify Nuclear Respiratory Gene (NRG) elements [60] in the non-coding sequences of Drosophilidae and non-Drosophilidae *aralar1* genes.

## 2.2. Reverse-transcription analyses of *aralar1* transcriptional isoforms

Oregon-R flies were raised on standard culture medium at 24 °C. Total RNA for gene expression analysis was achieved from 0.5- to 1-g samples of Oregon-R individuals at different developmental stages (embryo, larvae, pupae and adult flies). Except for ovaries and testes, male and female tissues equally contributed to each dissection. Total RNA from all the developmental stages and tissues was extracted by employing Trizol. Purified RNA was quantified using a Nanodrop spectrophotometer (Thermo Scientific) and diluted to 1 mg/ml for reverse transcription. RNA (1 µg) was reverse transcribed by employing the Quantitect reverse transcription kit (QIAGEN) [61, 62] following the manufacturer’s protocol. Amplification was carried out using the Platinum Taq DNA Polymerase (Thermo Fisher).

Primers used for amplification were:

aralar\_RA\_F ATTAGACGCGGGAATTGCTC  
aralar\_RA\_R CTCCTCGTGAAAGTCGTGCAG  
aralar\_RB\_F ATAGTGCGAACGTGCCTGA  
aralar\_RB\_R ATGGCGAGATGAACCCAGTG  
aralar\_RC\_F CCGATGCCAAGAATCTCCGT  
aralar\_RC\_R TCCTCGTGAAAGTCGTGCAG  
aralar\_RE\_F CAAATCACGCCGCTGGAGAT  
aralar\_RE\_F GGCCCCTTTATCAAGCGCTA

### 2.3. Construction of the expression plasmids encoding *D. melanogaster* Aralar1 isoforms and mutants in *E. coli* and *S. cerevisiae*

The two protein isoforms Aralar1-PA and Aralar1-PE were considered for the functional characterization of *D. melanogaster* *CG2139* gene. Aralar1-RA and Aralar1-RE were amplified by polymerase chain reaction (PCR) from the cDNA of the fruit fly clones LD35441 and GH21613, respectively. Both clones were provided by Drosophila Genomics Resource Center (Indiana University 1001 East Third St., Bloomington IN, 47405-7107). The oligonucleotide primers (sense and antisense) used in PCR reactions carried suitable restriction sites at their 5' ends for the further cloning of the amplified inserts in the pET-21b/V5-His *E. coli* expression vector [51]. The absence of a stop codon in the reverse primer sequence led to the expression of Aralar1 proteins containing V5/His-tag at their C-termini [63].

The WT Aralar1-RE cDNA was employed as a template to generate mutants named  $\Delta 5$  (deletion from residue 301 to 305),  $\Delta 8$  (deletion from residue 301 to 308 ),  $\Delta 12$  (deletion from residue 299 to 310 ), and 5Ala (replacement of residues K<sub>301</sub>RRR<sub>K305</sub> by consecutive alanines). All of the mutations were introduced by the overlap extension PCR method [64, 65], using oligonucleotides with suitable mutations in their sequences. Primers used for amplification were:

aralar\_PE\_FTAGGAATTCACCAATGCACATCCCGTTTCC and

aralar\_PE\_R CGAAAGCTTGGATCCCGTGGCCGTCG for all mutants.

The following specific primers were used to generate the above-mentioned mutants:

aralar\_PE\_Δ5\_F CCATCAAGCAGGCTGGTGGATACCTCCGAGTAGCCGCA

aralar\_PE\_Δ5\_R TGCGGCTACTCGGAGGTATCCACCAGCCTGCTTGATGG

aralar\_PE\_Δ8\_F CCATCAAGCAGGCTGGTGGAGTAGCCGCATCGACTATAGTGAC

aralar\_PE\_Δ8\_R GTCACTATAGTCGATGCGGCTACTCCACCAGCCTGCTTGATGG

aralar\_PE\_Δ12\_F GCGCCGTCCATCAAGCAGGCCGCATCGACTATAGTGACCTGAGCAA

aralar\_PE\_Δ12\_R TTGCTCAGGTCACTATAGTCGATGCGGCCTGCTTGATGGACGGCGC

aralar\_PE\_5Ala\_F

CCATCAAGCAGGCTGGTGGGCGGCTGCCGCAGCGATACCTCCGAGTAGCCGCA

aralar\_RE\_5Ala\_R

TGCGGCTACTCGGAGGTATCGCTGCGGCAGCCGCCACCAGCCTGCTTGATGG

The aralar1-RA and aralar1-RE ORFs were recovered from pET-21b/V5-His clones by a EcoRI/AgeI digestion and cloned in the modified yeast expression vector pYES2/ V5-His [49], in which the inducible GAL1 promoter had been replaced with the constitutive TDH3 promoter. The

frameshift of transcripts was avoided cloning a KpnI/EcoRI fragment carrying the ATG start codon at '5-end. Fragments used were: GGTACCAGGATCCGATCTTGAAGTACTGACTGAGATGGCGAATTC and GGTACCAGGATCCGATCTTGAAGTACTGACTGAGATGGCGAATTC for aralar1-RA and for aralar1-RE, respectively.

#### 2.4. Bacterial expression and purification of the recombinant proteins

Aralar1 proteins were overexpressed at high levels in *E. coli* BL21(DE3) [49]. Their identities were assessed by MALDI-TOFMS of trypsin digests of the corresponding bands excised from a Coomassie blue-stained polyacrylamide gel [66, 67]. Inclusion bodies were purified using sucrose density gradient centrifugation, next they were washed at 4°C, firstly with TE buffer (10 mM Tris/HCl, 1 mM EDTA, pH 8), then twice with a buffer containing Triton X-114 (2%, w/v) and 10 mM HEPES (pH 8), and finally with 10 mM PIPES pH 6.5. Aralar1-PA and Aralar1-PE were solubilized in 2% sarkosyl (w/v), and a small residue was removed by centrifugation (258000 g, 30 min). Solubilized proteins were diluted 10-fold with 10 mM PIPES pH 6.5 and reconstituted into liposomes [68].

#### 2.5. Reconstitution into liposomes and transport assays

Reconstitution mixture (700 µl) contained 0.5-1 µg of solubilized proteins, Triton X-114 (1,3 % w/v), L- $\alpha$ -phosphatidylcholine from egg yolk (1,3 % w/v), as sonicated liposomes, 10 mM glutamate (except where otherwise indicated), and 20 mM PIPES at pH 6.5 [69]. These components were carefully blended, and the blend was recycled 13 times through the same Amberlite column (Bio-Rad) [69]. External substrate was eliminated from proteoliposomes on Sephadex G-75 columns, pre-equilibrated with 50 mM NaCl and 10 mM PIPES at pH 6.5. Transport at 25°C was started by adding L-[<sup>14</sup>C]glutamate (Scopus Research BV, Wageningen, Netherlands) at the indicated concentrations to substrate-loaded proteoliposomes (exchange reaction), or to empty proteoliposomes (uniport reaction). In both cases, transport was terminated by adding 30 mM pyridoxal phosphate (PLP). In control samples, inhibitor was added together with the external radioactive substrate based on the inhibitor stop method [70, 71]. Finally, external substrate was removed and radioactivity into proteoliposomes was measured. The experimental values were adjusted by subtracting control values. The initial transport rate was measured from the radioactivity taken up by proteoliposomes after 1 min (in the initial linear range of substrate uptake). The free Ca<sup>2+</sup> concentrations were determined fluorimetrically with fura-2-acetoxymethyl ester (Fura-2 AM) (Thermo Fischer Scientific). Fura-2 AM is a membrane-permeable, non-invasive

1 derivative of the ratiometric calcium indicator fura-2. The excitation wavelengths used are 340 nm  
2 and 380 nm for Ca<sup>2+</sup>-bound and Ca<sup>2+</sup>-free fura-2 AM, respectively. In both states, the emission  
3 maximum is about 510 nm. The ratios 510 nm/340 nm and 510 nm/380 nm are directly related to  
4 the amount of Ca<sup>2+</sup> [72]. Calcium dependence on transport activity was determined using de-ionized  
5 ultrapure water. In experiments for evaluating the influence of the membrane potential on the  
6 activity of the recombinant proteins, valinomycin was added to proteoliposomes in order to provide  
7 de-energized conditions. K<sup>+</sup> diffusion potentials were generated using valinomycin and K<sup>+</sup>  
8 gradients. In these experiments, substrate and buffer were neutralized with NaOH [4].  
9  
10  
11  
12  
13  
14  
15

## 16 **2.6. Yeast strains, growth conditions and functional complementation of yeast AGC1Δ by** 17 **ARALAR1-PA and ARALAR1-PE**

18 W303 (wild-type) (*MATa {leu2-3,112 trp1-1 can1-100 ura3-1 ade2-1 his3-11,15}*) yeast strain was  
19 provided by the EUROFAN resource center EUROSCARF (Frankfurt, Germany). The yeast  
20 AGC1 gene deletion (*agc1Δ*) and the cloning of endogenous yeast deleted gene AGC1 were  
21 achieved as described before [73].  
22  
23  
24  
25  
26

27 The recombinant aralar1-RA-pYES2 and aralar1-RE-pYES2 plasmids were introduced into the  
28 *agc1Δ* yeast strain using the lithium acetate method [74], and transformants were selected on  
29 minimal medium lacking uracil, supplemented with 2% glucose.  
30  
31

32 Functional complementation was achieved growing cells on liquid complete medium (1% Bacto  
33 yeast extract, 2% Bacto Peptone, pH 5.0) supplemented with 2% glucose (YPD) or 0.5 mM oleic  
34 acid dissolved in 10% Tween40 (YPO) as carbon sources. Growths were started from medium log  
35 precultures grown on complete medium YPD and diluted with YPO to an optical density of 0.01 at  
36 600 nm.  
37  
38  
39  
40  
41

42 Simultaneously, washed cells were diluted and spotted on complete solid medium YPO, then plates  
43 were incubated for 72 h at 30 °C. Four-fold serial dilutions of both the transformed strains, wild-  
44 type and AGC1Δ cells were analyzed.  
45  
46  
47  
48  
49

## 50 **2.7. Other methods**

51 Proteins were resolved by SDS-PAGE and stained with Coomassie blue dye [75]. The amounts of  
52 recombinant pure Aralar1-PA and Aralar1-PE incorporated into liposomes were measured as  
53 previously described [76] and proved to be approximately 20% of the protein amount added to the  
54 reconstitution mixture. Moreover, recombinant proteins were resolved by SDS-PAGE analysis [77,  
55 78], then transferred to a nitrocellulose membrane and analyzed by Western blotting employing a  
56 mouse anti-V5 monoclonal antibody (Sigma-Aldrich) [79, 80]. A multiple sequence alignment  
57  
58  
59  
60  
61  
62  
63  
64  
65

(MSA) of the fruit fly Aralar1 proteins, human aralar and citrin isoforms was obtained by using ClustalW to insert gaps in the MSA [81]. All data were analyzed using the statistical software GraphPad Prism Software (7.0 version). Pairwise comparisons between means of different groups were performed using a Student's t-test (two tailed, unpaired). Multiple comparisons were performed using a univariate ANOVA. Values at  $P \leq 0.05$  were considered statistically significant, while values at  $P \leq 0.01$  and  $P < 0.001$  were considered very significant [82, 83]. Orientation of functional Aralar-1 in the membrane of reconstituted proteoliposomes was investigated by ELISA assay performed as previously described [84]. ELISA tests were carried out on intact and permeabilized proteoliposomes by using either the rabbit polyclonal antiserum generated against 35-177 amino acids of Drosophila Aralar-1 proteins as described in [85] or the anti-V5 antibody directed against the V5 epitope placed at their C-termini (Sigma-Aldrich).

### 3. Results

#### 3.1. Identification of genes encoding the aspartate/glutamate carrier in Drosophilaspecies

A single gene, annotated in FlyBase as *CG2139* or *alarar1*, encodes a *D. melanogaster* ortholog of the human AGC isoforms (also known as aralar and citrin) [4], with no additional hits obtained throughout database mining. *Aralar1* locus spans roughly 10 Kbp on the third chromosome (3R:30,445,635..30,455,867 [-]) in the 99F4-99F5 cytogenetic band of polytene chromosomes of *D. melanogaster*. The transcriptional organization of *alarar1* reported in FlyBase (Figure 1A) comprises six transcriptional isoforms. The utilization of alternative transcriptional start sites, alternative splicing and alternative UTRs, produces five different transcriptional isoforms (namely RA, RB, RC, RD, RE), which in turn can be translated into four different proteins (PA/PD, PB, PC, PE). An additional translational isoform is reported in FlyBase, Aralar1-PF, which is translated from the *alarar1-RF* transcript that is structurally identical to *alarar1-RA* isoform by mean of a read-through translational mechanism [86]. In this regard, *alarar1-RA* transcript is translated into a 682 amino acids long protein (Aralar1-PA), whereas *alarar1-RF* transcriptional isoform is translated into a polypeptide having 12 additional aminoacids at its C-terminus due to translation progression beyond the canonical stop codon. Three different promoters contribute to the transcription of *alarar1* locus. *Aralar1-RA* (identical to *alarar1-RF*) and *alarar1-RD* are transcribed from the same downstream promoter, with *alarar1-RD* transcript possessing a shorter 3'UTR if compared to that of *alarar1-RA/RF* isoforms. *Aralar1-RB* arises from the central promoter, whereas *alarar1-RC* and *alarar1-RE* are originated from the upstream promoter. The two latter isoforms differ by a short, 36 bp long exon, which is specifically incorporated into the *alarar1-RE* transcript. Given the availability of a wide range of sequenced Arthropoda genomes, we have surveyed *alarar1* gene structure in Arthropoda.



1 Orthologous genes in Drosophilidae have been retrieved using a BLAST strategy, and locus  
2 structure has been inferred with the aid of ESTs and cDNA sequences annotated in FlyBase and  
3 NCBI databases. Sequences with significant similarity to *D. melanogaster aralar1* gene have been  
4 detected in the genome of 22 additional Drosophila species (Supplementary Table 1), and their  
5 organization has been compared. Similarly to *D. melanogaster* annotation, in all the investigated  
6 Drosophila species three transcriptional start sites can be inferred from ESTs and cDNAs comparison  
7 and from inter-species similarity. In order to give a better snapshot of *aralar1* locus, its organization  
8 has been divided into three schemes highlighting the exon/intron organization relative to the three  
9 TSSs (Transcriptional Start Site) (Supplementary Tables 2-5). The comparison clearly suggests that  
10 the exon-intron structure of the locus is highly conserved in the 23 analyzed species. As can be  
11 observed, exon length is poorly variable. The first exon of all transcriptional isoforms is the most  
12 variable in length. Indeed, they encode the 5' UTRs and the leader peptides that are expected to be  
13 divergent in sequence, even if closely related species are compared. The length of the coding region  
14 of the last exon, encoding the protein C-terminus, also presents variable length and sequence in the  
15 analyzed Drosophila species. Internal coding exons are instead extremely conserved in length. As  
16 expected, introns are the most plastic regions of eukaryotic genes, and they are longer in species  
17 distantly related to *D. melanogaster*. It is worth to note that although the presence of the *aralar1-RE*  
18 specific exon is not supported by ESTs or cDNAs in the vast majority of the Drosophilidae species  
19 (not shown), it can be inferred by sequence similarity, suggesting that it could be also a functional  
20 exon in other species. In support of this hypothesis, the *aralar1-RE* specific exon, which can be 33-  
21 39 bp long depending upon the species, is flanked by a non-canonical donor splice site  
22 (GC) conserved in all the Drosophila species, suggesting the usage of an atypical splice site in the  
23 common ancestor of Drosophila and Sophophora genera (Supplementary Figure 1).  
24  
25  
26  
27  
28  
29  
30  
31  
32  
33  
34  
35  
36  
37  
38  
39  
40  
41  
42  
43

### 44 **3.2. Conservation of regulatory elements**

45 Inter-species DNA sequence comparison is an excellent tool for the identification of cis-regulatory  
46 DNA sequences interested in eukaryotic gene expression regulation, especially in non-coding DNA  
47 sequence. In the noncoding sequences of Drosophilidae *aralar1* genes we have searched for  
48 conserved motifs by using phylogenetic footprinting and DNA pattern discovery softwares. The  
49 nuclear respiratory gene (NRG) element has been previously reported as a palindromic 8-bp motif  
50 (TTAYRTAA) that is shared by all nuclear OXPHOS genes [87], as well as by many other nuclear  
51 genes involved in biogenesis and function of mitochondria in insects [60]. In *D. melanogaster*,  
52 NRG elements are usually located within an intron, in close proximity to the transcription start site  
53 (TSS), but it can be found in different gene locations, such as upstream the TSS. A NRG element  
54  
55  
56  
57  
58  
59  
60  
61  
62  
63  
64  
65

1 (TTATATAA) associated with high weight and low P value in the RSAT output (8,2 and 6.0e<sup>-05</sup>  
2 respectively) is located in the first intron, 518 bp downstream of the transcription start site related to  
3 *D. melanogaster aralar1-RB* transcriptional isoform. This 8-bp motif is extremely conserved and  
4 located in the first intron in all the Drosophilidae *aralar1* orthologs with high frequency (Figure  
5 1B). An additional NRG element, associated with a slightly lower score and a moderately higher P-  
6 value in the RSAT output (6,7 and 1,5e<sup>-04</sup> respectively), is located downstream within the same  
7 intron, 686 bp upstream the TSS related to the RA/RD/RF transcriptional isoforms (Figure 1C).

8 The functional importance of the NRG element in *aralar1* genes is suggested by its presence in the  
9 non-coding regions of *aralar1* genes belonging to the 32 non-Drosophilidae Arthropoda species  
10 investigated in this work (Supplementary Table 1). Notwithstanding, the very long divergence times  
11 (divergence between Drosophila and Parasteatoda/Limulus genera is estimated approximately 600  
12 MYA, from Treebase <http://www.timetree.org>) [88], single or multiple NRG elements have been  
13 detected in *aralar1* genes of the majority of Arthropoda species, and their intragenic localization is  
14 often strictly conserved (not shown). However, standing to the availability of transcriptional data in  
15 the vast majority of the studied cases, we have reconstructed the complete exon/intron structure of  
16 *aralar1* related to the shortest transcriptional isoform, which we have arbitrarily assumed to be  
17 homologous to *D. melanogaster* RA-RD-RF transcripts. In many of these species, the NRG  
18 elements have been found in the first intron related to the shortest transcriptional isoform,  
19 suggesting that their positions could have been remodeled during insects' evolution. Also the length  
20 of the first intron, with respect to the most proximal TSS, is on average longer in non-Drosophilidae  
21 insects (mean length=15149 bp, 29 species) than in *D. melanogaster* homologs (mean length=245  
22 bp, 23 species), supporting the hypothesis of a functional role of the NRG elements, although in a  
23 different position.  
24  
25  
26  
27  
28  
29  
30  
31  
32  
33  
34  
35  
36  
37  
38  
39  
40  
41  
42  
43

### 44 **3.3. All eukaryotic *aralar1* genes have a common evolutionary origin.**

45 Sequences homologous to *D. melanogaster aralar1* gene have been found in the genomes of 23  
46 Drosophilidae species. They share not only significant sequence similarity with *D. melanogaster*  
47 genes, but also a strikingly conserved exon/intron organization (Figure 2 and Supplementary Tables  
48 2-5). As a first step towards understanding the evolutionary history of *aralar1* genes, we have  
49 compared the Drosophilidae gene organization with their counterparts in an informative range of 32  
50 Arthropod species consisting of 30 insects species (namely 7 Diptera, two Lepidoptera 1  
51 Coleoptera, 18 Hymenoptera and 2 Hemiptera), an Arachnida (*Parasteatoda tepidariorum*) and a  
52 Xiphosurida (*Limulus polyphemus*).  
53  
54  
55  
56  
57  
58  
59  
60  
61  
62  
63  
64  
65

1 Similarly to what found in Drosophilidae, a single *aralar1* gene has been detected in the genome of  
2 all these species. The complete list of the identified *aralar1* genes and the accession numbers in  
3 which they have been found in the respective genomes is shown in Supplementary Table 1.  
4 Variations in the exon/intron organization of the investigated genes are reported in Supplementary  
5 Table 6. Comparison of all the investigated genes, in particular those in insects and Arachnida  
6 (*Parasteatoda tepidariorum*), as well as in Xiphosura (*Limulus polyphemus*), suggests the presence  
7 of a common ancestor before Arthropods' divergence. Intron loss seemingly occurred in Diptera-  
8 Lepidoptera-Coleoptera, while intron gain suggests a lineage-specific process.

9 The existence of an internal exon, specific for a transcriptional isoform homologous to *D.*  
10 *melanogasteraralar1-RE*, can be inferred in a subset of the analyzed species including Hymenoptera  
11 (14 out of 18 species) and Diptera (6 out of 7 non-Drosophilid species), whereas we have not  
12 detected it in Coleoptera (one species) and Lepidoptera (two species), as well as in the evolutionary  
13 distant Hemiptera species.

14 In humans, the nearly identical exon/intron organization of *ARALAR* (*SLC25A12*) and *CITRIN*  
15 (*SLC25A13*) genes (19 and 21 coding exons, respectively) is consistent with a duplication of an  
16 ancestral gene, which was probably present in the genome of the Vertebrate's ancestor, due to the  
17 existence of two paralogue genes in the genome of extant vertebrate species so far sequenced (not  
18 shown). Alternatively spliced transcript variants have been reported for the human *ARALAR* gene  
19 (as provided by ac.nos NM\_003705, NR\_047549, XM\_011512070). While the NM\_003705 is  
20 translated into the Aralar1 protein (NP\_003696), the functional roles of the predicted  
21 (XM\_011512070) and the putatively non-coding (NR\_047549) transcriptional isoforms are currently  
22 unknown. Comparisons of exon phase, exon length, and intron positions, suggest that Arthropod  
23 and human genes have a unique intron-rich ancestor predating the divergence of such lineages.  
24 Since position conservation in humans and in numerous Arthropod lineages can be supposed in order  
25 to identify retained ancestral introns, we have deduced that such common ancestor gene contained at  
26 least 15 introns.

### 27 **3.4. Expression pattern of *Drosophila melanogasteraralar1* gene**

28 The developmental expression pattern of *aralar1* in *D. melanogaster* is widely described in  
29 FlyBase, which reports the modENCODE mRNA-Seq temporal expression data (mRNA-Seq\_U,  
30 [89]). Relative data are summarized in Figure 3. In order to integrate these data with the expression  
31 pattern of *aralar1* transcriptional isoforms, we have carried out a Reverse Transcriptase-PCR  
32 analysis (RT-PCR) on total RNA samples isolated from distinct *Drosophila* developmental stages  
33 (Figure 4A) or from dissected adult tissues (Figure 4B).

1  
2  
3  
4  
5  
6  
7  
8  
9  
10  
11  
12  
13  
14  
15  
16  
17  
18  
19  
20  
21  
22  
23  
24  
25  
26  
27  
28  
29  
30  
31  
32  
33  
34  
35  
36  
37  
38  
39  
40  
41  
42  
43  
44  
45  
46  
47  
48  
49  
50  
51  
52  
53  
54  
55  
56  
57  
58  
59  
60  
61  
62  
63  
64  
65

With this aim, we have devised a set of primers specific to easily discriminate the five reported isoforms. Unfortunately, we were not able to find oligos suitable for performing quantitative analysis, so we could only conduct semiquantitative analyses based on RT-PCR. However, RA/RF and RD, cannot be distinguished, due to their nearly identical sequence, as described above. We will refer to *aralar1-RA* to indicate the RA/RD/RF isoforms through this paragraph.

The obtained results have revealed a constitutive expression of *aralar1-RA* transcript throughout development (Figure 4A). By contrast, the expression of the other isoforms is patchy distributed during the development or in different tissues. *Aralar1-RB* isoforms detected in early embryo development, during all the pupal stages and in adults, being only limited to females. Finally, *aralar1-RC* is detected in embryos (at least until 12-15 hours after egg laying), in all the pupal stages and in both sexes during the adult stage, while *aralar1-RE* is expressed in the early-embryo development and in both sexes during the adult stage. Consistent with the expression pattern detected in whole adult males and females, we have found that *aralar1-RA*, *aralar1-RC* and *aralar1-RE* are ubiquitously expressed in all the main fruit fly body regions (namely head, thorax and abdomen), whereas *aralar1-RB* expression is limited to the abdomens of females, due to its ovary-specific expression (Figure 4B).

### 3.5. Bacterial expression and functional characterisation of recombinant Aralar1 proteins

A ClustalW alignment of Drosophila Aralar1 with the human AGC isoforms has revealed that all the proteins conserve the same domain structure organization consisting of an N-terminal domain with 8 EF-hands, a carrier domain and a C-terminal domain with unknown function (Figure 5) [23]. Five out of the six Drosophila Aralar1 protein isoforms do not present any difference in their N-terminal EF-hands and carrier domains (Figure 5). Aralar1-PE diverges from the other isoforms because of an insertion of 12 additional amino acid residues in the loop of its eighth EF-hand (EF-hand 8) [23]. In order to check if this peculiarity may affect its transport activity, we have chosen Aralar1-PE to be biochemically characterized together with Aralar1-PA that also shows a shorter N-terminus similar to that found in Aralar1-PD and Aralar1-PF (Figure 5).

Aralar1-PA and Aralar1-PE have been overexpressed at high levels in *E. coli* BL21(DE3) (Figure 6A, lane 3 for Aralar1-PA, lane 4 for Aralar1-PE). They accumulate as inclusion bodies and have been purified by centrifugation on sucrose gradient and washing (Figure 6A, lane 5 for Aralar1-PA, lane 6 for Aralar1-PE), with a yield of 50 – 60 mg/ml bacterial culture. These proteins have been not revealed in bacterial cells harvested just before the induction of expression (Figure 6A, lane 1 for Aralar1-PA, lane 2 for Aralar1-PE), or in cells harvested after induction but do not carrying the coding sequence for Aralar1-PA and Aralar1-PE in the expression vector (data not shown). Their

1 identities have been assessed by western blot analysis employing a mouse anti-V5 monoclonal  
2 antibody (Figure 6A, lanes 1-6).

3 Aralar1-PA and Aralar1-PE have been functionally reconstituted into liposomes and the orientation  
4 of their N- and C-terminal regions in the proteoliposomes was performed by ELISA assay,  
5 indicating that both termini of Aralar1 proteins reconstituted into the proteoliposomal membrane  
6 protrude toward the outside, which in intact proteoliposomes is the only side of the membrane  
7 accessible to antibodies (Supplementary Figure 2). Aralar1-PA and Aralar1-PE transport activity  
8 have been tested in homo-exchange experiments (same substrate inside and outside). Using external  
9 and internal substrate concentrations of 1 and 10 mM, respectively, both proteins efficiently  
10 catalyze [<sup>14</sup>C]glutamate/glutamate and [<sup>14</sup>C]aspartate/aspartate exchange reactions. A very active  
11 uptake of [<sup>14</sup>C]glutamate and [<sup>14</sup>C]aspartate has also been observed when proteoliposomes had been  
12 preloaded with 10 mM aspartate or glutamate, respectively (hetero-exchange reactions). Both  
13 proteins do not catalyze any homo-exchange of phosphate, ADP, ATP, malonate, malate,  
14 oxoglutarate, ketoisocaproate, citrate, carnitine, ornithine, lysine, arginine, glutathione, choline,  
15 proline, and threonine (data not shown). No [<sup>14</sup>C]glutamate/aspartate exchange has been observed  
16 using boiled Aralar1-PA and Aralar1-PE for incorporation into liposomes or reconstituting  
17 sarcosyl-solubilized bacterial material deriving either from cells not carrying any expression vector  
18 for Aralar1-PA and Aralar1-PE or from cells collected just before the induction of expression.

19 We have displayed kinetics of Aralar1-PA and Aralar1-PE uptake in Figure 6B. Each protein  
20 reconstituted into proteoliposomes contains 10 mM internal glutamate, and uptake has been  
21 measured in the presence of external 0.5 mM [<sup>14</sup>C]glutamate (exchange). Exchange reactions follow  
22 first-order kinetics, and isotopic equilibrium is approached exponentially, maximum uptake is  
23 reached after 90 min (rate constants 0.066 and 0.080 min<sup>-1</sup> and initial rates of 20.78 and 59.51  
24 nmol/min x mg protein for Aralar1-PA and Aralar1-PE, respectively). Conversely, no  
25 [<sup>14</sup>C]glutamate uptake is observed in the absence of an internal substrate (uniport), highlighting that  
26 both proteins are unable to catalyze a unidirectional transport of glutamate (Figure 6B). After 50  
27 min incubation, when radioactive uptake by proteoliposomes has approached equilibrium, the  
28 addition of 20 mM unlabeled aspartate leads to an extensive efflux of radiolabeled glutamate from  
29 glutamate-loaded proteoliposomes (Figure 6B). A similar efflux of labeled substrate is observed by  
30 adding 20 mM unlabeled glutamate (not shown). This efflux further confirms the strict exchange  
31 mechanism catalyzed by Aralar1-PA and Aralar1-PE. The unidirectional transport has been further  
32 investigated in backward experiment, as it provides a more convenient assay [53], i.e., by  
33 measuring the efflux of [<sup>14</sup>C]glutamate from prelabeled active proteoliposomes; in the absence of an  
34 external substrate no efflux of [<sup>14</sup>C]glutamate has been observed, even after 60 minutes of

1 incubation, but an extensive efflux has occurred upon the addition of 10 mM external glutamate or  
2 aspartate (data not shown).

3 Substrate specificity of recombinant Aralar1-PA and Aralar1-PE has been examined in detail by  
4 measuring the uptake of [<sup>14</sup>C]glutamate into proteoliposomes preloaded with different possible  
5 substrates. Table I reports the results of our explorative statistical analysis. Both proteins efficiently  
6 exchange external [<sup>14</sup>C]glutamate for internal L-glutamate or L-aspartate. Aralar1-PA also catalyzes  
7 a lower but significant uptake of [<sup>14</sup>C]glutamate in the presence of internal L-cysteinesulfinate,  
8 whereas no transport activity has been found with L- $\alpha$ -amino adipate, L-glutamine and L-asparagine  
9 (Table I). Differently from Aralar1-PA and yeast AGC [90], but similarly to the human AGC  
10 isoforms [4], Aralar1-PE exchanges external [<sup>14</sup>C]glutamate for internal cysteinesulfinate at the  
11 same rate as aspartate, and it shows a significantly high [<sup>14</sup>C]glutamate uptake in the presence of  
12 internal L- $\alpha$ -amino adipate and L-glutamine. Both isoforms are virtually unable to exchange  
13 [<sup>14</sup>C]glutamate for internal D-aspartate and D-glutamate, indicating a high degree of stereo  
14 specificity.  
15

16 The [<sup>14</sup>C]glutamate/glutamate exchange reactions catalyzed by Aralar1-PA and Aralar1-PE are  
17 hampered by many well-known inhibitors of several MCF members, being completely inhibited by  
18 50  $\mu$ M *p*-chloromercuribenzoate [4] and 1 mM pyrocarbonate [90] (100 and 96% inhibition,  
19 respectively for both proteins) and, to a slightly lesser extent by 50  $\mu$ M mersalyl [76] and 0.1%  
20 tannic acid [53] (80 and 85% inhibition, respectively for both proteins), and also by 1 mM *N*-  
21 ethylmaleimide [53] (40 and 50% inhibition for Aralar1-PA and Aralar1-PE, respectively).  
22 Moreover, 10 mM bathophenanthroline or 0.1 mM bromocresol purple [53] are unable to exert a  
23 significant inhibition. Additionally, no inhibition has been observed with 10  $\mu$ M bongkreikic acid  
24 [68] and 2.5 mM 1,2,3-benzenetricarboxylate [81], which are specific inhibitors of the mitochondrial  
25 ADP/ATP and citrate carrier, respectively.  
26

27 Considering that the AGC-catalyzed aspartate/glutamate antiport reaction is electrogenic [4], the  
28 effect of membrane potential has been examined on the aspartate/glutamate exchange reaction  
29 mediated by our Aralar1 carriers. A K<sup>+</sup> diffusion potential has been created across the membrane of  
30 proteoliposomes using valinomycin/KCl (calculated value  $\sim$ 100 mV, positive inside). In such  
31 conditions, the rates of the [<sup>14</sup>C]aspartate<sub>out</sub>/glutamate<sub>in</sub> exchanges of Aralar1-PA and Aralar1-PE are  
32 stimulated (Table II). In the absence of a membrane potential or when homo-exchanges have been  
33 measured, no effect has been observed. As a consequence, Aralar1-PA and Aralar1-PE are able to  
34 catalyze an electrogenic exchange of aspartate for glutamate.  
35

36 We have determined the kinetic constants of the recombinant purified Aralar1-PA and Aralar1-  
37 PE by measuring the initial transport rate at various external [<sup>14</sup>C]glutamate or [<sup>14</sup>C]aspartate  
38  
39  
40  
41  
42  
43  
44  
45  
46  
47  
48  
49  
50  
51  
52  
53  
54  
55  
56  
57  
58  
59  
60  
61  
62  
63  
64  
65

1 concentrations, in the presence of a constant internal saturating concentration (10 mM) of unlabeled  
2 substrates. In five independent experiments carried out at the same internal and external pH (6.5),  
3 the half-saturation constants ( $K_m$ ) of reconstituted Aralar1-PA and Aralar1-PE for glutamate are  
4  $0.26 \pm 0.03$  and  $0.29 \pm 0.07$  mM, respectively, and for aspartate are  $47 \pm 2.3$  and  $51 \pm 2.6$   $\mu$ M,  
5 respectively. Interestingly, the two isoforms significantly differ in their  $V_{max}$  values, which are  $32.25$   
6  $\pm 1.69$  and  $94.29 \pm 5.40$  nmol/min/mg protein, for Aralar1-PA and Aralar1-PE, respectively for  
7 both substrates. The activity has been normalized by determining the amount of recombinant  
8 proteins recovered into proteoliposomes after reconstitution. We have further analyzed whether the  
9 differences in transport rates (Table I) and  $V_{max}$  values found between the two isoforms could arise  
10 from the 12 additional amino acid residues present in the loop of the helix-loop-helix structure of  
11 the eighth EF-hand (EF-hand 8) of Aralar1-PE. First of all, we have checked, in de-ionized  
12 ultrapure water, the effect of  $Ca^{2+}$  or EGTA (a divalent ion chelator) on Aralar1-PA and Aralar1-PE  
13 transport activity (Figure 6C). The activities of both isoforms are increased of about 35% by the  
14 addition of 1 mM  $CaCl_2$  and diminished by the addition of 0.5 mM EGTA. The inhibitory effect of  
15 EGTA is abolished in the presence of 1 mM  $CaCl_2$  (Figure 6C). These results indicate that both  
16 isoforms are highly sensitive to calcium, since low calcium contamination in the reconstitution  
17 mixture is able to activate transport activity of both isoforms, whereas its removal by a  $Ca^{2+}$   
18 chelator exerts an inhibitory effect. The  $Ca^{2+}$ -dependence of the transport activities of Aralar1-PA  
19 and Aralar1-PE has been further studied by measuring their transport rates as a function of the free  
20  $Ca^{2+}$  concentration (Figure 6D). Both isoforms are highly  $Ca^{2+}$ -sensitive, since Aralar1-PA and  
21 Aralar1-PE have a half-maximal activation of about 0.34 and 0.15  $\mu$ M, respectively.  
22  
23  
24  
25  
26  
27  
28  
29  
30  
31  
32  
33  
34  
35  
36  
37  
38  
39

### 40 **3.6. Influence of the eighth EF-hand on the activity of ARALAR1 PE isoform**

41 Once established that in our reconstituted system calcium is able to regulate transport activity of both  
42 isoforms, we have checked if the shortening of the insertion consisting of 12 additional residues in  
43 Aralar1-PE or the replacement of some residues might affect its transport activity. In particular, the  
44 five positive charged residues (KRRRK from 301 to 305) have been replaced by consecutive  
45 alanine residues (5Ala mutant) or deleted ( $\Delta 5$  mutant). Two further deletions have also been  
46 investigated, the first encompassing residues 301-308 ( $\Delta 8$  mutant), and the second including  
47 residues 299-310 ( $\Delta 12$  mutant); in this latter mutant the insertion characterizing Aralar1-PE has  
48 been completely removed. Substrate specificity of recombinant Aralar1-PE mutants has been  
49 examined in detail by measuring the uptake of [ $^{14}C$ ]glutamate into proteoliposomes preloaded with  
50 different possible substrates. As reported in figure 7, the substitution of the five charged residues  
51 with Ala deeply increases transport activity of all the tested substrates, whereas its deletion  
52  
53  
54  
55  
56  
57  
58  
59  
60  
61  
62  
63  
64  
65

1  
2  
3  
4  
5  
6  
7  
8  
9  
10  
11  
12  
13  
14  
15  
16  
17  
18  
19  
20  
21  
22  
23  
24  
25  
26  
27  
28  
29  
30  
31  
32  
33  
34  
35  
36  
37  
38  
39  
40  
41  
42  
43  
44  
45  
46  
47  
48  
49  
50  
51  
52  
53  
54  
55  
56  
57  
58  
59  
60  
61  
62  
63  
64  
65

decreases transport activity proportionally with the size of the deletion gradually leading Aralar1-PE to have the same substrate specificity of Aralar1-PA. The kinetic constants of the recombinant Aralar1-PE mutants are reported in Table III. The half-saturation constants ( $K_m$ ) of reconstituted mutants do not vary with respect to the wild type, whereas as regards transport activity a significant change has been observed. In particular, 5Ala mutant shows a transport activity three-fold higher than that of the wild-type protein, whereas deletions negatively affect transport activity, which decreases proportionally with the size of the deletion. Interestingly,  $\Delta 12$  mutant exhibits the same transport activity as Aralar1-PA.

### 3.7. Aralar1-PA and Aralar1-PE function as an AGC transporter in *S. cerevisiae*

The yeast *AGC1* null mutant does not grow on oleate even in rich medium [90]. This phenotype is explained since MAS is required for reduction of the cytosolic NADH derived from peroxisomal oleate oxidation [90]. Thus, the expression of a mitochondrial carrier protein able to exchange aspartate with glutamate should abolish the growth defect of the *agc1* $\Delta$  knockout. Aralar1-PA and Aralar1-PE expressed in *AGC1* null cells have fully restored growth of the *agc1* $\Delta$  strain on oleate, similarly to the yeast Agc1p (Figure 8), indicating that both Drosophila proteins function as AGC transporters. By contrast, in *agc1* $\Delta$  cells transformed with the empty vector no growth rescue has been observed.

## Discussion

By allowing the mitochondrial re-oxidation of the cytosolic NADH, the MAS plays a central role in the redox homeostasis and in different metabolisms such as glucose homeostasis and nitrogen metabolism. The MAS requires the concerted functioning of six proteins, two located in the cytosol, the malate dehydrogenase 1 (MDH1) and the aspartate aminotransferase 1 (GOT1), two located in the mitochondrial matrix, the malate dehydrogenase 2 (MDH2) and the aspartate aminotransferase 2 (GOT2), and the last two located in the inner mitochondrial membrane, the aspartate/glutamate and the oxoglutarate/malate (OGC) carriers, which connect MAS cytosolic reactions to the mitochondrial ones. Despite the central role in energetic metabolism, very little is known about MAS components in the fruit fly, and up to date no functional data are available on AGC and OGC. In mammals, there are two genes encoding AGC, *ARALAR*, also known as AGC1, more widely expressed but absent in the liver, and *CITRIN* also known as AGC2, expressed in fewer tissues but present in the liver [24]. By searching the FlyBase database (<http://flybase.org/>) for human AGC homologs, we have found 6 alternatively spliced-isoforms annotated as *aralar1* and none as citrin.



1 The expression profile of *aralar1* transcriptional variants studied in this work suggests that three  
2 isoforms (namely *aralar1-RA/RF* and *aralar1-RD*) are constitutively transcribed throughout the  
3 development and in adult tissues. Due to their overlapping sequences, it is not possible to  
4 discriminate the expression profile of these transcriptional isoforms, which are transcribed from the  
5 innermost promoter. The slight differences observed in their organization suggest that they might  
6 have a different stability (i.e. half-life of their mRNA molecules) due to the length of the 3' UTR  
7 (*aralar1-RD* and *aralar1-RA* isoforms). Similarly, the stability of Aralar1-PF protein, encoded by  
8 *aralar1-RF* transcript (identical to *aralar1-RA* transcript), could be affected by the presence of the  
9 additional 12 amino acids introduced upon the translational read-through process [86].

10 Conversely, *aralar1-RB*, *aralar1-RC* and *aralar1-RE* transcriptional isoforms have a more complex  
11 expression pattern, as described in the Results section. While *aralar1-RB* is undetectable by RT-  
12 PCR in adult males, it can be specifically detected in adult ovary, suggesting its role in oogenesis.  
13 We do not know whether *aralar1-RB* detected during the early embryo development is the result of  
14 a maternal contribution or of the active transcription in embryos, as instead appears evident for  
15 *aralar1-RC* and *aralar1-RE*, which are undetectable in female germline and are present in early  
16 embryo developmental stages. Furthermore, while *aralar1-RC* expression persists in the whole  
17 adult tissues with the exclusion of the germline tissues, *aralar1-RE* expression is confined in the  
18 early stages of embryo development and in somatic adult tissues. The expression of the more active  
19 *aralar1-RE* in the early embryogenesis might be related to the very active aspartate and glutamate  
20 metabolism occurring in this stage [91]. *Aralar1-RB* and *aralar1-RC*, together with the  
21 constitutively expressed isoforms, seem to be also important during metamorphosis. It is  
22 noteworthy that all the *aralar1* transcriptional isoforms contribute to the strong *aralar1* expression  
23 observed in adult fat bodies (mainly located in the abdomen), as can be inferred by the combination  
24 of our results (see Figure 4) and the modENCODE Tissue Expression Data. Fat bodies are  
25 important energy storages and utilization organs in *Drosophila*, as well as in other insects [92], and  
26 they play a fundamental role in the post-metamorphic energy metabolism and egg development.  
27 Taken together, these results suggest that an isoform-specific expression pattern becomes defined  
28 after the initial embryo development, when all the isoforms are transcribed, and its establishment  
29 appears to be important for certain developmental stages or in specific adult tissues.

30 It can be speculated that the observed transcriptional pattern could be related to the presence of two  
31 evolutionary conserved DNA motifs, located between the TSSs of *aralar1-RB* and *aralar1-  
32 RA/RF/RD* transcripts. Although we have not performed functional studies aimed to demonstrate  
33 their involvement in transcriptional regulation, it could be hypothesized that NRG elements might  
34 influence *aralar1* gene expression for two reasons. Firstly, its evolutionary conservation in 23

1 Drosophila species belonging to two distinct sub-genera indicates a constrained role. Indeed, intron  
2 sequences are less conserved, even in related species, and only functionally constrained motifs are  
3 maintained. The divergence between *D. melanogaster* and *D. grimshawi* is thought to have occurred  
4 50Mya (Russo et al. 2003), and the conservation of such putative *cis*-acting sequence suggests a  
5 functional role. The NRG element can also be detected in non-Drosophilidae insects  
6 (Supplementary Table 6), thus enforcing its putative functional role, although its position related to  
7 the expressed transcriptional isoforms in these organisms is not easy to be determined.

8  
9 Secondly, previous studies reported that NRG elements are conserved in a subset of Drosophila  
10 genes encoding mitochondrial proteins, while they have been lost in duplicated genes, which in turn  
11 have acquired testis-specific transcription patterns. Since *alarar1* gene lacks paralogues in *D.*  
12 *melanogaster* (and in all the analyzed Drosophila species), the presence of two NRG elements  
13 within it might have acquired a different role, such as the establishment of a regulated expression  
14 pattern of all, or at least some, of the transcriptional *alarar1* isoforms. In this view, the two NRG  
15 elements detected could act either cooperatively or independently, as positive or negative  
16 regulators. Whether or not the two NRG elements are functional to *alarar1* expression cannot be  
17 determined without the aid of mutant or transgenic strains carrying *alarar1* genes containing  
18 disrupted NRG elements, which necessarily calls for future analyses.

19  
20 In order to verify if this complex tissue- and developmental stage-specific transcriptional regulation  
21 is associated to the expression of functionally different isoforms, the transport properties of Aralar1-  
22 PA and Aralar1-PE, representing the two main encoded products of all *alarar1* transcripts, have  
23 been determined. The two recombinant proteins, once reconstituted into liposomes, catalyze a very  
24 efficient aspartate/glutamate electrogenic exchange reaction and are able to restore the yeast defect  
25 of the *AGC1* null gene (Figure 8), confirming their identity as the *D. melanogaster* mitochondrial  
26 AGC. Similarly to the human isoforms [4], fruit fly Aralar1 isoforms do not show any significant  
27 difference in their substrate affinity, moreover, as the human isoforms, the Km value for aspartate  
28 was significantly lower than that for glutamate. Interestingly, although Aralar1-PA and Aralar1-PE  
29 differ only in their N-terminal halves, i.e., region known to interact with calcium [23], they showed  
30 a significant different specific activity, being Aralar1-PE more active than Aralar1-PA. A similar  
31 situation had been previously found in *H. sapiens*, where citrin resulted more active than aralar [4].  
32 Although fruit fly and human AGC isoforms showed this overlapping behavior, it should be  
33 emphasized that the different specific activities found in the latter are mainly due to their different  
34 carrier domains [4], whereas all *D. melanogaster* AGC isoforms share the same carrier domain and  
35 differ in their N-terminal domains. In fact, the recombinant carrier domain reconstituted into  
36 liposomes, shows the same kinetic properties of Aralar1-PA (data not shown).

1  
2  
3  
4  
5  
6  
7  
8  
9  
10  
11  
12  
13  
14  
15  
16  
17  
18  
19  
20  
21  
22  
23  
24  
25  
26  
27  
28  
29  
30  
31  
32  
33  
34  
35  
36  
37  
38  
39  
40  
41  
42  
43  
44  
45  
46  
47  
48  
49  
50  
51  
52  
53  
54  
55  
56  
57  
58  
59  
60  
61  
62  
63  
64  
65

Interestingly, this N-terminal domain was also able to alter substrate specificity of the fruit fly AGC isoforms; since Aralar1-PE, similarly to human citrin [4], is able to exchange glutamate against cysteinesulfinatate at the same rate as that of aspartate, while Aralar1-PA, similarly to human aralar, shows a glutamate/cysteinesulfinatate exchange rate about one half lower than that of glutamate/aspartate. Furthermore, Aralar1-PE, differently from Aralar1-PA, significantly exchanges glutamate for L- $\alpha$ -aminoadipate and L-glutamine, suggesting a wider range of substrate specificity if compared to the latter.

A ClustalW alignment of *Drosophila* Aralar1 with human AGC isoforms has clarified that all proteins conserved the same structural organization including an N-terminal domain having 8 EF-hands with different functions (i.e. EF-hands 1-3 constitute a calcium-responsive unit, whereas EF-hands 4-8 are part of a static unit), a carrier domain and a C-terminal domain with unknown role (Figure 5) [23]. Furthermore, calcium (EF-hands 1-3) and substrate binding sites are almost completely conserved between man and *Drosophila*, with a single conservative variation present in the calcium-binding site, where a threonine was replaced by a serine in the fruit fly isoforms (Figure 5). The most variable regions in the fruit fly Aralar1 isoforms are located in the N-terminus and into the loop of the helix-loop-helix structure of EF-hand 8 (Figure 5, green shaded) [23], where Aralar1-PE has an extra highly positive charged amino acid sequence. In the light of this observation, it is evident that N-terminus variations could play a fundamental role on the functional differences found between Aralar1-PA and Aralar1-PE. Site-direct mutagenesis experiments conducted on this additional region in EF-hand 8 have showed that the substitution of the charged residues by alanine can significantly affect substrate specificity and increase initial transport rate, whereas the progressive removal of these extra amino acids reduce initial transport rate and change substrate specificity until making Aralar1-PE similar to Aralar1-PA. Furthermore, this data are in agreement with the role proposed for the human AGC isoforms, in which the EF-hands 1–3 form a calcium-responsive mobile unit, EF-hands 4–8 form a static unit while the N-terminus region, external to the first EF-hand motif, seems not to be involved in any crucial regulatory function [23]. Finally, we have demonstrated that both proteins are Ca<sup>2+</sup>-dependent, and similarly to citrin, Aralar1-PE shows a higher sensitivity to calcium being S<sub>0.5</sub> about 2 times lower than that of Aralar1-PA. Hence, biochemical characterization and calcium sensitivity have identified Aralar1-PA and Aralar1-PE as the human aralar and citrin counterparts, respectively (Figure 6 C-D).

The functional characterization of the fruit fly mitochondrial AGC transporter represents a crucial step toward a complete understanding of the metabolic events acting during early embryogenesis, and it might strengthen the use of *D. melanogaster* as a model for genetics and developmental biology. Nevertheless, further studies of gain and loss of function are required to better understand

1  
2 how the complex transcriptional and expression patterns of Aralar1 regulates specific metabolic  
3 pathways in the different developmental stages of the fruit fly.  
4

## 5 **Acknowledgements**

6 This work was supported by Associazione Italiana per la Ricerca sul Cancro (FG grant n.  
7 15404/2014); by the Italian Ministero dell'Istruzione, dell'Università e della Ricerca, MIUR,  
8 2017PAB8EM\_003; Drosophila clones were provided by Drosophila Genomics Resource Center  
9 NIH grant 2P40OD010949. The authors acknowledge “Sistema Integrato di Laboratori per  
10 L’Ambiente — SILA for providing lab tools.  
11  
12  
13

## 14 **References**

- 15  
16 [1] R. Curcio, P. Lunetti, V. Zara, A. Ferramosca, F. Marra, G. Fiermonte, A.R. Cappello, F. De  
17 Leonardis, L. Capobianco, V. Dolce, Drosophila melanogaster Mitochondrial Carriers: Similarities  
18 and Differences with the Human Carriers, *Int J Mol Sci* 21(17) (2020).  
19 [2] F. Palmieri, The mitochondrial transporter family SLC25: identification, properties and  
20 physiopathology, *Molecular aspects of medicine* 34(2-3) (2013) 465-84.  
21 [3] F. Palmieri, M. Monne, Discoveries, metabolic roles and diseases of mitochondrial carriers: A  
22 review, *Biochimica et biophysica acta* 1863(10) (2016) 2362-78.  
23 [4] L. Palmieri, B. Pardo, F.M. Lasorsa, A. del Arco, K. Kobayashi, M. Iijima, M.J. Runswick, J.E.  
24 Walker, T. Saheki, J. Satrustegui, F. Palmieri, Citrin and aralar1 are Ca(2+)-stimulated  
25 aspartate/glutamate transporters in mitochondria, *The EMBO journal* 20(18) (2001) 5060-9.  
26 [5] F. Palmieri, The mitochondrial transporter family (SLC25): physiological and pathological  
27 implications, *Pflugers Arch* 447(5) (2004) 689-709.  
28 [6] B. Pardo, L. Contreras, A. Serrano, M. Ramos, K. Kobayashi, M. Iijima, T. Saheki, J.  
29 Satrustegui, Essential role of aralar in the transduction of small Ca<sup>2+</sup> signals to neuronal  
30 mitochondria, *The Journal of biological chemistry* 281(2) (2006) 1039-47.  
31 [7] F.M. Lasorsa, P. Pinton, L. Palmieri, G. Fiermonte, R. Rizzuto, F. Palmieri, Recombinant  
32 expression of the Ca(2+)-sensitive aspartate/glutamate carrier increases mitochondrial ATP  
33 production in agonist-stimulated Chinese hamster ovary cells, *The Journal of biological chemistry*  
34 278(40) (2003) 38686-92.  
35 [8] F.N. Gellerich, Z. Gizatullina, O. Arandarcikaite, D. Jerzembek, S. Vielhaber, E. Seppet, F.  
36 Striggow, Extramitochondrial Ca<sup>2+</sup> in the nanomolar range regulates glutamate-dependent  
37 oxidative phosphorylation on demand, *PloS one* 4(12) (2009) e8181.  
38 [9] I. Llorente-Folch, C.B. Rueda, I. Amigo, A. del Arco, T. Saheki, B. Pardo, J. Satrustegui,  
39 Calcium-regulation of mitochondrial respiration maintains ATP homeostasis and requires  
40 ARALAR/AGC1-malate aspartate shuttle in intact cortical neurons, *The Journal of neuroscience :*  
41 *the official journal of the Society for Neuroscience* 33(35) (2013) 13957-71, 13971a.  
42 [10] B. Rubi, A. del Arco, C. Bartley, J. Satrustegui, P. Maechler, The malate-aspartate NADH  
43 shuttle member Aralar1 determines glucose metabolic fate, mitochondrial activity, and insulin  
44 secretion in beta cells, *The Journal of biological chemistry* 279(53) (2004) 55659-66.  
45 [11] M. Lane, D.K. Gardner, Mitochondrial malate-aspartate shuttle regulates mouse embryo  
46 nutrient consumption, *The Journal of biological chemistry* 280(18) (2005) 18361-7.  
47 [12] N. Moscatelli, P. Lunetti, C. Braccia, A. Armirotti, F. Pisanello, M. De Vittorio, V. Zara, A.  
48 Ferramosca, Comparative Proteomic Analysis of Proteins Involved in Bioenergetics Pathways  
49 Associated with Human Sperm Motility, *Int J Mol Sci* 20(12) (2019).  
50 [13] M. Ramos, B. Pardo, I. Llorente-Folch, T. Saheki, A. Del Arco, J. Satrustegui, Deficiency of  
51 the mitochondrial transporter of aspartate/glutamate aralar/AGC1 causes hypomyelination and  
52 neuronal defects unrelated to myelin deficits in mouse brain, *Journal of neuroscience research*  
53 89(12) (2011) 2008-17.  
54  
55  
56  
57  
58  
59  
60  
61  
62  
63  
64  
65

- 1 [14] E. Profilo, L.E. Pena-Altamira, M. Corricelli, A. Castegna, A. Danese, G. Agrimi, S. Petralla,  
2 G. Giannuzzi, V. Porcelli, L. Sbano, C. Viscomi, F. Massenzio, E.M. Palmieri, C. Giorgi, G.  
3 Fiermonte, M. Virgili, L. Palmieri, M. Zeviani, P. Pinton, B. Monti, F. Palmieri, F.M. Lasorsa,  
4 Down-regulation of the mitochondrial aspartate-glutamate carrier isoform 1 AGC1 inhibits  
5 proliferation and N-acetylaspartate synthesis in Neuro2A cells, *Biochimica et biophysica acta*  
6 1863(6) (2017) 1422-1435.
- 7 [15] R. Wibom, F.M. Lasorsa, V. Tohonen, M. Barbaro, F.H. Sterky, T. Kucinski, K. Naess, M.  
8 Jonsson, C.L. Pierri, F. Palmieri, A. Wedell, AGC1 deficiency associated with global cerebral  
9 hypomyelination, *The New England journal of medicine* 361(5) (2009) 489-95.
- 10 [16] M.A. Jalil, L. Begum, L. Contreras, B. Pardo, M. Iijima, M.X. Li, M. Ramos, P. Marmol, M.  
11 Horiuchi, K. Shimotsu, S. Nakagawa, A. Okubo, M. Sameshima, Y. Isashiki, A. Del Arco, K.  
12 Kobayashi, J. Satrustegui, T. Saheki, Reduced N-acetylaspartate levels in mice lacking aralar, a  
13 brain- and muscle-type mitochondrial aspartate-glutamate carrier, *The Journal of biological*  
14 *chemistry* 280(35) (2005) 31333-9.
- 15 [17] B. Pardo, L. Contreras, J. Satrustegui, De novo Synthesis of Glial Glutamate and Glutamine in  
16 Young Mice Requires Aspartate Provided by the Neuronal Mitochondrial Aspartate-Glutamate  
17 Carrier Aralar/AGC1, *Frontiers in endocrinology* 4 (2013) 149.
- 18 [18] J.M. Thornburg, K.K. Nelson, B.F. Clem, A.N. Lane, S. Arumugam, A. Simmons, J.W. Eaton,  
19 S. Telang, J. Chesney, Targeting aspartate aminotransferase in breast cancer, *Breast cancer research*  
20 : BCR 10(5) (2008) R84.
- 21 [19] C. Wang, H. Chen, M. Zhang, J. Zhang, X. Wei, W. Ying, Malate-aspartate shuttle inhibitor  
22 aminooxyacetic acid leads to decreased intracellular ATP levels and altered cell cycle of C6 glioma  
23 cells by inhibiting glycolysis, *Cancer letters* 378(1) (2016) 1-7.
- 24 [20] F. Palmieri, I. Stipani, V. Iacobazzi, The transport of L-cysteinesulfinatate in rat liver  
25 mitochondria, *Biochimica et biophysica acta* 555(3) (1979) 531-46.
- 26 [21] T. Ubuka, A. Okada, H. Nakamura, Production of hypotaurine from L-cysteinesulfinatate by rat  
27 liver mitochondria, *Amino acids* 35(1) (2008) 53-8.
- 28 [22] K. Kobayashi, D.S. Sinasac, M. Iijima, A.P. Boright, L. Begum, J.R. Lee, T. Yasuda, S. Ikeda,  
29 R. Hirano, H. Terazono, M.A. Crackower, I. Kondo, L.C. Tsui, S.W. Scherer, T. Saheki, The gene  
30 mutated in adult-onset type II citrullinaemia encodes a putative mitochondrial carrier protein, *Nat*  
31 *Genet* 22(2) (1999) 159-63.
- 32 [23] C. Thangaratnarajah, J.J. Ruprecht, E.R. Kunji, Calcium-induced conformational changes of  
33 the regulatory domain of human mitochondrial aspartate/glutamate carriers, *Nature communications*  
34 5 (2014) 5491.
- 35 [24] A. del Arco, J. Morcillo, J.R. Martinez-Morales, C. Galian, V. Martos, P. Bovolenta, J.  
36 Satrustegui, Expression of the aspartate/glutamate mitochondrial carriers aralar1 and citrin during  
37 development and in adult rat tissues, *European journal of biochemistry* 269(13) (2002) 3313-20.
- 38 [25] J. Liu, A. Yang, Q. Zhang, G. Yang, W. Yang, H. Lei, J. Quan, F. Qu, M. Wang, Z. Zhang, K.  
39 Yu, Association between genetic variants in SLC25A12 and risk of autism spectrum disorders: An  
40 integrated meta-analysis, *American journal of medical genetics. Part B, Neuropsychiatric genetics :*  
41 *the official publication of the International Society of Psychiatric Genetics* 168B(4) (2015) 236-46.
- 42 [26] J. Du, A. Rountree, W.M. Cleghorn, L. Contreras, K.J. Lindsay, M. Sadilek, H. Gu, D.  
43 Djukovic, D. Raftery, J. Satrustegui, M. Kanow, L. Chan, S.H. Tsang, I.R. Sweet, J.B. Hurley,  
44 Phototransduction Influences Metabolic Flux and Nucleotide Metabolism in Mouse Retina, *The*  
45 *Journal of biological chemistry* 291(9) (2016) 4698-710.
- 46 [27] L. Contreras, L. Ramirez, J. Du, J.B. Hurley, J. Satrustegui, P. de la Villa, Deficient glucose  
47 and glutamine metabolism in Aralar/AGC1/Slc25a12 knockout mice contributes to altered visual  
48 function, *Mol Vis* 22 (2016) 1198-1212.
- 49 [28] I. Llorente-Folch, C.B. Rueda, I. Perez-Liebana, J. Satrustegui, B. Pardo, L-Lactate-Mediated  
50 Neuroprotection against Glutamate-Induced Excitotoxicity Requires ARALAR/AGC1, *The Journal*  
51 *of neuroscience : the official journal of the Society for Neuroscience* 36(16) (2016) 4443-56.
- 52  
53  
54  
55  
56  
57  
58  
59  
60  
61  
62  
63  
64  
65

- 1 [29] C.B. Rueda, I. Llorente-Folch, J. Traba, I. Amigo, P. Gonzalez-Sanchez, L. Contreras, I.  
2 Juaristi, P. Martinez-Valero, B. Pardo, A. Del Arco, J. Satrustegui, Glutamate excitotoxicity and  
3 Ca<sup>2+</sup>-regulation of respiration: Role of the Ca<sup>2+</sup> activated mitochondrial transporters (CaMCs),  
4 *Biochimica et biophysica acta* 1857(8) (2016) 1158-1166.
- 5 [30] L. Palmieri, V. Papaleo, V. Porcelli, P. Scarcia, L. Gaita, R. Sacco, J. Hager, F. Rousseau, P.  
6 Curatolo, B. Manzi, R. Militerni, C. Bravaccio, S. Trillo, C. Schneider, R. Melmed, M. Elia, C.  
7 Lenti, M. Saccani, T. Pascucci, S. Puglisi-Allegra, K.L. Reichelt, A.M. Persico, Altered calcium  
8 homeostasis in autism-spectrum disorders: evidence from biochemical and genetic studies of the  
9 mitochondrial aspartate/glutamate carrier AGC1, *Molecular psychiatry* 15(1) (2010) 38-52.
- 10 [31] N. Ramoz, J.G. Reichert, C.J. Smith, J.M. Silverman, I.N. Bespalova, K.L. Davis, J.D.  
11 Buxbaum, Linkage and association of the mitochondrial aspartate/glutamate carrier SLC25A12  
12 gene with autism, *The American journal of psychiatry* 161(4) (2004) 662-9.
- 13 [32] J.A. Turunen, K. Rehnstrom, H. Kilpinen, M. Kuokkanen, E. Kempas, T. Ylisaukko-Oja,  
14 Mitochondrial aspartate/glutamate carrier SLC25A12 gene is associated with autism, *Autism*  
15 *research : official journal of the International Society for Autism Research* 1(3) (2008) 189-92.
- 16 [33] M.J. Falk, D. Li, X. Gai, E. McCormick, E. Place, F.M. Lasorsa, F.G. Otieno, C. Hou, C.E.  
17 Kim, N. Abdel-Magid, L. Vazquez, F.D. Mentch, R. Chiavacci, J. Liang, X. Liu, H. Jiang, G.  
18 Giannuzzi, E.D. Marsh, Y. Guo, L. Tian, F. Palmieri, H. Hakonarson, Erratum to: AGC1  
19 Deficiency Causes Infantile Epilepsy, Abnormal Myelination, and Reduced N-Acetylaspartate,  
20 *JIMD reports* 14 (2014) 119.
- 21 [34] T. Saheki, K. Kobayashi, M. Iijima, M. Horiuchi, L. Begum, M.A. Jalil, M.X. Li, Y.B. Lu, M.  
22 Ushikai, A. Tabata, M. Moriyama, K.J. Hsiao, Y. Yang, Adult-onset type II citrullinemia and  
23 idiopathic neonatal hepatitis caused by citrin deficiency: involvement of the aspartate glutamate  
24 carrier for urea synthesis and maintenance of the urea cycle, *Molecular genetics and metabolism* 81  
25 Suppl 1 (2004) S20-6.
- 26 [35] Z.H. Zhang, Z.G. Yang, F.P. Chen, A. Kikuchi, Z.H. Liu, L.Z. Kuang, W.M. Li, Y.Z. Song, S.  
27 Kure, T. Saheki, Screening for five prevalent mutations of SLC25A13 gene in Guangdong, China: a  
28 molecular epidemiologic survey of citrin deficiency, *The Tohoku journal of experimental medicine*  
29 233(4) (2014) 275-81.
- 30 [36] Y.Z. Song, Z.H. Zhang, W.X. Lin, X.J. Zhao, M. Deng, Y.L. Ma, L. Guo, F.P. Chen, X.L.  
31 Long, X.L. He, Y. Sunada, S. Soneda, A. Nakatomi, S. Dateki, L.H. Ngu, K. Kobayashi, T. Saheki,  
32 SLC25A13 gene analysis in citrin deficiency: sixteen novel mutations in East Asian patients, and  
33 the mutation distribution in a large pediatric cohort in China, *PloS one* 8(9) (2013) e74544.
- 34 [37] Y.Z. Song, M. Deng, F.P. Chen, F. Wen, L. Guo, S.L. Cao, J. Gong, H. Xu, G.Y. Jiang, L.  
35 Zhong, K. Kobayashi, T. Saheki, Z.N. Wang, Genotypic and phenotypic features of citrin  
36 deficiency: five-year experience in a Chinese pediatric center, *International journal of molecular*  
37 *medicine* 28(1) (2011) 33-40.
- 38 [38] G. Fiermonte, G. Parisi, D. Martinelli, F. De Leonardis, G. Torre, C.L. Pierri, A. Saccari, F.M.  
39 Lasorsa, A. Voza, F. Palmieri, C. Dionisi-Vici, A new Caucasian case of neonatal intrahepatic  
40 cholestasis caused by citrin deficiency (NICCD): a clinical, molecular, and functional study,  
41 *Molecular genetics and metabolism* 104(4) (2011) 501-6.
- 42 [39] G. Fiermonte, D. Soon, A. Chaudhuri, E. Paradies, P.J. Lee, S. Krywawych, F. Palmieri, R.H.  
43 Lachmann, An adult with type 2 citrullinemia presenting in Europe, *The New England journal of*  
44 *medicine* 358(13) (2008) 1408-9.
- 45 [40] T. Saheki, Y.Z. Song, Citrin Deficiency, in: M.P. Adam, H.H. Ardinger, R.A. Pagon, S.E.  
46 Wallace, L.J.H. Bean, K. Stephens, A. Amemiya (Eds.), *GeneReviews((R))*, Seattle (WA), 1993.
- 47 [41] A. Del Arco, M. Agudo, J. Satrustegui, Characterization of a second member of the subfamily  
48 of calcium-binding mitochondrial carriers expressed in human non-excitabile tissues, *The*  
49 *Biochemical journal* 345 Pt 3 (2000) 725-32.

- 1 [42] I. Campos, J.A. Geiger, A.C. Santos, V. Carlos, A. Jacinto, Genetic screen in *Drosophila*  
2 *melanogaster* uncovers a novel set of genes required for embryonic epithelial repair, *Genetics*  
3 184(1) (2010) 129-40.
- 4 [43] C.L. Dilda, T.F. Mackay, The genetic architecture of *Drosophila* sensory bristle number,  
5 *Genetics* 162(4) (2002) 1655-74.
- 6 [44] H. Okada, H.A. Ebhardt, S.C. Vonesch, R. Aebersold, E. Hafen, Proteome-wide association  
7 studies identify biochemical modules associated with a wing-size phenotype in *Drosophila*  
8 *melanogaster*, *Nature communications* 7 (2016) 12649.
- 9 [45] M.D. Brand, J.L. Pakay, A. Ocloo, J. Kokoszka, D.C. Wallace, P.S. Brookes, E.J. Cornwall,  
10 The basal proton conductance of mitochondria depends on adenine nucleotide translocase content,  
11 *The Biochemical journal* 392(Pt 2) (2005) 353-62.
- 12 [46] I.M. Sokolova, E.P. Sokolov, Evolution of mitochondrial uncoupling proteins: novel  
13 invertebrate UCP homologues suggest early evolutionary divergence of the UCP family, *FEBS*  
14 *letters* 579(2) (2005) 313-7.
- 15 [47] M. Ulgherait, A. Chen, S.F. McAllister, H.X. Kim, R. Delventhal, C.R. Wayne, C.J. Garcia, Y.  
16 Recinos, M. Oliva, J.C. Canman, M. Picard, E. Owusu-Ansah, M. Shirasu-Hiza, Circadian  
17 regulation of mitochondrial uncoupling and lifespan, *Nature communications* 11(1) (2020) 1927.
- 18 [48] D. Iacopetta, M. Madeo, G. Tasco, C. Carrisi, R. Curcio, E. Martello, R. Casadio, L.  
19 Capobianco, V. Dolce, A novel subfamily of mitochondrial dicarboxylate carriers from *Drosophila*  
20 *melanogaster*: biochemical and computational studies, *Biochimica et biophysica acta* 1807(3)  
21 (2011) 251-61.
- 22 [49] D. Iacopetta, C. Carrisi, G. De Filippis, V.M. Calcagnile, A.R. Cappello, A. Chimento, R.  
23 Curcio, A. Santoro, A. Voza, V. Dolce, F. Palmieri, L. Capobianco, The biochemical properties of  
24 the mitochondrial thiamine pyrophosphate carrier from *Drosophila melanogaster*, *FEBS J* 277(5)  
25 (2010) 1172-81.
- 26 [50] C. Carrisi, D. Antonucci, P. Lunetti, D. Migoni, C.R. Girelli, V. Dolce, F.P. Fanizzi, M.  
27 Benedetti, L. Capobianco, Transport of platinum bonded nucleotides into proteoliposomes,  
28 mediated by *Drosophila melanogaster* thiamine pyrophosphate carrier protein (DmTpc1), *J Inorg*  
29 *Biochem* 130 (2014) 28-31.
- 30 [51] P. Lunetti, A.R. Cappello, R.M. Marsano, C.L. Pierri, C. Carrisi, E. Martello, C. Caggese, V.  
31 Dolce, L. Capobianco, Mitochondrial glutamate carriers from *Drosophila melanogaster*:  
32 biochemical, evolutionary and modeling studies, *Biochimica et biophysica acta* 1827(10) (2013)  
33 1245-55.
- 34 [52] A. Louvi, S.G. Tsilou, A cDNA clone encoding the ADP/ATP translocase of *Drosophila*  
35 *melanogaster* shows a high degree of similarity with the mammalian ADP/ATP translocases, *J Mol*  
36 *Evol* 35(1) (1992) 44-50.
- 37 [53] A. Voza, F. De Leonadis, E. Paradies, A. De Grassi, C.L. Pierri, G. Parisi, C.M. Marobbio,  
38 F.M. Lasorsa, L. Muto, L. Capobianco, V. Dolce, S. Raho, G. Fiermonte, Biochemical  
39 characterization of a new mitochondrial transporter of dephosphocoenzyme A in *Drosophila*  
40 *melanogaster*, *Biochimica et biophysica acta* 1858(2) (2017) 137-146.
- 41 [54] J.P. Venables, J. Tazi, F. Juge, Regulated functional alternative splicing in *Drosophila*, *Nucleic*  
42 *acids research* 40(1) (2012) 1-10.
- 43 [55] V. Zara, V. Dolce, L. Capobianco, A. Ferramosca, P. Papatheodorou, J. Rassow, F. Palmieri,  
44 Biogenesis of eel liver citrate carrier (CIC): negative charges can substitute for positive charges in  
45 the presequence, *Journal of molecular biology* 365(4) (2007) 958-67.
- 46 [56] G. Moreno-Hagelsieb, K. Latimer, Choosing BLAST options for better detection of orthologs  
47 as reciprocal best hits, *Bioinformatics* 24(3) (2008) 319-24.
- 48 [57] C. Burge, S. Karlin, Prediction of complete gene structures in human genomic DNA, *Journal of*  
49 *molecular biology* 268(1) (1997) 78-94.
- 50 [58] R. Carrozzo, A. Torraco, G. Fiermonte, D. Martinelli, M. Di Nottia, T. Rizza, A. Voza, D.  
51 Verrigni, D. Diodato, G. Parisi, A. Maiorana, C. Rizzo, C.L. Pierri, S. Zucano, F. Piemonte, E.

1 Bertini, C. Dionisi-Vici, Riboflavin responsive mitochondrial myopathy is a new phenotype of  
2 dihydrolipoamide dehydrogenase deficiency. The chaperon-like effect of vitamin B2,  
3 Mitochondrion 18 (2014) 49-57.

4 [59] A.R. Cappello, R. Curcio, R. Lappano, M. Maggiolini, V. Dolce, The Physiopathological Role  
5 of the Exchangers Belonging to the SLC37 Family, Front Chem 6 (2018) 122.

6 [60] D. Porcelli, P. Barsanti, G. Pesole, C. Caggese, The nuclear OXPHOS genes in insecta: a  
7 common evolutionary origin, a common cis-regulatory motif, a common destiny for gene  
8 duplicates, BMC Evol Biol 7 (2007) 215.

9 [61] S. Avino, P. De Marco, F. Cirillo, M.F. Santolla, E.M. De Francesco, M.G. Perri, D.  
10 Rigracciolo, V. Dolce, A. Belfiore, M. Maggiolini, R. Lappano, A. Vivacqua, Stimulatory actions  
11 of IGF-I are mediated by IGF-IR cross-talk with GPER and DDR1 in mesothelioma and lung  
12 cancer cells, Oncotarget 7(33) (2016) 52710-52728.

13 [62] V. Bartella, E.M. De Francesco, M.G. Perri, R. Curcio, V. Dolce, M. Maggiolini, A. Vivacqua,  
14 The G protein estrogen receptor (GPER) is regulated by endothelin-1 mediated signaling in cancer  
15 cells, Cellular signalling 28(2) (2016) 61-71.

16 [63] A. Santoro, A.R. Cappello, M. Madeo, E. Martello, D. Iacopetta, V. Dolce, Interaction of  
17 fosfomycin with the glycerol 3-phosphate transporter of Escherichia coli, Biochimica et biophysica  
18 acta 1810(12) (2011) 1323-9.

19 [64] S.N. Ho, H.D. Hunt, R.M. Horton, J.K. Pullen, L.R. Pease, Site-directed mutagenesis by  
20 overlap extension using the polymerase chain reaction, Gene 77(1) (1989) 51-9.

21 [65] D. Bonofiglio, A. Santoro, E. Martello, D. Vizza, D. Rovito, A.R. Cappello, I. Barone, C.  
22 Giordano, S. Panza, S. Catalano, V. Iacobazzi, V. Dolce, S. Ando, Mechanisms of divergent effects  
23 of activated peroxisome proliferator-activated receptor-gamma on mitochondrial citrate carrier  
24 expression in 3T3-L1 fibroblasts and mature adipocytes, Biochimica et biophysica acta 1831(6)  
25 (2013) 1027-36.

26 [66] A. Napoli, D. Aiello, G. Aiello, M.S. Cappello, L. Di Donna, F. Mazzotti, S. Materazzi, M.  
27 Fiorillo, G. Sindona, Mass spectrometry-based proteomic approach in Oenococcus oeni enological  
28 starter, Journal of proteome research 13(6) (2014) 2856-66.

29 [67] R. Curcio, D. Aiello, A. Voza, L. Muto, E. Martello, A.R. Cappello, L. Capobianco, G.  
30 Fiermonte, C. Siciliano, A. Napoli, V. Dolce, Cloning, Purification, and Characterization of the  
31 Catalytic C-Terminal Domain of the Human 3-Hydroxy-3-methyl glutaryl-CoA Reductase: An  
32 Effective, Fast, and Easy Method for Testing Hypocholesterolemic Compounds, Mol Biotechnol  
33 62(2) (2020) 119-131.

34 [68] V. Kurauskas, A. Hessel, P. Ma, P. Lunetti, K. Weinhaupl, L. Imbert, B. Brutscher, M.S. King,  
35 R. Sounier, V. Dolce, E.R.S. Kunji, L. Capobianco, C. Chipot, F. Dehez, B. Bersch, P. Schanda,  
36 How Detergent Impacts Membrane Proteins: Atomic-Level Views of Mitochondrial Carriers in  
37 Dodecylphosphocholine, The journal of physical chemistry letters 9(5) (2018) 933-938.

38 [69] R. Curcio, L. Muto, C.L. Pierri, A. Montalto, G. Lauria, A. Onofrio, M. Fiorillo, G. Fiermonte,  
39 P. Lunetti, A. Voza, L. Capobianco, A.R. Cappello, V. Dolce, New insights about the structural  
40 rearrangements required for substrate translocation in the bovine mitochondrial oxoglutarate carrier,  
41 Biochimica et biophysica acta 1864(11) (2016) 1473-80.

42 [70] Y. Li, A.R. Cappello, L. Muto, E. Martello, M. Madeo, R. Curcio, P. Lunetti, S. Raho, F.  
43 Zaffino, L. Frattaruolo, R. Lappano, R. Malivindi, M. Maggiolini, D. Aiello, C. Piazzolla, L.  
44 Capobianco, G. Fiermonte, V. Dolce, Functional characterization of the partially purified Sac1p  
45 independent adenine nucleotide transport system (ANTS) from yeast endoplasmic reticulum, J  
46 Biochem 164(4) (2018) 313-322.

47 [71] F. Palmieri, M. Klingenberg, Direct methods for measuring metabolite transport and  
48 distribution in mitochondria, Methods Enzymol 56 (1979) 279-301.

49 [72] L. Contreras, P. Gomez-Puertas, M. Iijima, K. Kobayashi, T. Saheki, J. Satrustegui, Ca<sup>2+</sup>  
50 Activation kinetics of the two aspartate-glutamate mitochondrial carriers, aralar and citrin: role in  
51  
52  
53  
54  
55  
56  
57  
58  
59  
60  
61  
62  
63  
64  
65



1 the heart malate-aspartate NADH shuttle, *The Journal of biological chemistry* 282(10) (2007) 7098-  
2 106.

3 [73] S. Raho, L. Capobianco, R. Malivindi, A. Vozza, C. Piazzolla, F. De Leonadis, R.  
4 Gorgoglione, P. Scarcia, F. Pezzuto, G. Agrimi, S.N. Barile, I. Pisano, S.J. Reshkin, M.R. Greco,  
5 R.A. Cardone, V. Rago, Y. Li, C.M.T. Marobbio, W. Sommergruber, C.L. Riley, F.M. Lasorsa, E.  
6 Mills, M.C. Vegliante, G.E. De Benedetto, D. Fratantonio, L. Palmieri, V. Dolce, G. Fiermonte,  
7 KRAS-regulated glutamine metabolism requires UCP2-mediated aspartate transport to support  
8 pancreatic cancer growth, *Nat Metab* 2(12) (2020) 1373-1381.

9 [74] H. Ito, Y. Fukuda, K. Murata, A. Kimura, Transformation of intact yeast cells treated with  
10 alkali cations, *J Bacteriol* 153(1) (1983) 163-8.

11 [75] L. Frattaruolo, M. Fiorillo, M. Brindisi, R. Curcio, V. Dolce, R. Lacret, A.W. Truman, F.  
12 Sotgia, M.P. Lisanti, A.R. Cappello, Thioalbamide, A Thioamidated Peptide from *Amycolatopsis*  
13 *alba*, Affects Tumor Growth and Stemness by Inducing Metabolic Dysfunction and Oxidative  
14 Stress, *Cells* 8(11) (2019).

15 [76] M. Madeo, C. Carrisi, D. Iacopetta, L. Capobianco, A.R. Cappello, C. Bucci, F. Palmieri, G.  
16 Mazzeo, A. Montalto, V. Dolce, Abundant expression and purification of biologically active  
17 mitochondrial citrate carrier in baculovirus-infected insect cells, *Journal of bioenergetics and*  
18 *biomembranes* 41(3) (2009) 289-97.

19 [77] J. Dandurand, A. Ostuni, M.F. Armentano, M.A. Crudele, V. Dolce, F. Marra, V. Samouillan,  
20 F. Bisaccia, Calorimetry and FTIR reveal the ability of URG7 protein to modify the aggregation  
21 state of both cell lysate and amylogenic  $\alpha$ -synuclein, *AIMS Biophysics* 7(3) (2020) 189-203.

22 [78] O.I. Parisi, M. Fiorillo, L. Scrivano, M.S. Sinicropi, V. Dolce, D. Iacopetta, F. Puoci, A.R.  
23 Cappello, Sericin/Poly(ethylcyanoacrylate) Nanospheres by Interfacial Polymerization for  
24 Enhanced Bioefficacy of Fenofibrate: In Vitro and In Vivo Studies, *Biomacromolecules* 16(10)  
25 (2015) 3126-33.

26 [79] M. Fiorillo, M. Peiris-Pages, R. Sanchez-Alvarez, L. Bartella, L. Di Donna, V. Dolce, G.  
27 Sindona, F. Sotgia, A.R. Cappello, M.P. Lisanti, Bergamot natural products eradicate cancer stem  
28 cells (CSCs) by targeting mevalonate, Rho-GDI-signalling and mitochondrial metabolism,  
29 *Biochimica et biophysica acta* (2018).

30 [80] C. Carrisi, A. Romano, P. Lunetti, D. Antonucci, T. Verri, G.E. De Benedetto, V. Dolce, F.P.  
31 Fanizzi, M. Benedetti, L. Capobianco, Platinated Nucleotides are Substrates for the Human  
32 Mitochondrial Deoxynucleotide Carrier (DNC) and DNA Polymerase  $\gamma$ : Relevance for the  
33 Development of New Platinum-Based Drugs., *ChemistrySelect* 1(15) (2016) 4633-7

34 [81] V. Dolce, A.R. Cappello, L. Capobianco, Mitochondrial tricarboxylate and dicarboxylate-  
35 Tricarboxylate carriers: from animals to plants, *IUBMB Life* 66(7) (2014) 462-71.

36 [82] M. Santoro, C. Guido, F. De Amicis, D. Sisci, E. Cione, V. Dolce, A. Dona, M.L. Panno, S.  
37 Aquila, Bergapten induces metabolic reprogramming in breast cancer cells, *Oncol Rep* 35(1) (2016)  
38 568-76.

39 [83] M. Bonesi, M. Brindisi, B. Armentano, R. Curcio, V. Sicari, M.R. Loizzo, M.S. Cappello, G.  
40 Bedini, L. Peruzzi, R. Tundis, Exploring the anti-proliferative, pro-apoptotic, and antioxidant  
41 properties of *Santolina corsica* Jord. & Fourr. (Asteraceae), *Biomed Pharmacother* 107 (2018) 967-  
42 978.

43 [84] D. Vergara, M. Bianco, R. Pagano, P. Priore, P. Lunetti, F. Guerra, S. Bettini, S. Carallo, A.  
44 Zizzari, E. Pitotti, L. Giotta, L. Capobianco, C. Bucci, L. Valli, M. Maffia, V. Arima, A. Gaballo,  
45 An SPR based immunoassay for the sensitive detection of the soluble epithelial marker E-cadherin,  
46 *Nanomedicine* 14(7) (2018) 1963-1971.

47 [85] A. del Arco, J. Satrustegui, Molecular cloning of Aralar, a new member of the mitochondrial  
48 carrier superfamily that binds calcium and is present in human muscle and brain, *The Journal of*  
49 *biological chemistry* 273(36) (1998) 23327-34.

- 1 [86] I. Jungreis, C.S. Chan, R.M. Waterhouse, G. Fields, M.F. Lin, M. Kellis, Evolutionary  
2 Dynamics of Abundant Stop Codon Readthrough, *Molecular biology and evolution* 33(12) (2016)  
3 3108-3132.
- 4 [87] M. Sardiello, G. Tripoli, A. Romito, C. Minervini, L. Viggiano, C. Caggese, G. Pesole, Energy  
5 biogenesis: one key for coordinating two genomes, *Trends Genet* 21(1) (2005) 12-6.
- 6 [88] P. Rehm, J. Borner, K. Meusemann, B.M. von Reumont, S. Simon, H. Hadrys, B. Misof, T.  
7 Burmester, Dating the arthropod tree based on large-scale transcriptome data, *Molecular*  
8 *phylogenetics and evolution* 61(3) (2011) 880-7.
- 9 [89] J.B. Brown, N. Boley, R. Eisman, G.E. May, M.H. Stoiber, M.O. Duff, B.W. Booth, J. Wen, S.  
10 Park, A.M. Suzuki, K.H. Wan, C. Yu, D. Zhang, J.W. Carlson, L. Cherbas, B.D. Eads, D. Miller, K.  
11 Mockaitis, J. Roberts, C.A. Davis, E. Frise, A.S. Hammonds, S. Olson, S. Shenker, D. Sturgill,  
12 A.A. Samsonova, R. Weiszmann, G. Robinson, J. Hernandez, J. Andrews, P.J. Bickel, P. Carninci,  
13 P. Cherbas, T.R. Gingeras, R.A. Hoskins, T.C. Kaufman, E.C. Lai, B. Oliver, N. Perrimon, B.R.  
14 Graveley, S.E. Celniker, Diversity and dynamics of the *Drosophila* transcriptome, *Nature* 512(7515)  
15 (2014) 393-9.
- 16 [90] S. Cavero, A. Voza, A. del Arco, L. Palmieri, A. Villa, E. Blanco, M.J. Runswick, J.E.  
17 Walker, S. Cerdan, F. Palmieri, J. Satrustegui, Identification and metabolic role of the  
18 mitochondrial aspartate-glutamate transporter in *Saccharomyces cerevisiae*, *Molecular*  
19 *microbiology* 50(4) (2003) 1257-69.
- 20 [91] P.N. An, M. Yamaguchi, T. Bamba, E. Fukusaki, Metabolome analysis of *Drosophila*  
21 *melanogaster* during embryogenesis, *PloS one* 9(8) (2014) e99519.
- 22 [92] D.K. Hoshizaki, Fat-cell development, In *Complete Molecular Insect Science* 2 (2005) 315-  
23 345.
- 24  
25  
26  
27  
28  
29  
30  
31  
32  
33  
34  
35  
36  
37  
38  
39  
40  
41  
42  
43  
44  
45  
46  
47  
48  
49  
50  
51  
52  
53  
54  
55  
56  
57  
58  
59  
60  
61  
62  
63  
64  
65

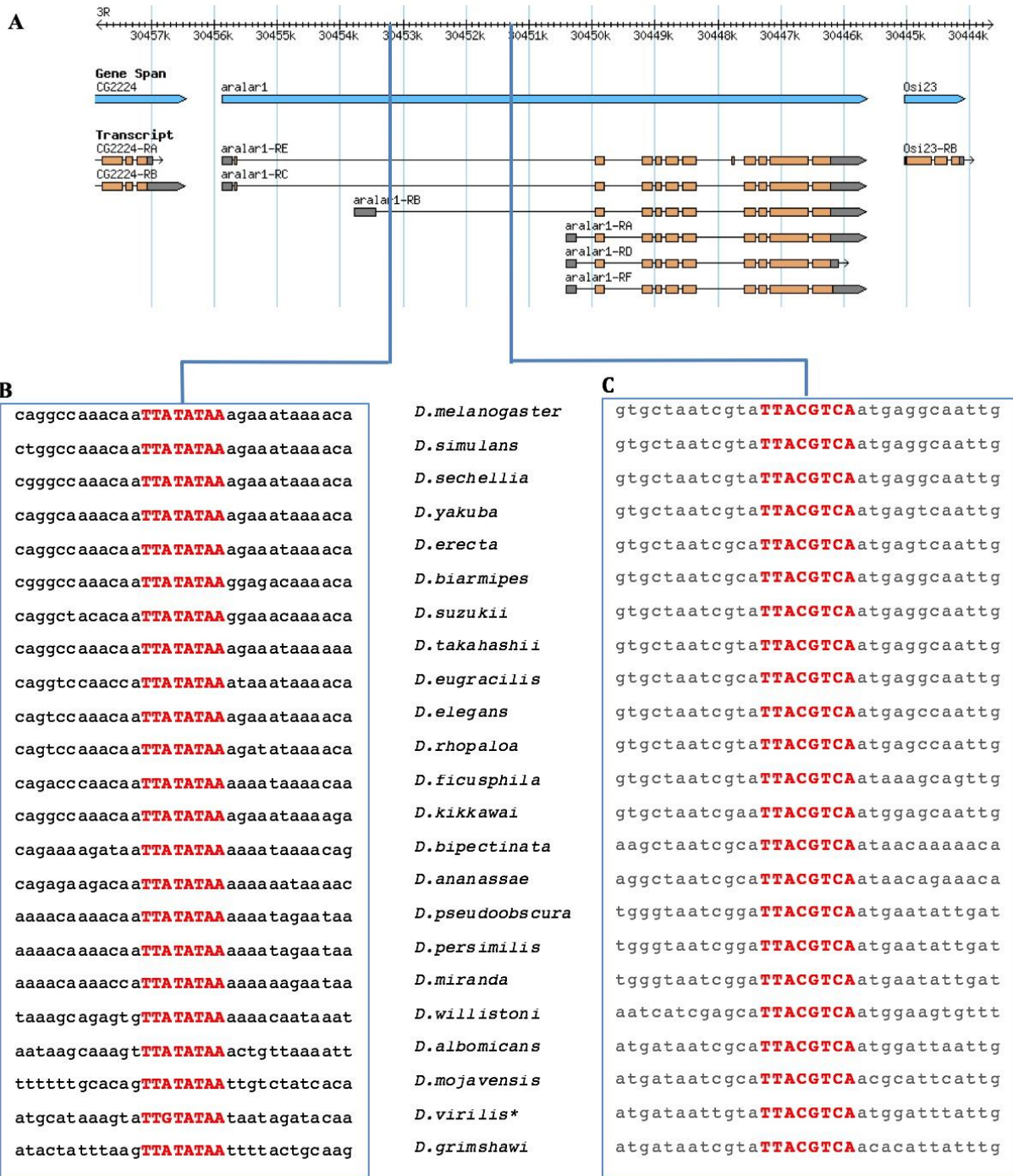


**Figure 1** Chromosomal organization of the *aralar1* gene in *D. melanogaster*. A) Overall organization of *aralar1* locus and its map position in *D. melanogaster*. B) and C) multiple sequence alignments encompassing the two conserved NRG elements in the *aralar1* gene of 23 *Drosophila* species. \* variant NRG motif in homologous position.

1  
2  
3  
4  
5  
6  
7  
8  
9  
10  
11  
12  
13  
14  
15  
16  
17  
18  
19  
20  
21  
22  
23  
24  
25  
26  
27  
28  
29  
30  
31  
32  
33  
34  
35  
36  
37  
38  
39  
40  
41  
42  
43  
44  
45  
46  
47  
48  
49  
50  
51  
52  
53  
54  
55  
56  
57  
58  
59  
60  
61  
62  
63  
64  
65

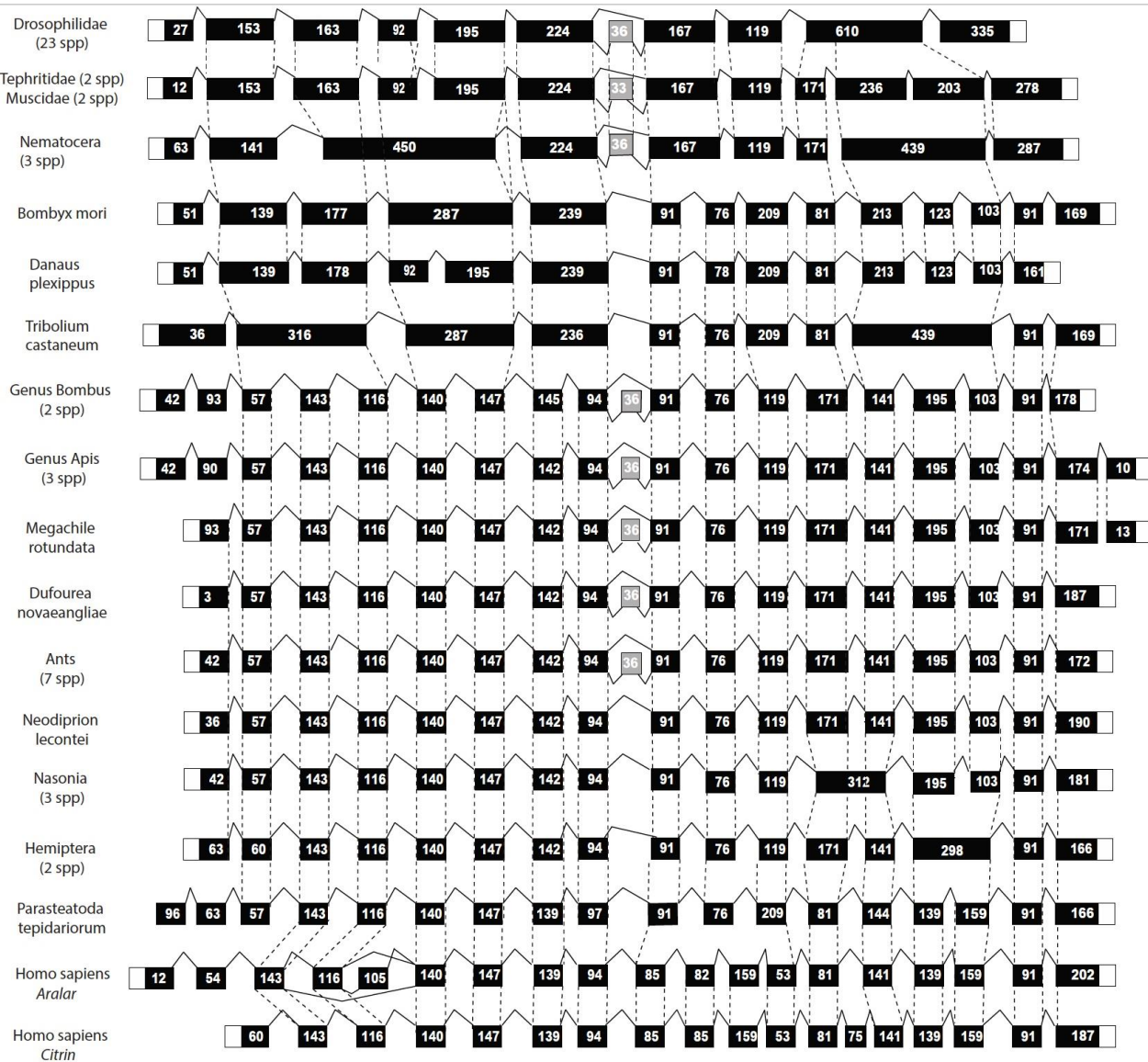


**Figure 2. Eukaryotic AGC-encoding genes share an ancient intron-rich ancestor.** The exon/intron structure of orthologous AGC-encoding genes of representative eukaryotic species is compared considering intron position, exon phase and length. Dashed lines indicate conservation of intron position. Translated AGC1-encoding regions are indicated in black, UTRs as white boxes. Internal *alarar1-RE* specific exons are indicated as gray boxes. Boxes are not in scale.

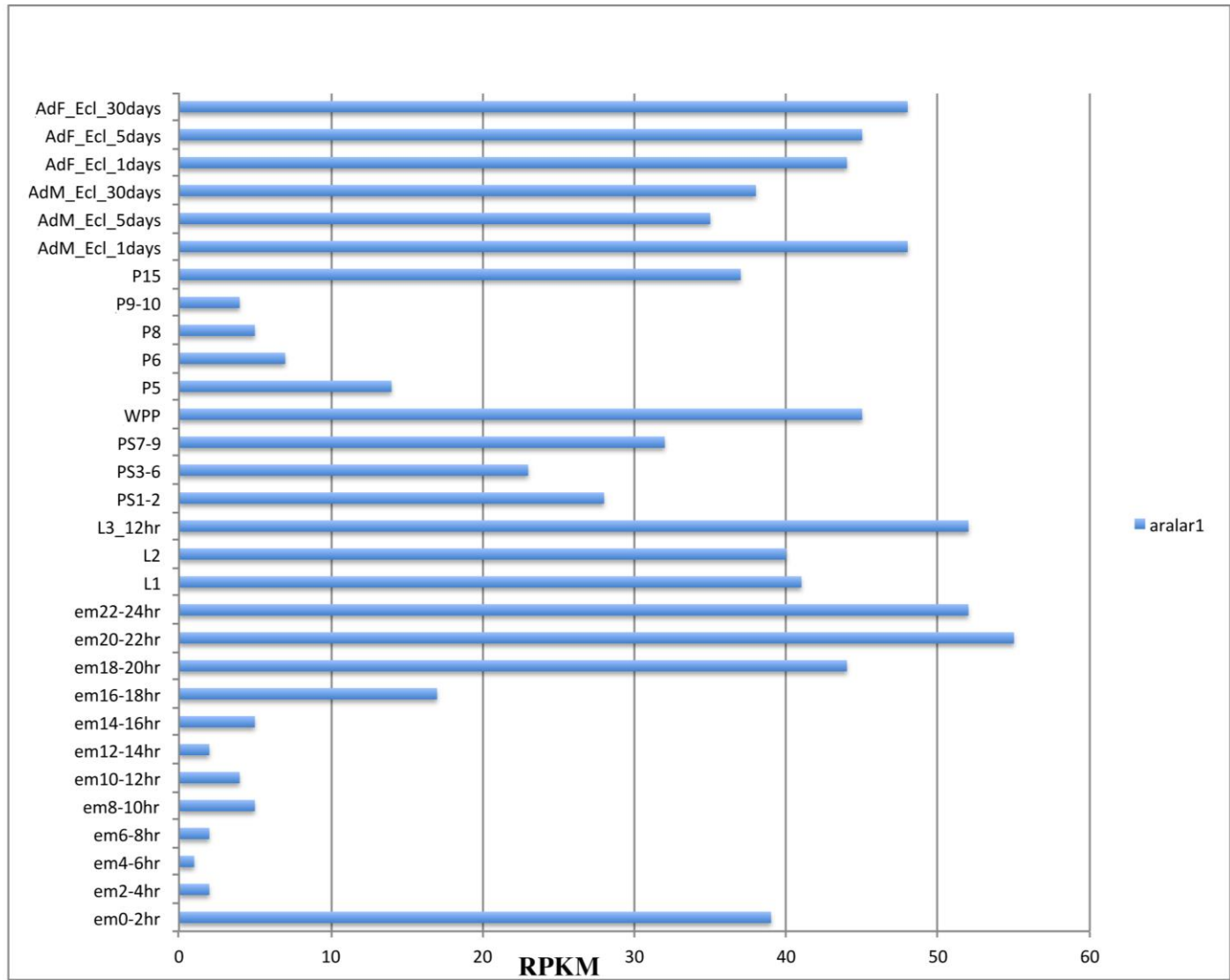


**Figure 3. modEncode expression of *alarar1* through the development.** Cumulative expression of all *alarar1* isoforms through the development is shown. Data were collected from modENCODE. Abbreviations legend. em: embryo stages; L: larval stages; P: pupae stages; AdM: adult males, various ages; AdF: adult females, various ages; RPKM: reads per kilobase million.

1  
2  
3  
4  
5  
6  
7  
8  
9  
10  
11  
12  
13  
14  
15  
16  
17  
18  
19  
20  
21  
22  
23  
24  
25  
26  
27  
28  
29  
30  
31  
32  
33  
34  
35  
36  
37  
38  
39  
40  
41  
42  
43  
44  
45  
46  
47  
48  
49  
50  
51  
52  
53  
54  
55  
56  
57  
58  
59  
60  
61  
62  
63  
64  
65

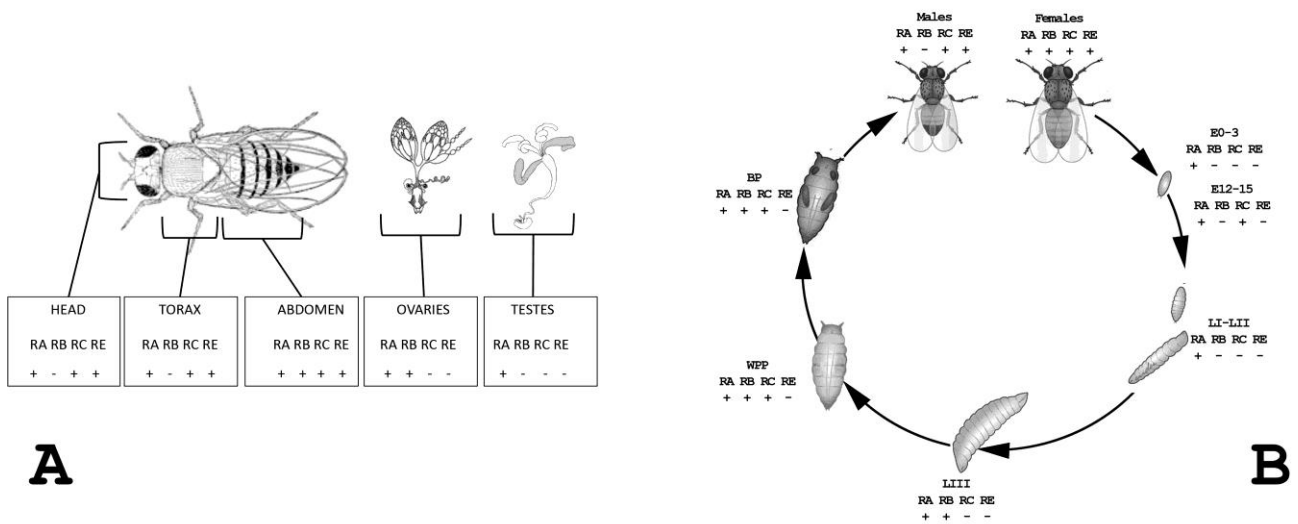


**Figure 4. Transcriptional analysis of *aralar1* in *Drosophila* adult tissues.**

The presence/absence of the indicated *aralar1* isoforms revealed by the detection of RT-PCR fragment in each analyzed RNA sample is indicated with “+” or “-”, respectively.

Panel A. The impact of the four transcriptional isoforms of *aralar1* analyzed in adult heads, thoraces and abdomens, and in the reproductive organs of males and females of *D. melanogaster*.

Panel B. The presence/absence of four transcriptional isoforms of *aralar1* was analyzed by RT-PCR through development in the indicated stages. RNA samples were collected from embryos at two stages of embryonic development (0–3, 12–15 after egg laying), mixed first and second instar larvae (LI-LII), third instar larvae (LIII), white prepupae (WPP), black pupae (BP), and adults (females and males).

1  
2  
3  
4  
5  
6  
7  
8  
9  
10  
11  
12  
13  
14  
15  
16  
17  
18  
19  
20  
21  
22  
23  
24  
25  
26  
27  
28  
29  
30  
31  
32  
33  
34  
35  
36  
37  
38  
39  
40  
41  
42  
43  
44  
45  
46  
47  
48  
49  
50  
51  
52  
53  
54  
55  
56  
57  
58  
59  
60  
61  
62  
63  
64  
65

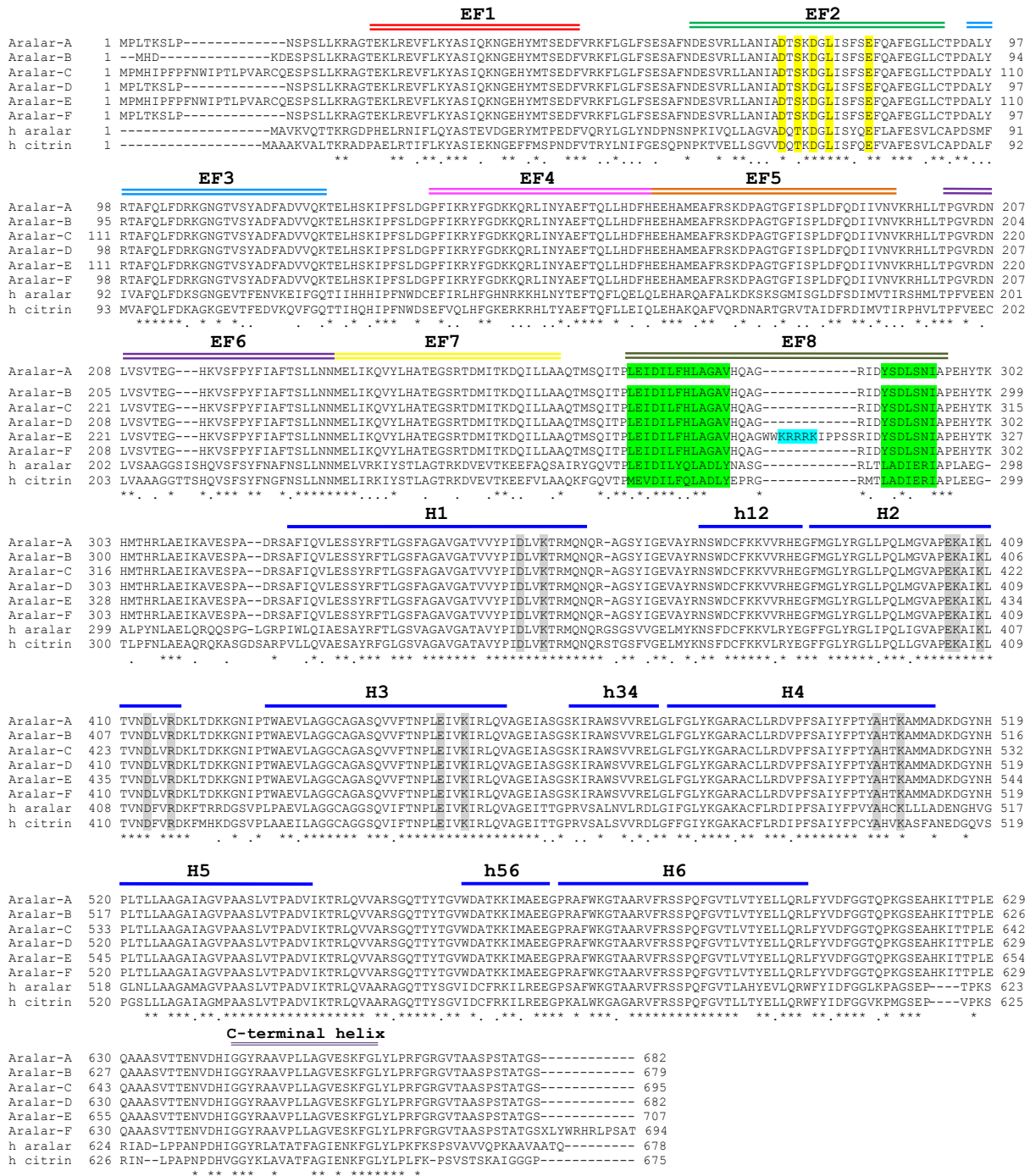


**Figure 5. Alignment of Drosophila Aralar1-PA-PF and human aralar and citrin.** Sequence conservation is indicated with an asterisk for identical residues, a dot for conserved substitutions, and a gap for non-conserved residues. The EF-hands, the six transmembrane helices H1-H6, the three small helices parallel to the membrane plane h12-h56, and the C-terminal  $\alpha$ -helix are indicated by coloured bars and labels. The two  $\alpha$ -helices of EF-hand 8 and the positive residues in

the loop of Aralar-1-PE are shaded in green and cyan, respectively. Residues that are involved in the coordination of calcium and the contact points of the substrate-binding site are shaded in yellow and gray, respectively. The alignment was obtained by using ClustalW.

1  
2  
3  
4  
5  
6  
7  
8  
9  
10  
11  
12  
13  
14  
15  
16  
17  
18  
19  
20  
21  
22  
23  
24  
25  
26  
27  
28  
29  
30  
31  
32  
33  
34  
35  
36  
37  
38  
39  
40  
41  
42  
43  
44  
45  
46  
47  
48  
49  
50  
51  
52  
53  
54  
55  
56  
57  
58  
59  
60  
61  
62  
63  
64  
65



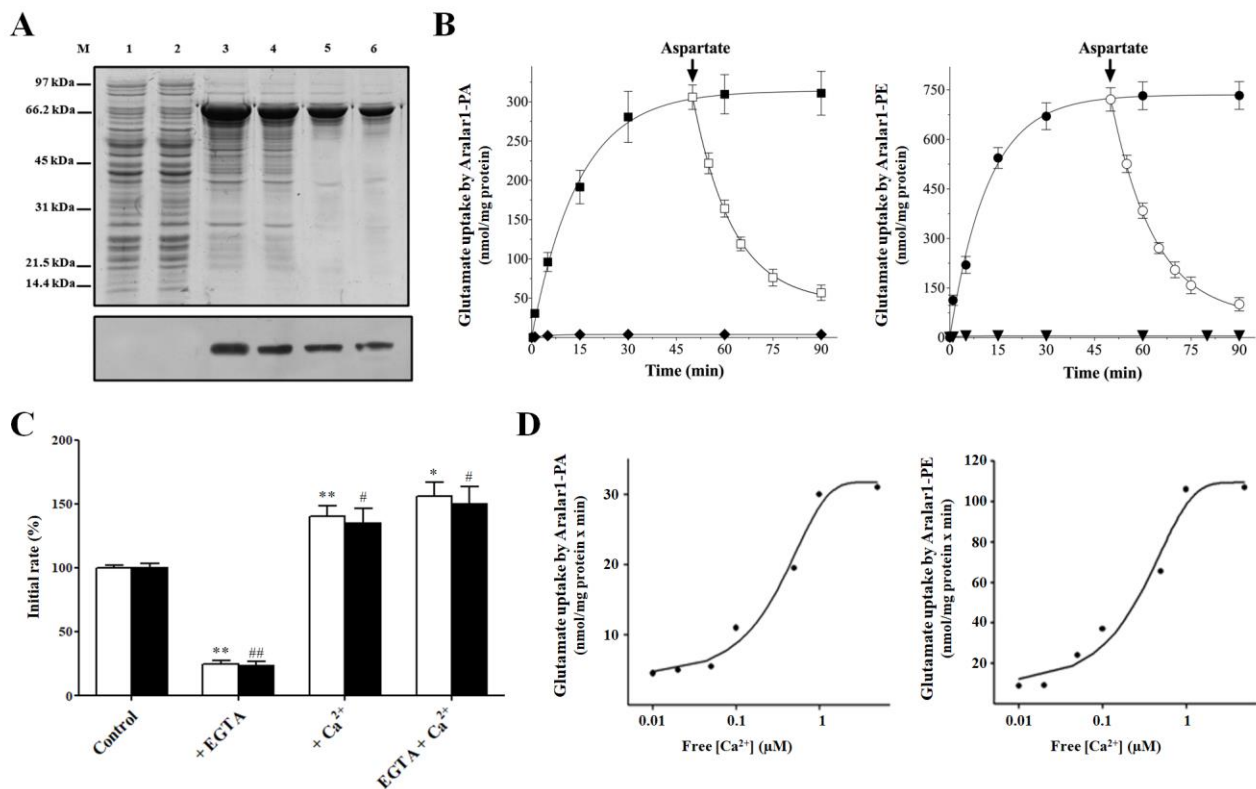


**Figure 6. Bacterial expression and functional characterization of Aralar1-PA and Aralar1-PE.** (A) Expression in *Escherichia coli* of recombinant Aralar1. Proteins were separated by SDS-PAGE and stained with Coomassie blue dye or transferred to nitrocellulose and immunodetected with an anti-V5 monoclonal antibody. Lane M, markers; lanes 1-6, *E. coli* BL21(DE3) containing the expression vector with the coding sequence for Aralar1-PA (lanes 1, 3 and 5) and Aralar1-PE (lanes 2, 4 and 6). Samples were taken at the time of the induction (lanes 1 and 2) and 4 h later (lanes 3 and 4). Lanes 5 and 6, Aralar1-PA and Aralar1-PE originating from bacteria shown in lanes 3 and 4, respectively, purified by centrifugation on sucrose gradient. The same number of bacteria was analyzed in each sample. (B) Kinetics of [<sup>14</sup>C]glutamate/glutamate exchange by Aralar1-PA and Aralar1-PE. Proteoliposomes were reconstituted with Aralar1-PA and Aralar1-PE. 0.5 mM [<sup>14</sup>C]glutamate was added to proteoliposomes containing 10 mM glutamate (■ and ●) or 10 mM NaCl (◆ and ▼). When the uptake approached equilibrium (50 min), 20 mM of aspartate was added outside the proteoliposomes (□ and ○). Similar results were obtained in four independent experiments. (C-D) Effect of Ca<sup>2+</sup> on transport activities of Aralar1-PA and Aralar1-PE. (C) Recombinant Aralar1-PA (open bars) and Aralar1-PE (filled bars), were reconstituted in proteoliposomes, the [<sup>14</sup>C]glutamate/glutamate transport rates were measured in de-ionized ultrapure water without additions (Control) or with the addition of 0.5 mM EGTA, or 1 mM CaCl<sub>2</sub>, or 0.5 mM EGTA in the presence of 1 mM CaCl<sub>2</sub>. Uptake rates of glutamate/glutamate exchange were measured at 60 s. Results are expressed as a percentage of the Aralar1-PA and Aralar1-PE values, which were on average 35.31 ± 1.24 and 110.58 ± 3.76 nmol/min x mg of protein, respectively. The average transport rates were calculated from the average of at least five independent experiments and displayed with the standard error. Different symbols indicate statistical differences, when occurring, between means of values as indicated by ANOVA. \**P* < 0.05, \*\**P* < 0.01 vs Aralar1-PA control, #*P* < 0.05, ##*P* < 0.01 vs Aralar1-PE control. (D) Dependence of Aralar1-PA and Aralar1-PE activities on the free Ca<sup>2+</sup> concentration. The [<sup>14</sup>C]glutamate transport rates were measured in de-ionized ultrapure water in the presence of 0.5 mM EGTA and various concentrations of Ca<sup>2+</sup>. Similar results were obtained in at least three independent experiments.

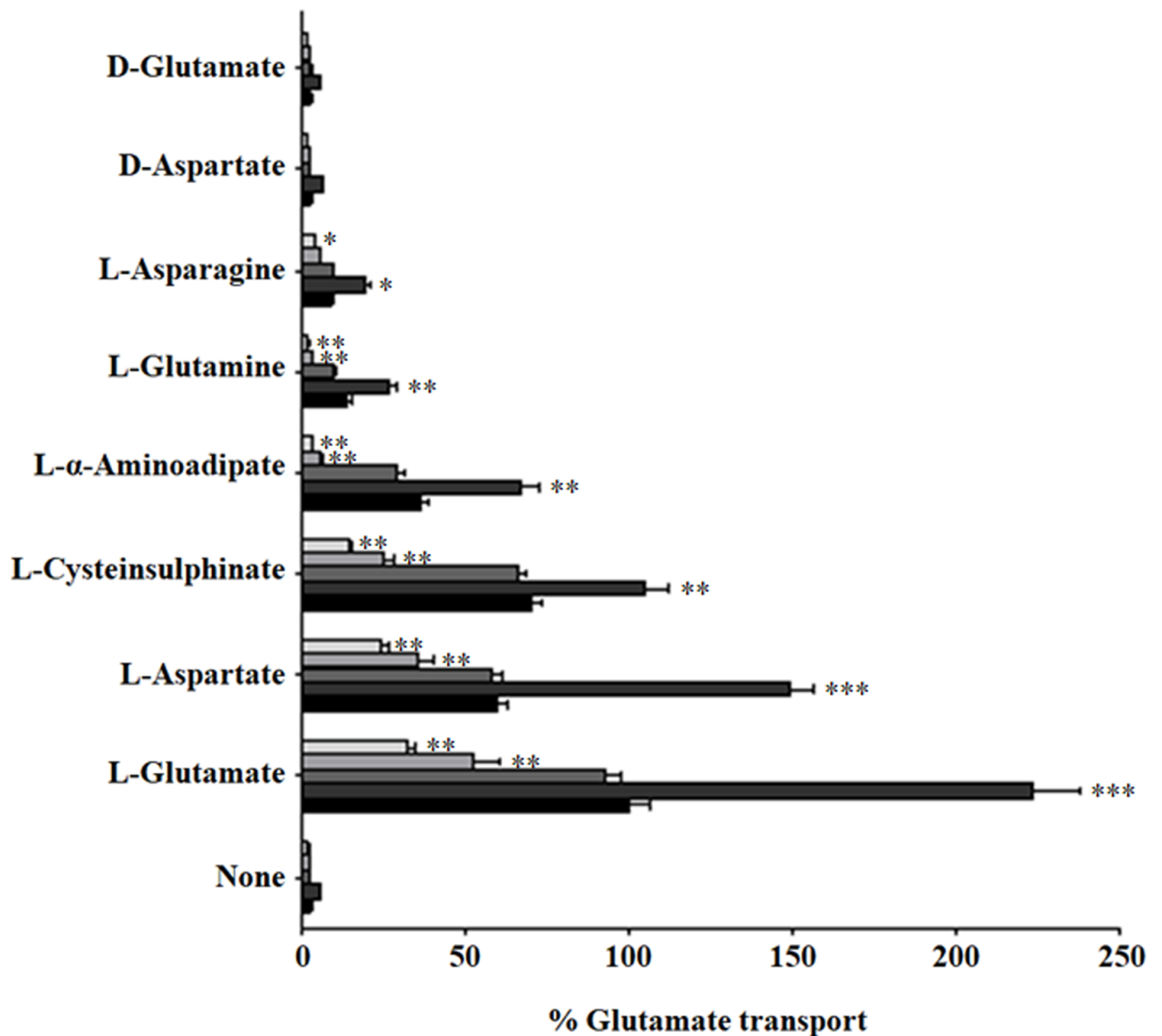


**Figure 7. Dependence on internal substrate of the transport properties of proteoliposomes reconstituted with recombinant Aralar1-PE, 5ALA, Δ5-Aralar1-PE, Δ8-Aralar1-PE and Δ12-Aralar1-PE mutants.** Proteoliposomes reconstituted with Aralar1-PE (black bars), 5ALA (very dark grey bars), Δ5-Aralar1-PE (dark grey bars), Δ8-Aralar1-PE (light grey bars) and Δ12-Aralar1-PE (very light grey bars) were preloaded internally with various substrates (concentration 10 mM). Transport was started by adding 0.5 mM [<sup>14</sup>C]glutamate to proteoliposomes and terminated after 1 min. Data represent the mean of three independent experiments reported as the percent of glutamate transport with respect to the rate of [<sup>14</sup>C]glutamate/glutamate exchange by Aralar1-PE (110 nmol/min/mg protein) setting at 100%. Asterisks indicate the level of statistical significance calculated comparing Aralar1-PE transport activity with that of its mutants in presence of each internal substrate. \**P* < 0.05, \*\**P* < 0.01, \*\*\**P* < 0.001, using ANOVA.

1  
2  
3  
4  
5  
6  
7  
8  
9  
10  
11  
12  
13  
14  
15  
16  
17  
18  
19  
20  
21  
22  
23  
24  
25  
26  
27  
28  
29  
30  
31  
32  
33  
34  
35  
36  
37  
38  
39  
40  
41  
42  
43  
44  
45  
46  
47  
48  
49  
50  
51  
52  
53  
54  
55  
56  
57  
58  
59  
60  
61  
62  
63  
64  
65

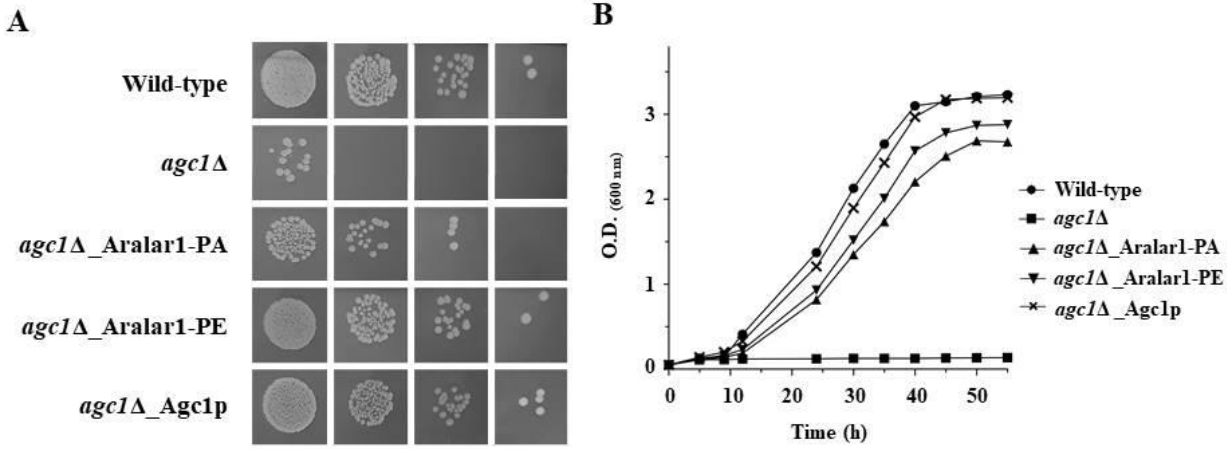


**Figure 8. Complementation of the growth defect of *agc1Δ* yeast strain by Aralar1-PA and Aralar1-PE.** Wild-type, *agc1Δ* cells transformed with the empty vector (*agc1Δ*) and *agc1Δ* cells expressing drosophila Aralar1-PA, Aralar1-PE and yeast Agc1p were plated by using a four-fold serial dilution (A) or inoculated (B) in YP medium supplemented with 0.5 mM oleate. Plates and cell cultures were placed at 30°C. Picture given in A was taken after 3 days to show yeast growth performance, whereas the optical density (O.D.) values at 600 nm given in B refer to cell cultures after the indicated growth times.

**TABLE I**

*Dependence on internal substrate of the transport properties of proteoliposomes reconstituted with recombinant Aralar1-PA and Aralar1-PE.*

Proteoliposomes were preloaded internally with various substrates (concentration 10 mM). Transport was started by adding 0.5 mM [<sup>14</sup>C]glutamate to proteoliposomes reconstituted with Aralar1-PA and Aralar1-PE, respectively, and terminated after 1 min. For each internal substrates four independent experiments have been carried out. The means and the standard deviations of Aralar1-PA and Aralar1-PE for each substrate are reported. Different symbols indicate statistical differences between means of values as indicated by ANOVA (\*P ≤ 0.05, \*\*\*P ≤ 0.001 vs uniport reaction by Aralar1-PA, #P ≤ 0.05, ##P ≤ 0.01, ###P ≤ 0.001 vs uniport reaction by Aralar1-PE).

Internal substrate	<sup>14</sup> C]Glutamate transport	
	Aralar1-PA	Aralar1-PE
	<i>nmol/min x mg of protein</i>	
None (Cl <sup>-</sup> present)	1.63 ± 0.11	2.85 ± 0.19
L-glutamate	31.27 ± 1.31 <sup>***</sup>	105.5 ± 6.89 <sup>###</sup>
L-aspartate	23.14 ± 1.21 <sup>***</sup>	63.34 ± 2.78 <sup>###</sup>
L-cysteinesulfinate	13.76 ± 0.78 <sup>***</sup>	73.91 ± 3.23 <sup>###</sup>
L-α-aminoadipate	2.34 ± 0.13 <sup>*</sup>	38.05 ± 2.98 <sup>###</sup>
L-glutamine	1.84 ± 0.16	14.68 ± 1.24 <sup>###</sup>
L-asparagine	3.63 ± 0.27 <sup>*</sup>	9.51 ± 1.02 <sup>#</sup>
D-aspartate	1.65 ± 0.10	2.99 ± 0.22
D-glutamate	1.34 ± 0.12	2.77 ± 0.25

**TABLE II**

*Influence of the membrane potential on the activity of recombinant Aralar1-PA and Aralar1-PE.*

The exchange was started by the addition of 50  $\mu\text{M}$  [ $^{14}\text{C}$ ]aspartate to proteoliposomes containing 10 mM of the indicated internal substrate.  $K^+_{\text{in}}$  was included as KCl in the reconstitution mixture, whereas  $K^+_{\text{out}}$  was added as KCl together with the labeled substrate. The differences in osmolarity were compensated for by the addition of appropriate concentrations of sucrose in the opposite compartment. Valinomycin (1.0  $\mu\text{g}/\text{mg}$  phospholipid) was added in 10  $\mu\text{l}$  ethanol/ml of proteoliposomes (+ valinomycin). In the samples without valinomycin (– valinomycin) the only ethanol was added. The exchange reactions were stopped after 1 min. Similar results were obtained in three independent experiments. Asterisks indicate values that are significantly different from those obtained in the same experiment but in absence of valinomycin (\*\* $P \leq 0.01$ , using Student's *t*-test)

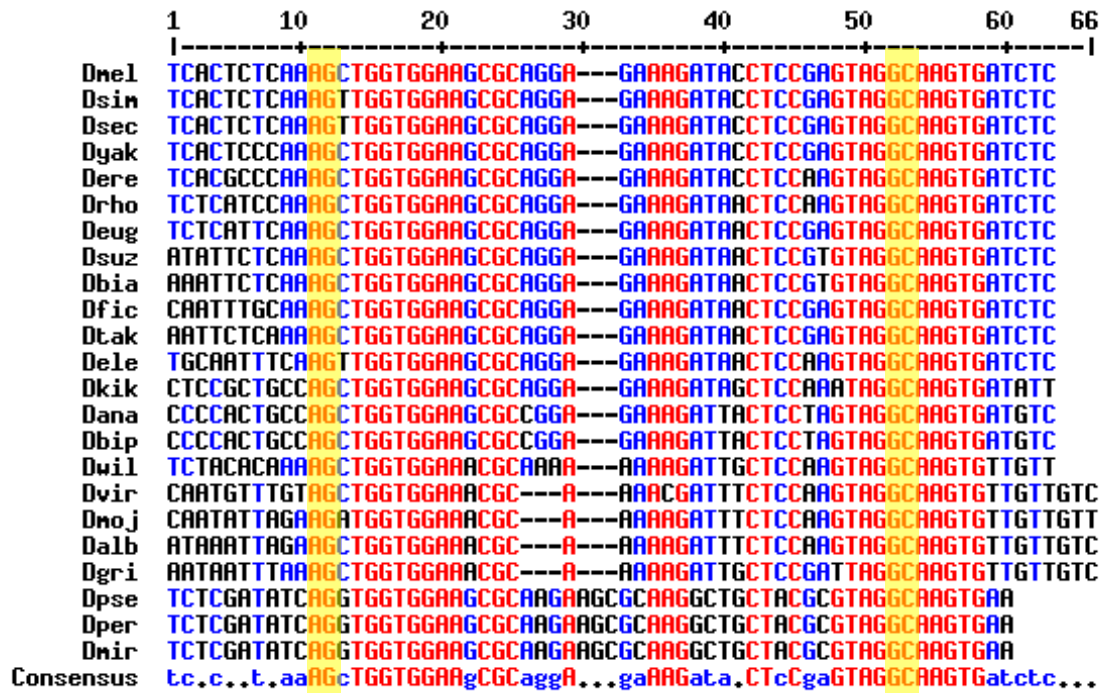
Internal substrate	$K^+_{\text{in}}/k^+_{\text{out}}$ (mM/mM)	$[^{14}\text{C}]$ Aspartate uptake (nmol/min x mg protein)			
		Aralar1-PA		Aralar1-PE	
		- valinomycin	+ valinomycin	- valinomycin	+ valinomycin
Aspartate	1/1	28.75 $\pm$ 2.11	30.05 $\pm$ 2.96	100.75 $\pm$ 8.55	102.21 $\pm$ 8.40
	1/50	27.37 $\pm$ 2.41	28.64 $\pm$ 2.05	103.25 $\pm$ 7.20	103.89 $\pm$ 9.10
Glutamate	1/1	21.52 $\pm$ 1.70	22.24 $\pm$ 1.45	76.33 $\pm$ 5.88	77.14 $\pm$ 6.39
	1/50	23.95 $\pm$ 2.35	57.48 $\pm$ 5.74**	75.68 $\pm$ 6.28	154.86 $\pm$ 7.50**

**TABLE III**

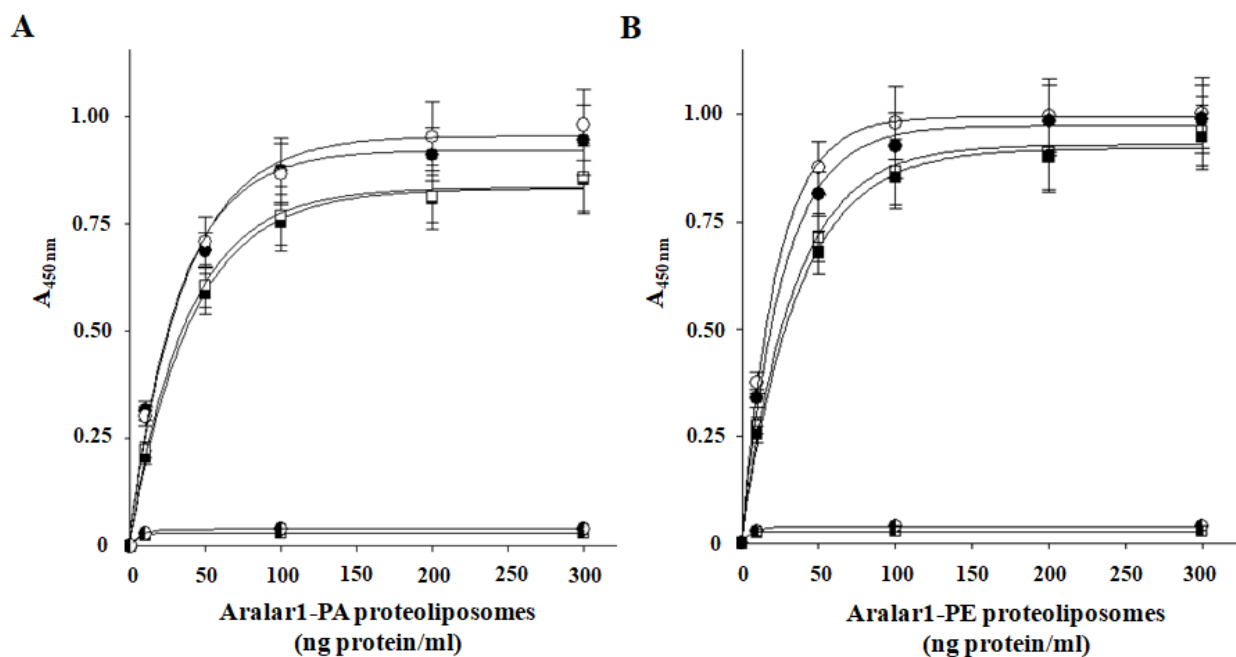
*Kinetic constants of recombinant Aralar1-PA, Aralar1-PE, 5ALA, Δ5-Aralar1-PE, Δ8-Aralar1-PE and Δ12-Aralar1-PE mutants.*

The values were calculated from double reciprocal plots of the rate of [<sup>14</sup>C]glutamate uptake versus substrate concentrations. Transport was started by adding 125-750 μM [<sup>14</sup>C]glutamate to proteoliposomes containing 10 mM glutamate, and terminated after 1 min. Similar results were obtained in at least three independent experiments.

<b>Carrier</b>	<b>K<sub>m</sub></b> <i>(mM)</i>	<b>V<sub>max</sub></b> <i>(nmol/min x mg protein)</i>
Aralar1-PA	0.26 ± 0.03	34.60 ± 2.11
Aralar1-PE	0.29 ± 0.07	92.08 ± 4.96
5ALA	0.31 ± 0.062	189.21 ± 10.50
Δ5-Aralar1-PE	0.33 ± 0.075	82.22 ± 7.55
Δ8-Aralar1-PE	0.31 ± 0.072	58.75 ± 5.10
Δ12-Aralar1-PE	0.30 ± 0.055	37.32 ± 3.15



Supplementary Figure 1. Multiple alignment of the aralar1-RE specific exon. the conservation of the acceptor (AG) and donor splice sites (GC) respectively of the upstream and downstream flanking introns are highlighted in yellow.



**Supplementary Figure 2. Reactivity of the anti-N-terminal amino acids 35-177 of Aralar1 and anti-V5 epitope tag antisera to the reconstituted Aralar1 proteins assessed by ELISA.** Reactivity was evaluated for both recombinant Aralar1-PA (A) and Aralar1-PE (B) isoforms by using either the anti-N-terminal peptide antiserum direct against 35-177 amino acids of Aralar1 proteins (●, ○ and ◐), or the anti-V5 antibody direct against the V5 epitope placed at their C-termini (■, □ and ◑). Microtiter plates were coated with the indicated amounts of intact (● and ■) or permeabilized (○ and □) proteoliposomes. In (◐ and ◑), each antibody, in presence of only not reconstituted liposomes, was used as a negative control.



**Supplementary Table S1.** List of the *aralar1* genes investigated in this study with their positions in the respective genome.

Species	Accession number	RA-RD-RF transcript Coding exons	RB Coding exons	RC(RE) Coding exons
<i>Drosophila melanogaster</i>	FBgn0028646	10	11	12(13)
<i>Drosophila simulans</i>	JMCE01000007.1	10	11	12(13)
<i>Drosophila sechellia</i>	AAKO01001326.1	10	11	12(13)
<i>Drosophila yakuba</i>	AAEU02000259	10	11	12(13)
<i>Drosophila erecta</i>	AAPQ01006792	10	11	12(13)
<i>Drosophila ficusphila</i>	AFFG02008687	10	11	12(13)
<i>Drosophila eugracilis</i>	AFPQ02005951	10	11	12(13)
<i>Drosophila biarmipes</i>	AFFD02006539.1	10	11	12(13)
<i>Drosophila takahashii</i>	AFFI02007371	10	11	12(13)
<i>Drosophila suzukii</i>	CAKG01025788	10	11	12(13)
<i>Drosophila elegans</i>	AFFF02008080	10	11	12(13)
<i>Drosophila rhopaloa</i>	AFPP02032380	10	11	12(13)
<i>Drosophila kikkawai</i>	AFFH02006507	10	11	12(13)
<i>Drosophila bipectinata</i>	AFFE02007958	10	11	12(13)
<i>Drosophila ananassae</i>	AAPP01015636	10	11	12(13)
<i>Drosophila miranda</i>	JXPA01005888	10	11	12(13)
<i>Drosophila pseudoobscura</i>	AAFS01000152	10	11	12(13)
<i>Drosophila persimilis</i>	AAIZ01003247	10	11	12(13)
<i>Drosophila willistoni</i>	AAQB01009418	10	11	12(13)
<i>Drosophila albomicans</i>	JXOX01003054	10	11	12(13)
<i>Drosophila mojavensis</i>	AAPU01011085	10	11	12(13)
<i>Drosophila virilis</i>	AANI01017206	10	11	12(13)
<i>Drosophila grimshawi</i>	AAPT01018777	10	11	12(13)
<i>Ceratitis capitata</i>	AOHK01020840	12	>=13	>=14(<=15)
<i>Musca domestica</i>	NW_004765104.1	12	>=13	>=14(<=15)
<i>Bactrocera cucurbitae</i>	NW_011863679	12	>=13	>=14(<=15)
<i>Stomoxys calcitrans</i>	NW_013172444.1	12	>=13	>=14(<=15)
<i>Anopheles gambiae</i>	AAAB01008811	9	ND	ND
<i>Culex quinquefasciatus</i>	NW_001886742 AAWU01004063	9	ND	ND
<i>Aedes aegypti</i>	NC_035107.1	9	ND	ND

<i>Bombyx mori</i>	NW_004582021	14	ND	ND
<i>Danaus plexippus</i>	AGBW02014362.1	14	ND	ND
<i>Tribolium castaneum</i>	NC_007417	11	ND	ND
<i>Apis mellifera</i>	NW_003378056	18	ND	ND
<i>Apis florea</i>	NW_003790556	18	ND	ND
<i>Apis dorsata</i>	NW_006263665	18	ND	ND
<i>Bombus impatiens</i>	NT_177753	18	ND	ND
<i>Bombus terrestris</i>	NC_015777	18	ND	ND
<i>Megachile rotundata</i>	NW_003797109	18	ND	ND
<i>Dufourea novaeangliae</i>	NW_015374267	17	ND	ND
<i>Acromyrmex echinator</i>	NW_011627086	18	ND	ND
<i>Atta cephalotes</i>	NW_012130091	16	ND	ND
<i>Solenopsis invicta</i>	NW_011795700	17	ND	ND
<i>Pogonomyrmex barbatus</i>	NW_011933718	18	ND	ND
<i>Harpegnathos saltator</i>	NW_011655019	17	ND	ND
<i>Linepithema humile</i>	NW_012160777	17	ND	ND
<i>Camponotus floridanus</i>	NW_011880404	16*	ND	ND
<i>Neodiprion lecontei</i>	NW_015383904	17	ND	ND
<i>Nasonia giraulti</i>	ADAO01244945	15**	ND	ND
<i>Nasonia longicornis</i>	ADAP01028838	15**	ND	ND
<i>Nasonia vitripennis</i>	NC_015869	16	ND	ND
<i>Acyrtosiphon pisum</i>	NW_003383605			
<i>Diuraphis noxia</i>	JOTR01000078			
<i>Limulus polyphemus</i>	NW_013667734			
<i>Parasteatoda tepidariorum</i>	NW_015458343			
<i>Homo sapiens aralar1</i>	NG_011781.1			
<i>Homo sapiens citrin</i>	NG_012247			

\* lacks exon 8 due to sequence gap

\*\* 1st exon not detected due to sequence limit

**Supplementary Table S2. aralar1 gene structure comparisons in Drosophila species.****Isoforms RA-RD-RF**

Key: UTR, CDS, intron \*length inferred by similarity, RA-RD-RF transcript specific exon

Subgenus	subgroup	Species	RA-RD-RF											
Sophophora	melanogaster subgroup	<i>Drosophila_melanogaster</i>	151	27	269	153	598	163	58	92	66	195	65	224
		<i>Drosophila_simulans</i>	151	27	264	153	585	163	58	92	64	195	63	224
		<i>Drosophila_yakuba</i>	156	27	306	153	595	163	59	92	64	195	63	224
		<i>Drosophila_erecta</i>	150	27	270	153	557	163	66	92	64	195	64	224
		<i>Drosophila_sechellia</i>	151	27	264	153	582	163	55	92	64	195	63	224
	suzukii subgroup	<i>Drosophila_biarmipes</i>	152*	27	237	153	601	163	63	92	78	195	64	224
		<i>Drosophila_takahashii</i>	145*	27	284	153	901	163	61	92	80	195	63	224
		<i>Drosophila_suzukii</i>	145*	27	240	153	744	163	66	92	68	195	64	224
	eugracilis subgroup	<i>Drosophila_eugracilis</i>	147*	24	284	153	657	163	67	92	75	195	62	224
	ficuspshila subgroup	<i>Drosophila_ficuspshila</i>	145*	27	309	153	514	163	63	92	68	195	62	224
	elegans subgroup	<i>Drosophila_elegans</i>	150*	27	261	153	818	163	59	92	66	195	64	224
montium subgroup	<i>Drosophila_rhopalooa</i>	154*	27	282	153	863	163	59	92	67	195	64	224	

		<i>Drosophila_kikkawai</i>	155*	27	470	153	698	163	65	92	72	195	65	224
	ananassae subgroup	<i>Drosophila_bipectinata</i>	154*	27	147	153	611	163	62	92	67	195	58	224
		<i>Drosophila_ananassae</i>	154*	27	142	153	631	163	59	92	61	195	58	224
willistoni subgroup	<i>Drosophila_willistoni</i>	156	27	169	153	476	163	65	92	167	195	66	224	
Drosophila	pseudoobscura subgroup	<i>Drosophila_miranda</i>	ND	27	177	153	535	163	50	92	67	195	62	224
		<i>Drosophila_pseudoobscura</i>	ND	27	177	153	504	163	57	92	67	195	62	224
		<i>Drosophila_persimilis</i>	ND	27	177	153	534	163	57	92	67	195	62	224
	nasuta subgroup	<i>Drosophila_albomicans</i>	136	18	233	153	1188	163	57	92	63	195	55	224
	mulleri subgroup	<i>Drosophila_mojavensis</i>	652	18	217	153	531	163	80	92	97	195	65	224
	virilis subgroup	<i>Drosophila_virilis</i>	139	18	215	153	521	163	69	92	70	195	68	224



**Supplementary Table S3. aralar1 gene structure comparisons in Drosophila species.****Isoform RB**

Key: UTR, CDS, intron \*length inferred by similarity, RB transcript specific exon

Subgenus	Subgroup		RB											
Sophophora	melanogaster	<i>Drosophila_melanogaster</i>	335	18	3468	153	598	163	58	92	66	195	65	22
		<i>Drosophila_simulans</i>	330	18	3548	153	585	163	58	92	64	195	63	22
		<i>Drosophila_yakuba</i>	376	18	3654	153	595	163	59	92	64	195	63	22
		<i>Drosophila_erecta</i>	353	18	6209	153	557	163	66	92	64	195	64	22
		<i>Drosophila_sechellia</i>	321	18	3445	153	582	163	55	92	64	195	63	22
	suzukii	<i>Drosophila_biarmipes</i>	393*	18	3545	153	601	163	63	92	78	195	64	22
		<i>Drosophila_takahashii</i>	389*	18	5299	153	901	163	61	92	80	195	63	22
		<i>Drosophila_suzukii</i>	386*	18	3806	153	744	163	66	92	68	195	64	22
	eugracilis	<i>Drosophila_eugracilis</i>	366*	18	3900	153	657	163	67	92	75	195	62	22
	ficuspila	<i>Drosophila_ficuspila</i>	385*	18	3582	153	514	163	63	92	68	195	62	22
	elegans	<i>Drosophila_elegans</i>	413*	18	3973	153	818	163	59	92	66	195	64	22
	montium	<i>Drosophila_rhopaloo</i>	254*	18	3963	153	863	163	59	92	67	195	64	22



**Supplementary Table S4. aralar1 gene structure comparisons in Drosophila species.****Isoform RC**

Key: UTR, CDS, intron \*length inferred by similarity, RC transcript specific exon

Subgenus	Subgroup	Species	RC				
Sophophora	melanogaster	<i>Drosophila_melanogaster</i>	151	66	5691	153	59
		<i>Drosophila_simulans</i>	151	66	5758	153	59
		<i>Drosophila_yakuba</i>	152	66	5910	153	59
		<i>Drosophila_erecta</i>	152	66	8315	153	59
		<i>Drosophila_sechellia</i>	151	66	5666	153	59
	suzukii	<i>Drosophila_biarmipes</i>	ND	60	6048	153	60
		<i>Drosophila_takahashii</i>	ND	63	7836	153	90
		<i>Drosophila_suzukii</i>	ND	60	6250	153	74
	eugracilis	<i>Drosophila_eugracilis</i>	ND	60	6186	153	60
	ficuspila	<i>Drosophila_ficuspila</i>	ND	60	5728	153	59
	elegans	<i>Drosophila_elegans</i>	ND	60	6552	153	80
	montium	<i>Drosophila_rhopaloo</i>	ND	66	6572	153	80
		<i>Drosophila_kikkawai</i>	ND	66	6262	153	60
ananassae	<i>Drosophila_bipectinata</i>	ND	66	5787	153	60	





**Supplementary Table S5. aralar1 gene structure comparisons in Drosophila species.****Isoform RE**

Key: UTR, CDS, intron \*length inferred by similarity, RE transcript specific exons

Subgenus	Subgroup		RE						
Sophophora	melanogaster	<i>Drosophila_melanogaster</i>	151	66	5691	153	598	163	58
		<i>Drosophila_simulans</i>	151	66	5758	153	585	163	58
		<i>Drosophila_yakuba</i>	152	66	5910	153	595	163	59
		<i>Drosophila_erecta</i>	152	66	8315	153	557	163	66
		<i>Drosophila_sechellia</i>	151	66	5666	153	582	163	55
	suzukii	<i>Drosophila_biarmipes</i>	ND	60	6048	153	601	163	63
		<i>Drosophila_takahashii</i>	ND	63	7836	153	901	163	61
		<i>Drosophila_suzukii</i>	ND	60	6250	153	744	163	66
	eugracilis	<i>Drosophila_eugracilis</i>	ND	60	6186	153	657	163	67
	ficuspila	<i>Drosophila_ficuspila</i>	ND	60	5728	153	514	163	63
	elegans	<i>Drosophila_elegans</i>	ND	60	6552	153	818	163	59
	montium	<i>Drosophila_rhopaloo</i>	ND	66	6572	153	863	163	59
		<i>Drosophila_kikkawai</i>	ND	66	6262	153	698	163	65
	ananassae	<i>Drosophila_bipectinata</i>	ND	66	5787	153	611	163	62



**Supplementary Table S6. aralar1 gene structure comparison in Arthropoda.**

Key: UTR, CDS, intron \*sequence gap; ND: Not detected

Order (Family)	Species	other TSSs	first exon of RB isoform													
			exon	intron	exon	intron	exon	intron	exon	intron	exon	intron	exon	intron	exon	
Diptera (Drosophilidae)	<i>Drosophila_melanogaster</i>	+ 1 alternative TSS	335	18	3021	151	27	269						153	598	163
Diptera (Tephritidae)	<i>Ceratitis_capitata</i> <i>OK</i>	+ 1 alternative TSS	361	21	7381	218	12	470						153	1334	163
	<i>Bactrocera_cucurbitae</i>		ND	ND	ND	328+ND +292	27	24806*						153	3360	163
Diptera (Muscidae)	<i>Stomoxys_calcitrans</i>	+ 1 alternative TSS	564	24	34157*	314	24	10080*						153	>=9 702	163

	<i>Musca_domestic a</i>	+ 1 altern ative TSS	141+48 1+137	2 4	28126*	309	2 4	4072	15 3	798 4	16 3
Diptera (Culicida e)	<i>Anopheles_gamb iae</i>		ND	ND	ND	136	3 0	3507	14 1	297	
	<i>Culex_pipiens_q uinq.</i>		ND	ND	ND		6 3	2117*	14 1	93	
	<i>Aedes_aegypti</i>		ND	ND	ND	520	6 3	50083*	14 1	70	

Lepidoptera	<i>Bombyx_mori</i>	+ 1 alternative TSS	ND	ND	ND	283	51	5746			139	1689	177		
	<i>Danaus_plexippus</i>		ND	ND	ND	ND	51	130482			139	70	177		
Coleoptera	<i>Tribolium_castaneum</i>		247	36	1516	54	36	81		316					
Hymenoptera	<i>Apis_mellifera</i>		ND	ND	ND	426	42	1720	90	8900	57	199	143	78	116
	<i>Apis_florea</i>		ND	ND	ND	306	42	10509		57	206	143	75	116	
	<i>Apis_dorsata</i>		ND	ND	ND	375	42	1680	93	6893	57	207	143	75	116

	<i>Bombus_impatiens</i>	ND	ND	ND	288	42	12665	57	118	143	106	116	
	<i>Bombus_terrestris</i>	ND	ND	ND	284	42	12543	57	111	143	104	116	
	<i>Megachile_rotundata</i>	182	44	2986	1108	93	85	57	70	143	121	116	





	<i>Harpegnathos_s altator</i>	ND	ND	ND	78	42	93341	57	147	143	1907	116	
	<i>Linepithema_hu mile</i>	ND	ND	ND	250	42	7691	57	152	143	151	116	
	<i>Camponotus_flor idanus</i>	ND	ND	ND	386	42	13515	57	1156	143	980	116	
	<i>Neodiprion_leco ntei</i>	ND		ND	25	36	3862	57	808	143	172	116	
	<i>Nasonia_vitripen nis</i>	253		339	75	42	10940	57	90	143	277*	116	
	<i>Nasonia_giraulti</i>	ND	ND	ND	ND	ND	ND	57	90	143	267	116	
	<i>Nasonia_longico rnis</i>	ND	ND	ND	ND	ND	364*	57	90	143	277	116	
Hemipter a	<i>Acyrtosiphon_p isum</i>	ND	ND	ND	173	63	554	60	75	143	1612	116	

	<i>Diuraphis_noxia</i>		ND	ND	ND	643	63	570	60	67	143	1610	116				
Xiphosura (Limulidae)	<i>Limulus_polyphemus</i>		ND	ND	ND	105	42	3641	60	8494	143	2534	116				
Arachnida	<i>Parasteatoda_tetranychus</i>		ND	ND	ND	ND	96	103	63	5434	57	2636	143	1018	116		
	<i>Homo_sapiens_raral</i>					92	12	944	54	24381	143	12731	116	75			

	<i>Homo_sapiens</i> \ <i>citrin</i>	+ 1 altern ative TSS	94	4 8	125 87	5 4	121 73	51	6 0	7279	14 3	422 78	11 6		

NOTE: the CITRIN locus has been depicted using the X1-X4 mRNA isoforms annotated in NCBI. The first ex

Credit Author Statement

P.L., R.C, L.C. and V.D. conceived the project, designed experiments, and wrote the manuscript. P.L., R.C, F.M, Y.L., G.L. and F.D. performed the biochemical and molecular biology experiments. R.M.M., R.M. performed the genetic experiments. D.A. performed the calcium experiments. A. A. M. provided antiserum and contributed to ELISA experiments. P. L. and F.M. analyzed the yeast phenotype. A.R.C. A.F. and G.F. assisted in data interpretation. G.F. and V. Z. participated in the discussion of the project and were involved in the revision of the manuscript. L.C. and V.D. directed and supervised the project. G.F. and V.Z. acquired the funding. All authors read and approved the final manuscript.